PFG

Photogrammetrie Fernerkundung Geoinformation

Organ der Deutschen Gesellschaft für Photogrammetrie, Fernerkundung und Geoinformation (DGPF) e.V.

Jahrgang 2006, Heft 4

E. Schweizerbart'sche Verlagsbuchhandlung
(Nägele u. Obermiller) Stuttgart 2006

Deutsche Gesellschaft für Photogrammetrie, Fernerkundung
und Geoinformation (DGPF) e.V.
Gegründet 1909

Die *Deutsche Gesellschaft für Photogrammetrie, Fernerkundung und Geoinformation* (DGPF) e.V. unterstützt als Mitglieds- bzw. Trägergesellschaft die folgenden Dachverbände:

International Society
for Photogrammetry
and Remote Sensing

Deutsche Arbeits-
gemeinschaft für
Mustererkennung e.V.

GeoUnion
Alfred-Wegener-Stiftung

Herausgeber:

Präsident: Prof. Dr.-Ing. Thomas Luhmann, Fachhochschule Oldenburg Ostfriesland Wilhelmshaven, Institut für Angewandte Photogrammetrie und Geoinformatik, Ofener Str. 16, D-26121 Oldenburg, Tel.: +49-441-7708-3172, e-mail: Praesident@dgpf.de, www.dgpf.de
Geschäftsstelle: Dr. Klaus-Ulrich Komp, c/o EFTAS Fernerkundung Technologietransfer GmbH, Ostmarkstraße 92, D-48145 Münster, e-mail: klaus.komp@eftas.com
Published by:
E. Schweizerbart'sche Verlagsbuchhandlung (Nägele u. Obermiller), Johannesstraße 3A, D-70176 Stuttgart. Tel.: 0711/351456-0, Fax: 0711/351456-99, e-mail: mail@schweizerbart.de
Internet: http://www.schweizerbart.de
℗ Gedruckt auf alterungsbeständigem Papier nach ISO 9706-1994

ISSN 1432-8364

Hauptschriftleiter: Prof. Dr.-Ing. habil. Klaus Szangolies, Closewitzer Str. 44, D-07743 Jena. e-mail: Klaus.Szangolies@t-online.de
Schriftleiter: Prof. Dr. rer. nat. Carsten Jürgens, Ruhr-Universität Bochum, Geographisches Institut, Gebäude NA 7/133, D-44780 Bochum, e-mail: carsten.juergens@rub.de und Dr.-Ing. Eckhardt Seyfert, Landesvermessung und Geobasisinformation Brandenburg, Heinrich-Mann-Allee 107, D-14473 Potsdam, e-mail: eckhardt.seyfert@geobasis-bb.de
Erscheinungsweise: 7 Hefte pro Jahrgang.
Bezugspreis im Abonnement: € 122,– pro Jahrgang. Mitglieder der DGPF erhalten die Zeitschrift kostenlos.
Anzeigenverwaltung: Dr. E. Nägele, E. Schweizerbart'sche Verlagsbuchhandlung (Nägele u. Obermiller), Johannesstraße 3A, D-70176 Stuttgart, Tel.: 0711/351456-0; Fax: 0711/351456-99.
e-mail: mail@schweizerbart.de, Internet: http://www.schweizerbart.de
Bernhard Harzer Verlag GmbH, Westmarkstraße 59/59a, D-76227 Karlsruhe, Tel.: 0721/944020, Fax: 0721/944023 0, e-mail: Info@harzer.de, Internet: www.harzer.de
Printed in Germany by Tutte Druckerei GmbH, D-94121 Salzweg bei Passau

PFG – Jahrgang 2006, Heft 4

Inhaltsverzeichnis

Originalbeiträge zum Thema „Urban Remote Sensing“

Berichte

Zusammenfassungen der Originalbeiträge (deutsch und englisch) sind auch verfügbar unter
http://www.dgpf.de/Texten/pfgvor.html

EUROSENSE®

EUROSENSE is probably one of the most prominent commercial remote sensing organizations, existing since 1964. All services offered by EUROSENSE are fully integrated within the company: aerial photography, photo interpretation, processing and interpretation of digital satellite images, production of photogrammetric and topographic maps, airborne laser scanning (LIDAR) for height measurements, GIS/LIS and AM/FM database development and consultancy, city and landscape planning, inventory of forests and natural resources, digital orthophotography, cartography, hydrography, environmental studies and lots of other activities. In all of these disciplines, EUROSENSE offers highly accurate and technologically high-grade solutions.

Due to our expanding activities we are looking for a

PRODUCTION MANAGER PHOTOGRAMMETRY

for our headquarters in Wemmel (Belgium)

Your profile :

- University degree in Photogrammetry or equal knowledge through experience
- Organizational, planning and communication skills
- Good active knowledge of English
- Ability to work in a team

Your responsibilities :

- Leading the Photogrammetric Department
- Coordination between all production sites of the EUROSENSE group
- Intensive travel activities to our production sites in Europe
- Daily management of running projects
- Management of human resources in the Photogrammetric Department
- Support to the Sales Department
- Follow up of developments in Photogrammetry

Our offer :

- Work within a renowned company
- Interesting work in the field of Photogrammetry, GIS and Remote Sensing
- Possibility to further develop your knowledge through training
- Possibility to travel abroad (a.o. to the other EUROSENSE branches in Europe, workshops, symposia, ...)

How to apply :
only by letter or e-mail in English (with CV and photo) to :

EUROSENSE GmbH
Richard-Byrd-Str. 43A
D-50829 Köln
e-mail: hubert.minten@eurosense.com

EUR 1848/2006

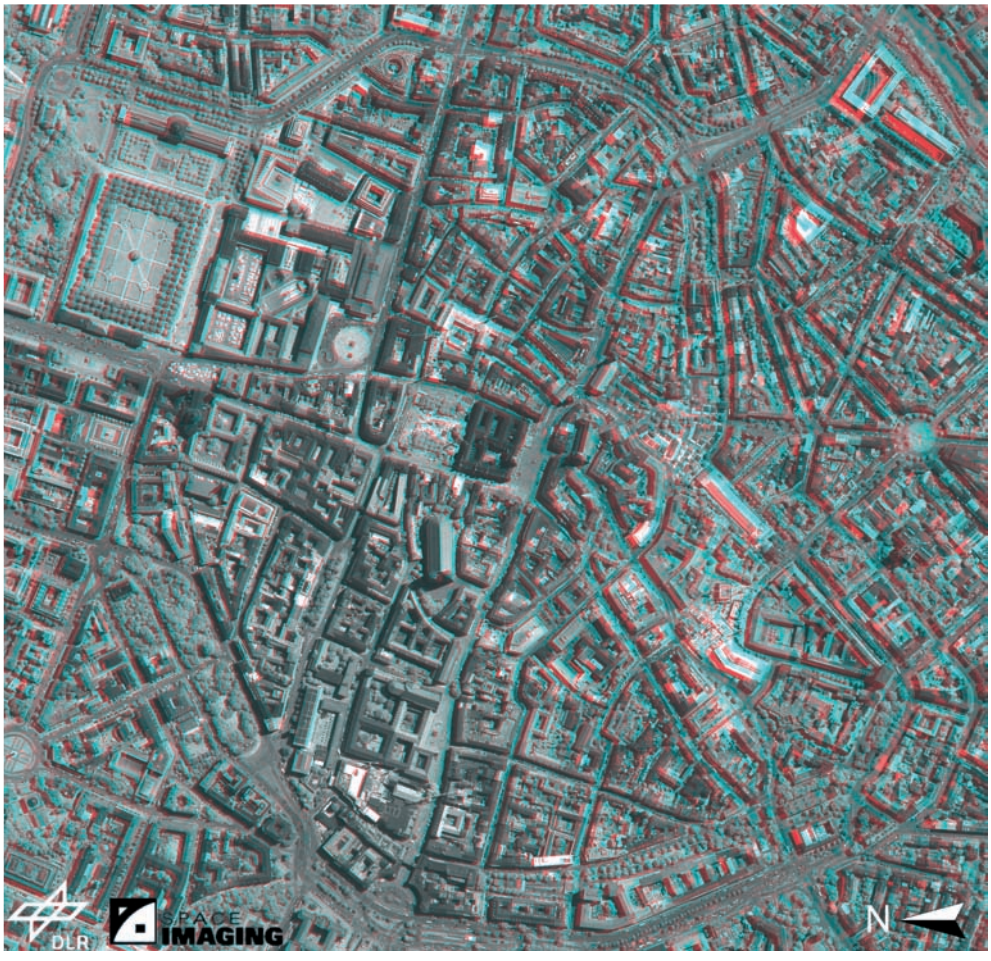

München – City im Anaglyphenbild

Please use the complimentary 3D glasses in this issue for looking at the anaglyph image above. You will have a realistic 3D impression looking through the red glasses with you left eye in a reading distance. The anaglyph imagery shows a subset of the city center of Munich and can be seen as an extension of the several imagery you may have already detected on the front cover. This 3D image has been computed by the German Aerospace Center (DLR) in Oberpfaffenhofen from two IKONOS panchromatic imagery. This imagery has been recorded from different viewing angles providing stereoscopy. DLR operates the European IKONOS satellite downlink receiving station for European Spaceimaging (see also section ''about the front cover'' oder ''Zum Titelbild'', page 356).

VAKAT

Photogrammetrie • Fernerkundung • Geoinformation 4/2006, S. 263–264

Remote Sensing of Urban Areas, Editorial

MATTHIAS S. MOELLER, Tempe, Arizona

Keywords: Remote Sensing, Feature extraction, Metropolitan survey, IKONOS, QuickBird

Since the mid 1990s, the analysis of urban areas by means of digitally remotely sensed image data has become popular amongst the scientific community. Application driven demands have evolved from the field of telecommunications, including the introduction of new radio techniques (UMTS) requiring very accurate and highly detailed geoinformation in both 2D and 3D (compare to RICHTER et al. in this issue), the development of location based services and wireless navigation systems that rely on precise geolocation information, and the improvement of virtual representation and realistic reproduction of real world objects.

This PFG special issue contains seven single publications related to urban remote sensing. Each of them represents excellent state-of-the-art information within their respective fields emphasizing, in an impressive way, that the evolution of urban remote sensing is still ongoing.

Almost every georelated research question – including the monitoring of urban areas – is strongly scale dependent. Scale in terms of remote sensing is inherently linked to resolution:

- spatial resolution,
- temporal resolution,
- spectral resolution and
- radiometric resolution.

Each of these study components has been improved significantly over the last half decade leading to interesting challenges for urban remote sensing research.

Pixel size determines the number and detail of detectable objects. As the number of objects increases and the pixel size decreases, remotely sensed images become more attractive to both scientists and the general public. A recent popular technological development called Google Earth (www.google.earth.com) provides, for the first time, imagery with a very high spatial resolution covering many parts of the Earth.

In fact, the availability of very high resolution optical imagery acquired from space started in 1999 with a series of three satellites all using roughly the same techniques: Ikonos satellite launched in 1999, Quickbird in 2001, and Orbview in 2003. This new kind of space borne imagery enables the clear detection and mapping of man made urban objects such as buildings, streets and even cars. LEITLOFF et al. have successfully used Quickbird imagery for the monitoring of traffic and the detection of vehicles. A differentiation of vegetation is also possible by the use of infrared vs. red spectral reflection highlighting the improvement of increased spectral properties. The limitation to three bands for aerial imagery (either true color or color infrared) is also no longer present. The Ikonos satellite in addition provides stereoscopic capabilities. First results of analyzed Ikonos stereo pairs will be presented in this issue by KRAUSS et al. from the German Center for Aerospace (DLR).

A key advantage of today's space borne satellites is an entire digital processing chain. After digital images are acquired (with high bit rates up to 2^{12}), data can be corrected for system inherited disturbances and geo-processed into products of different spatial position accuracy.

A higher temporal resolution is possible by increasing the number of space borne

1432-8364/06/2006/0263 $ 0.50

sensors, in effect equivalent to increasing the instrument repeat time. A series of small Rapid Eye satellites will soon provide daily images with a spatial resolution of 6.5 m. This will enable near real-time monitoring of temporally active targets, such as areas affected by earthquakes or volcanic eruptions or sites which are constructed on a temporal basis. In this issue, Lang & Tiede demonstrate how remote sensing can effectively be used to help monitor a refugee camp in the Darfur region.

A limiting factor for most of these optical sensor systems is the apparent cloud coverage and the actual illumination. Active micro wave systems such as Synthetic Aperture Radar (SAR) can be used to acquire imagery with more consistent quality and fewer atmospheric limitations. The DLR operated Terra SAR X, the next generation SAR instrument, is scheduled for launch in 2006 and will provide spatial resolutions up to 1 m. At this resolution, radar data will provide a potentially powerful tool for urban mapping applications.

In monitoring urban areas, observations at a moderate scale (1:50.000–1:100.000) are also very important. Schöpfer & Moeller (in this issue), perform LULC classifications for two rapidly growing cities of the southwestern U.S., Phoenix and Las Vegas, using multi-spectral data from the ASTER instrument. Object based image analysis methods appear to provide a more accurate detection and representation of urban objects compared to the common statistical image analysis approaches. Further, a number of adapted algorithms can be used in classifying multiple cities and ultimately to measure the growth of urban areas. In another moderate scale approach, Forsythe and Waters utilized pan-sharpened 15 meter Landsat imagery for the differentiation of urban areas using textural measurements.

Other applications of new remote sensing technology for the urban environment include monitoring polluted air and water using better spectral and spatial resolution sensors, and even developing near real-time crime fighting tools. Future developments will also include unmanned airborne platforms temporary or permanently placed above metropolitan areas, equipped with multiple remote sensing instruments and telecommunication devices. Imagery acquired by these sensors can be used for real time traffic management or the monitoring for security issues like crime prevention at big events with many visitors. It must be emphasized, however, that the benefits, risks, and ethics of such security structures be discussed thoroughly before any systems are established. The notion of 'Big Brother' is controversial for most people, and with good reason. When examining the evolution of urban remote sensing, a number of application driven tasks should be considered. One big issue is the rapid speed of changes in terms of phenology for urban areas; cities contain some of the most dynamic landscapes and environments. The automated mapping of new construction on a cadastral scale level and processing those data to a Geographic Information System (GIS) ready database is an area of intense research. For longer term changes, remotely sensed images can be combined with other data inputs to create urban growth scenarios, one is presented by Herold in this issue. Important urban features, such as streets and vegetated areas (urban parks, yards and trees) change frequently, but can be mapped using the latest high spectral and spatial resolution imagery.

The scientific urban remote sensing community has established specific discussion and meeting platforms. One of this is 100 cities urban environmental monitoring project located at Arizona State University. The biannual URS and Data Fusion over Urban Areas conferences were merged into one conference in 2005 in Tempe, AZ, USA under the umbrella of the ISPRS. This PFG special issue is partly an outcome of this conference and it also gives an outlook to the next joint conferences which will be held April 11–13, 2007 in Paris.

Sources: Google Earth (www.google.earth.com)

Photogrammetrie • Fernerkundung • Geoinformation 4/2006, S. 265–276, 7 figs., 1 tab.

Urban Patterns and Processes: a Remote Sensing Perspective

MARTIN HEROLD, Jena

Keywords: Remote Sensing, urban land cover features, urban pattern, urbanizing of California

Abstract: Remote sensing is a significant, yet under-used, data source for the study of urban phenomena; the key being a freeze-frame view on the spatio-temporal urban patterns, albeit in unprecedented detail. Quantitative descriptors of the characteristics and geometry of urban land cover features (spatial metrics) can describe the structure of urban environments and so allow the detailed exploration of urban patterns and dynamics of change. Several examples are discussed for using remote sensing in the analysis of rapidly urbanizing areas in California. The studies focus on urban land cover and land use, urban morphology and socio-economic characteristics, spatial pattern and growth process characteristics, and empirical observations and urban theory. Future emphasis is needed in the field of urban remote sensing to integrate the different levels of observations that, so far, has widely remain blind to pattern and processes.

Zusammenfassung: *Fernerkundung städtischer Muster und Prozesse*. Das Potential der Fernerkundung zur detaillierten Erfassung städtischer Raumstrukturen und -muster wird nur unzureichend zur Erarbeitung eines besseren theoretischen Verständnisses urbaner Systeme und Wachstumsprozesse angewandt. Diese Studie erarbeitet eine Synthese verschiedener Beispiele aus dem kalifornischen Raum. Auf der Basis von Satellitendaten und Raumstrukturmaßen werden Zusammenhänge zwischen städtischer Landbedeckung und Landnutzung, urbaner Morphologie und sozioökonomischer Eigenschaften, räumlicher Muster und Wachstumsprozessen bzw. empirischer Ergebnisse und urbanen Modellen vorgestellt.

1 Introduction

Understanding urban patterns, dynamic processes, and their relationships is a primary objective in the urban research agenda with a wide consensus among scientists, resource managers, and planners that future development and management of urban areas requires detailed information about ongoing processes. Central questions to be addressed are on how cities are spatially organized, where and when developments happen, and ultimately why and how did urban processes result in specific spatial pattern. Remote sensing, although challenged by the spatial and spectral heterogeneity of urban environments (JENSEN & COWEN 1999, HEROLD et al. 2004) seems to be an appropriate source of urban data to support such studies (DONNAY et al. 2001, HEROLD et al. 2005). Detailed spatial and temporal information of urban morphology, infrastructure, land cover and use patterns, population distributions, and drivers behind urban dynamics are essential to be observed and understood. Urban remote sensing has attempted to provide such information. But, despite proven advantages, remote sensing based urban mapping and monitoring has largely focused on technical aspects of data assembly and physical image classification and thus has widely remained "blind to pattern and processes" (LONGLEY 2002, LO 2004). In fact, the comprehensive spatial and temporal detail provided by remote sensing observations and quantitative measure-

1432-8364/06/2006/0265 $ 3.00

ments of urban structures have only rarely been explored in the context of understanding, representation and modeling spatial process characteristics (Longley & Mesev 2000, Herold et al. 2005).

The aim of this paper is to evolve a better understanding on what is possible to observe using urban remote sensing and how such information can be integrated to improve our theoretical knowledge about urban areas and their dynamics. Different approaches will be presented from California case studies. Their description will be brief and with a minimum of technical detail. But they emphasize different avenues taken to study urban patterns and link them with urban processes.

Concluding discussions will attempt to structure the different indicators and approaches. The discussions will follow a main line of argumentation: urban remote sensing is missing key contributions and potentials to both scientific progress and applications if it remains widely focused on simply observing patterns or detecting changes without asking questions of "How?" and "Why?" related to urban processes.

2 Linking land cover to land use

Analysis on a per-pixel (spectral) basis provides urban land cover or material characterization rather than urban land use information. As in visual air photo interpretation, the most important information for a more detailed mapping of urban land use characteristics is derived from image context, pattern, and texture (Barnsley & Barr 1997). One successful approach for describing spatial land cover heterogeneities in urban areas are spatial metrics (Herold et al. 2002). They can be defined as measurements derived from the digital analysis of thematic-categorical maps exhibiting spatial heterogeneity at a specific scale and resolution. They have been developed for categorical, patch-based representations of landscapes. Patches are defined as homogenous regions for a specific landscape property of interest such as land cover categories "building" or "vegetation" or "urban". In contrast to natural environments, man made structures have been identified as one of the few examples of objects within a landscape that have distinct and crisp bound-

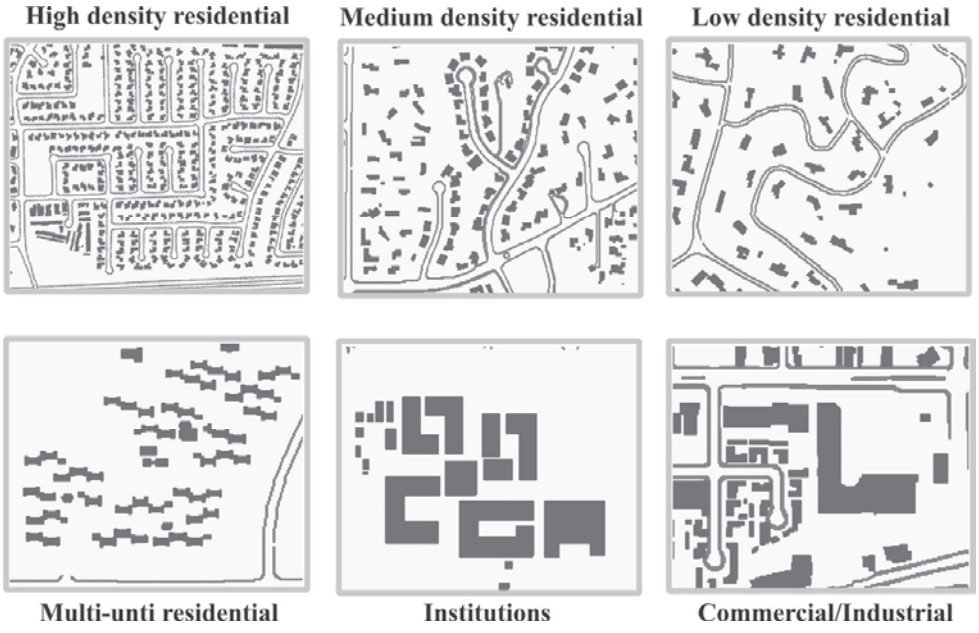

Fig. 1: Examples of spatial configuration for major urban land use categories.

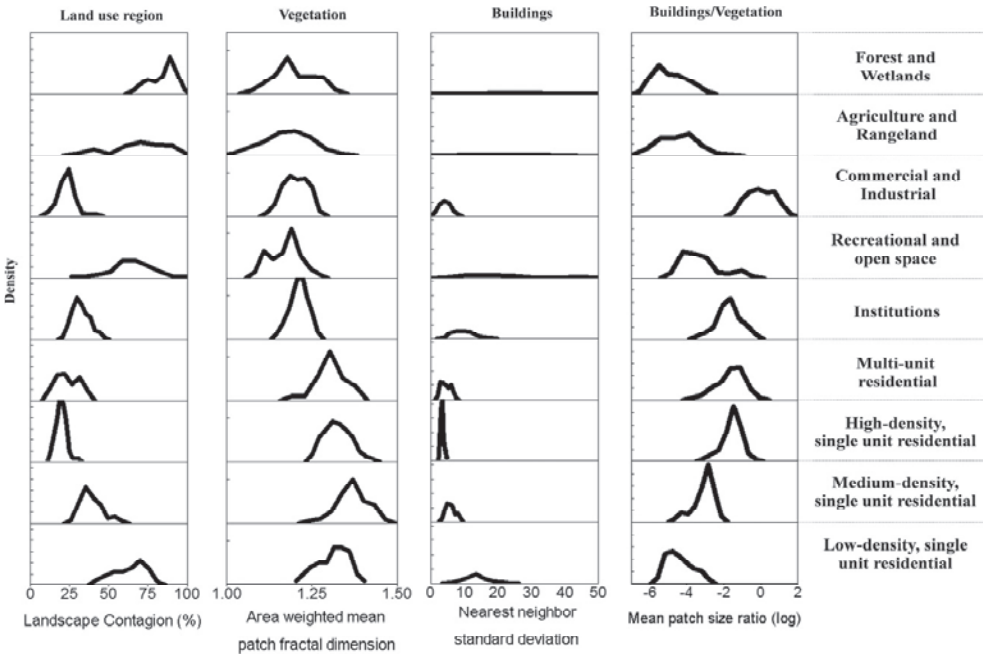

Fig. 2: Density graphs of four spatial metrics for nine types of land uses found within urban areas from IKONOS data. The metrics represent different spatial features noted on top of each graph. The last metric the log ratio of the mean building size and the mean vegetation patch size.

aries. Metrics represent spatial heterogeneity at a specific spatial scale, determined by the spatial resolution, the spatial domain, and the thematic definition of the map categories at a given point in time (Herold et al. 2005). When applied to multi-scale or multi-temporal datasets, spatial metrics can be used to analyze and describe change in the degree of spatial heterogeneity (O'Neill et al. 1988, Herold et al. 2003a).

For studying urban land use patterns the question for spatial metric analysis becomes: What characterizes the spatial land cover heterogeneity of urban areas and how can they describe urban characteristics? For example, the heterogeneity of the class ''buildings'' can be related to the size of structures (small versus large buildings), their shape (compact versus complex and fragmented), and the spatial configuration (regular versus irregular).

Size is measured by the ''mean patch size''; the variation in size by the ''patch size standard deviation'' metric. Shape can be quantified by the ''fractal dimension'' metric, an area/peri-meter ratio that increases as spatial forms get more complex, and by the number of edges or edge length of a patch. Spatial building patterns are described by the ''mean nearest neighbor distance'' and the ''nearest neighbor distance standard deviation'' metrics, with the latter metric increasing as the spatial pattern of buildings gets more irregular. Similar measures can be applied to explore the heterogeneity of the vegetation areas. For more detail on the spatial metrics, please refer to McGarigal et al. (2002).

The spatial metrics for typical Santa Barbara, CA land use region (derived from remote sensing data interpretations, Fig. 1 and 2) are based on a land cover discrimination of the urban environment in the three main classes: buildings, vegetation, and the rest. The contagion is lowest for single unit high density residential, multi-unit residential and commercial/industrial areas (Fig. 2). These land uses represent a most

heterogeneous, fragmented type of urban landscape. High contagion is found for forest, wetlands, agriculture, rangelands and a distinct residential gradient with lower contagion for higher residential density. The fractal dimension of the vegetation areas reflects high fragmentation for all residential land uses, e. g. residential development pattern results in disperse vegetation structures. Although having less area vegetation coverage, urban land uses like commercial or public institutions show more compact vegetated areas. The nearest neighbor standard deviation describes the regularity of the building pattern. The values for forest, wetlands, agriculture, recreational and open spaces are indistinct as they have no inherent or characteristic built up pattern. High density single unit residential areas have the most distinct regular building configuration reflecting the typical American block pattern. Commercial and industrial, multi-unit residential and medium density single unit residential also indicate a high degree of regularity. The building configurations in low density residential area are significantly more detached resulting in more irregularity in the spatial pattern.

This thematic exploration of commonly applied spatial metrics emphasizes that the

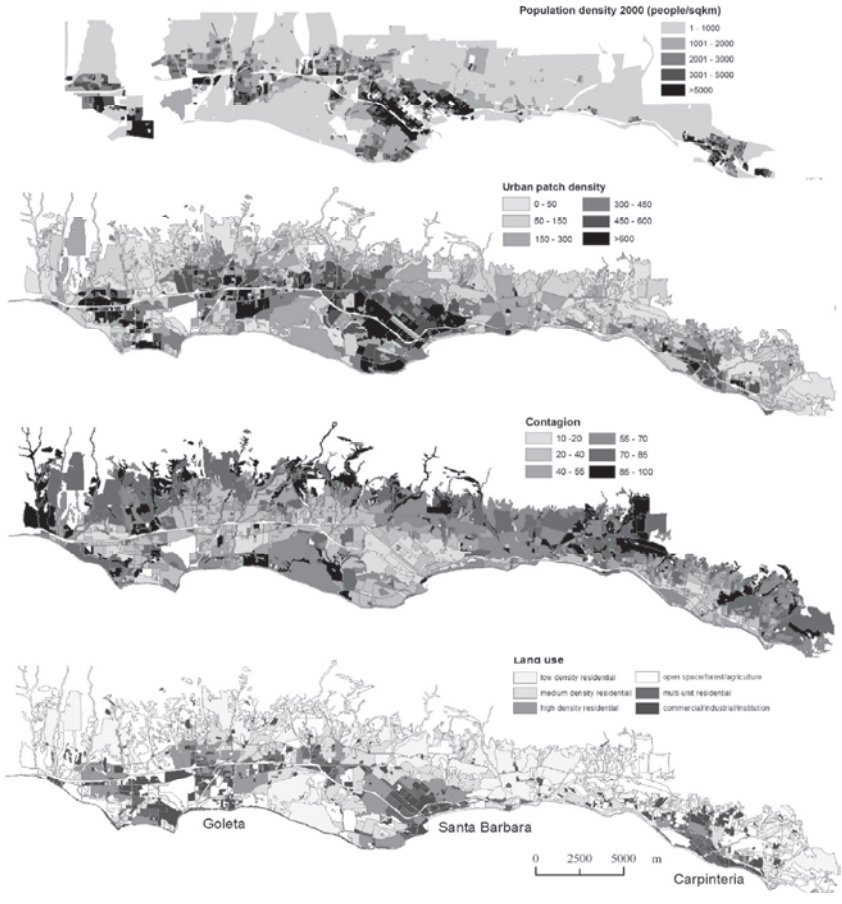

Fig. 3: Spatial urban characteristics of two spatial metrics and major land uses in the Santa Barbara South Coast urban area derived from IKONOS data and CENSUS population density. The metrics describe the spatial heterogeneity for each land use region (see HEROLD et al. 2003a). The population density and land use map highlights the three urban core areas in the region of Santa Barbara, Goleta, and Carpinteria.

metrics itself are fairly simple statistical measurements. They require comprehensive interpretation to be used in describing intra-urban environments based on their land cover characteristics. Ultimately it would be useful to identify or develop a set of ''urban metrics'' transferable and comparable among different urban areas and to adjust the skew and range of the values to apply further analysis method, e. g. urban land use classification based on the metrics. An example of an aggregated metric is the mean patch size ratio in Fig. 2. This metric describes the ratio of mean building size versus the mean size of the vegetation patches. Except for commercial and industrial uses, the vegetation patches are larger than the buildings and represent the spatial characteristics of the individual land uses.

In correspondence to Fig. 2, intra-urban patterns of spatial metric distributions are presented in Fig. 3. The building patch density shows an obvious correspondence with the population density. High values of this metric reflect high and medium density residential land uses with high numbers of individual buildings per area unit. The contagion is lowest for single unit high-density residential, multi-unit residential and commercial/industrial areas. In fact, the contagion metric follows a concentric pattern with heterogeneous urban environments near the central urban (low contagion) and a gradient of increasing contagion towards the peripheral rural areas. This goes along with a distinct residential gradient of lower contagion for higher residential density (see Fig. 1 and 2). In a related study, Herold et al. (2003a) show that metric and texture measurements can be used to accurately classify different land use types from this IKONOS dataset.

3 Linking urban form to population density

The previous section highlighted the relationship between urban land cover pattern and land use. Describing discrete land use categories, however, does not take full advantage of the spatial metrics that quantify urban form on a continuous scale. Residential land use types are intrinsically related to demographic characteristics. Spatial patterns shown in Fig. 3 suggest an obvious relationship between spatial metrics (describing urban form) and population density. Based on US 2000 Census block level data and IKONOS spatial metric measurements, Fig. 4 highlights the relationship between the metrics and population densities.

A positive correlation exists between population density and the amount area covered by buildings patches. This seems intuitive since a larger area covered building usually coincides with higher population density for each census block. A negative relationship is shown for the Contagion. The more homogenous the urban environ-

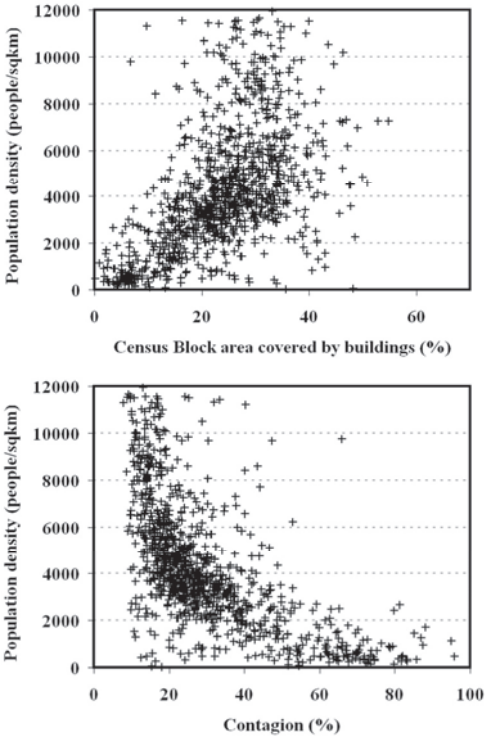

Fig. 4: Relationship between two spatial metrics and population density for n = 1092 Census 2000 block with residential land use in the Santa Barbara South Coast. The spatial metrics describe the land cover class buildings and have been derived from classified IKONOS data for each Census block.

ment is, the lower the population density. High-density residential areas represent fragmented urban landscapes with the heterogeneity decreasing for lower-density residential areas (Fig. 2).

Thus, building area proportions and the spatial heterogeneity are linked to the population density. The graphs in Fig. 4, however, show a fair amount of scattering indicating problems for direct estimation of population densities from remote sensing derived spatial metrics. The variance in the relationship increases for higher population densities, thus the metrics would better predict low population densities are less sensitive to changes in areas for high population densities. This is further emphasized by the non-linear correlation between Contagion and population density. Low Contagion values ($\sim$ 20 %) do not allow for a clear distinction between areas with 6000–12000 people/sqkm. High-resolution remote sensing and spatial metrics can indeed help to estimate population density, but a quantitative derivation may not be able without considering additional data or specific spatial methods (Liu et al. 2006). A determinant relationship was not expected since the spatial urban patterns are diverse and not only driven by the number of people living there. However, a distinct link exists and a changing physical structure of an urban residential landscape would be clear indicator of ongoing demographic processes.

4 Linking spatial patterns and processes

From an urban process perspective it is important to study spatial urban land cover and land use characteristics as outcome of specific development characteristics. Existing and measurable urban pattern result from growth processes that, controlled and constrained by spatial growth factors, created the urban landscape in the first place. It should be possible to link the current urban landscape configurations to spatial distribution of the underlying growth factors. Such an investigation can be attempted through a combination of high-resolution remote sensing land cover mapping products and spatial metrics as quantitative descriptors of urban form. The method to link the remote sensing/spatial metric measurements and the spatial growth factors is provided by Geographically Weighted Regression (GWR) analysis. The method of Geographically Weighted Regression (GWR) has been developed in response to the need for locally specific spatial regression models (Fortheringham et al. 2002). GWR addresses the issue of spatial non-stationarity directly and allows regression relationships to vary over space, e. g. the predictors and regression parameters might vary for urban versus rural areas. In a case study, GWR was applied to explore the relationship between growth factors (independent predictor variables) and the spatial metrics (dependent variables). The study was conducted for residential areas in the Santa Barbara urban area (see Fig. 3). The three urban growth factors identified to have a major influence in the urban evolution of the area are topographic slope, distance to highways, and distance to the central urban core. Basically, the GWR analysis emphasizes how well the spatial urban structure as cumulative outcome of urban development processes (described by the metrics) is explained by spatial distribution of urban growth factors. The application of GWR is essential to assess the relationship of growth factors versus metrics on a more local, intra-urban level (e. g. different city districts) rather than as a global model for the whole urban area.

Tab. 1 shows the GWR regression parameters for the multivariate prediction of five spatial metrics from the spatial growth factors. The local sample sizes (bandwidth) are in the order of 38 to 88 points, which corresponds to 8–20 % of the total number 484 observations. The value *Global R-sq* or global coefficient of determination represents the R-squared of the global regression model including all observations; the *GWR R-s* describes the overall strengths of spatially weighted regression. The significance of each predictor in the global regression analysis is reflected in the t-values (*T-slope,*

Tab. 1: Results of the GWR analysis for multivariate regression models considering three growth factors (distance to urban core, distance to highways, and slope) versus five spatial metrics. One metric represent the heterogeneity whole landscape (land use region, Contagion), two metrics describe characteristics of the land cover class buildings (PL = area percentage of buildings, PD = patch density), two the class vegetation (PD = patch density, AR_S = Standard deviation of vegetation patch sizes).

	Landscape	***Buildings***		***Vegetation***	
	CONTAG	PL	PD	PD	AR_S
Local sample	70	94	88	88	38
Global R-sq	0.55	0.30	0.34	0.30	0.34
T-slope	7.12	−6.39	−6.62	−5.94	0.13
T-core	7.91	−2.06	−3.8	−4.44	7.89
T-highway	8.05	−4.27	−4.02	−3.21	7.33
GWR R-sq	0.73	0.47	0.51	0.47	0.68

T-core, T-highway). If the absolute t-value is above 1.96 the predictor can be considered significant and useful for the regression model. T-values below 0 indicate a negative linear relationship between the growth factor and the spatial metric. Except for one regression model were one growth factor is not significant (the factor slope in predicting the patch area standard deviation – AREA_SD).

Comparing the Global CoD and GWR CoD indicate the improvements in the regression models using geographically weighted regression. This result is not surprising since the local regression models better adjust to specific local characteristics and relationships than the global approach. The overall GWR CoD for these metrics are pretty high and range from 46 to 72% of described variance (Tab. 1); hence the growth factors are able to predict most of the spatial urban patterns of the area as emerging characteristics of historical urban growth processes. The study has further shown that areas with highly predictable urban patterns represent historically grown or planned urban characteristics that are representative for the major urban development processes in this region. The internal urban system is in balance or in some stage of desired development. The areas with lower predictability reflect an internal gradient in spatial urban structure to more unplanned urban or rural development patterns. They are under particular development pressure and it can be expected that the urban structures will gradually become a part of the balanced existing system if urban expansion continues. In this context, these areas are also of major importance for urban planning. Important regional planning actions in this region like protection of agricultural land, the establishment of an urban growth boundary, or fostering of highly desired land use types (affordable housing), can be expected to have a main impact in these regions where internal urban evolution seems not completed. These conclusions show that the combined use of remote sensing, spatial metrics and GWR improves our understanding of the internal structure of cities and provide further empirical evidence on the relationship between urban form and growth processes (Geoghegan et al. 1997).

5 Linking empirical observations and urban theory

Of particular potential is the combined application of multitemporal remote sensing with spatial metrics. Monitoring and analysis using this technique can provide a unique source of information on how various spatial characteristics of cities change over time. Temporal change 'signatures' of metrics can reflect specific dynamic change processes effecting spatial urban structure. Several studies have shown that the empirical observation of temporal urban growth signatures with spatial metrics contributes to a better understanding and representation of urban dynamics. It offers a new perspective into urban change theory and has the potential to contribute to urban growth and land use change modeling (Herold et al. 2003b, 2005).

However, one important step in such empirical analysis is to synthesize the observations into a more general theoretical under-

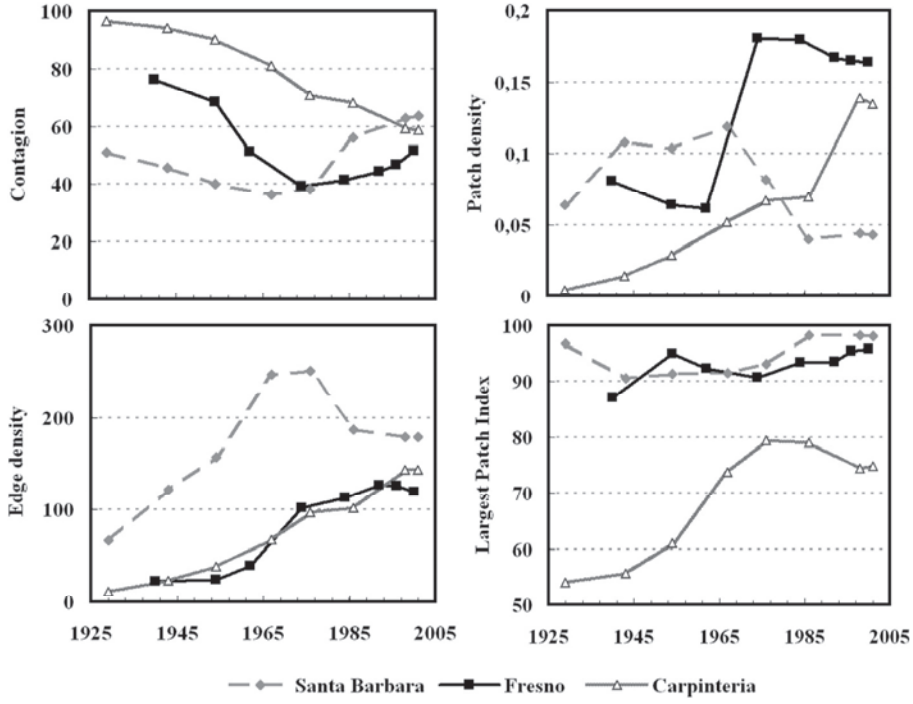

Fig. 5: Temporal growth signatures of three different cities of California: Santa Barbara, Fresno, Carpinteria, derived from remote sensing observations using spatial metrics.

standing of urban dynamics (Dietzel et al. 2005). Remote sensing observations usually follow an inductive, bottom up perspective: to provide empirical observations of actual spatial structures in great spatial and temporal detail and linking their changes over time to specific processes at work (from structure to process). The rather traditional perspective followed by the urban modeling and spatial urban theory community is deductive or top-down. Their focus is on deriving urban structures as the spatial outcomes of pre-specified processes of urban change (from process to structure). Linking both perspectives is a central task both deductive and inductive approaches could benefit by being used in combination. This avenue has only recently been explored with a combination of remote sensing, spatial analysis and spatial metrics to establish the link between empirical observations and urban theory (Dietzel et al. 2005, Herold et al. 2005).

Fig. 5 compares temporal signatures of metrics mapped for different cities in California. These cities vary in size (50.000–1.000.000 inhabitants) and the regional growth characteristics have been quite different (Central Valley versus South Coast). Santa Barbara showed major growth during the 50ies and 60ies of the last century, Fresno in the 1970–90ies, and Carpinteria is just currently developing as subsidiary center near Santa Barbara. The temporal signatures (Fig. 5) emphasize that similar growth pattern exists for all of this three different areas considering that the timing and the absolute values are shifted due to specific local growth characteristics. Dietzel et al. (2005) have attributed these observations into phases of Coalescence and Diffusion that is characteristics for several investigated cities (Fig. 6). Urbanization, as it is reflected by the contagion metric, results in a transformation from homogenous non-urban to a heterogeneous mix of urban and

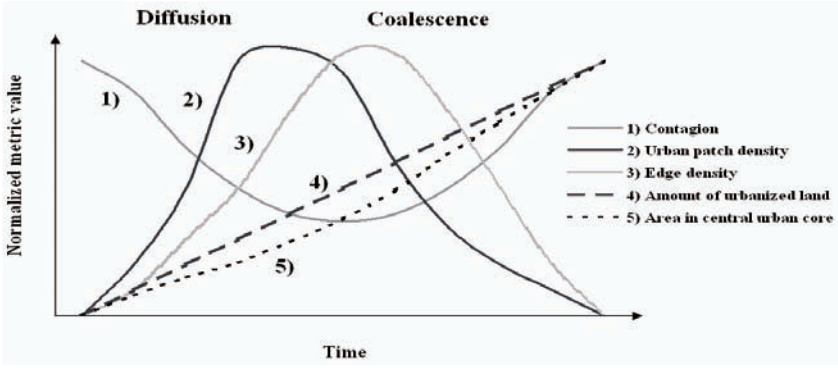

Fig. 6: Theoretical spatial metric signatures for a full cycle of urbanization for uniform isotropic growth at a specific scale (after DIETZEL et al. 2005).

non-urban. At some time in the progression of development there is a transition to a homogenous urban landscape. The other spatial metrics capture spatio-temporal phases. The diffusion phase is characterized by a large number of new urban areas in the nascent urban system comprised by the original core and peripheral development centers. The patch density peaks and amount of urban land in the largest patch is the lowest at this point. The low point in the contagion metric marks the transition from diffusion to coalescence. Coalescence starts as urban areas spatially aggregate. This is reflected by a decrease in the patch density and an increase in the edge density metrics. The terminal point of coalescence is complete urban build out when all, or nearly all, of the available land has been urbanized. This "final" stage can be seen as an initial urban core for further urbanization at a less detailed scale. Similar growth pattern, hence with different temporal dimension, can be observed on these different scales (DIETZEL et al. 2005).

In Fig. 5, the phase of diffusion corresponds to 1940–1960ies for Santa Barbara and 1960–70ies for Fresno. While Santa Barbara and Fresno are currently in the process of coalescence, Carpinteria is at the end of the urban diffusion process. However, the link between empirical measurements (Fig. 5) and the theoretical concept (Fig. 6) is, for now, only of a qualitative nature. A quantitative comparison reveals differences among metric signatures, in amplitude, duration, location and extent. These differences were anticipated since urban growth is not constant over time and the different regions. Furthermore, the spatial configuration of these areas are not uniform nor are the initial conditions for each developing city system identical with regard to the starting point for empirical observations. Local urban growth factors such as topography, transportation infrastructure, growth barriers or planning efforts affect the spatial growth pattern. However, the local variations yield important information about the ongoing processes. They can be interpreted as "distortions" i. e. amplifications, lagging, or damping the metric signatures. As in other urban models, the distortions can be thought of as the residual between the growth pattern under uniform, isotropic spatial and temporal conditions and the observed existing urbanization dynamics. Considering that understanding of patterns and processes through urban modeling is largely limited by the available data (LONGLEY & MESEV 2000), these examples show that time-series analysis of remotely sensed imagery using spatial metrics can provide an addition to urban theory. In fact, spatial metrics are one key to build a bridge between remote sensing analysis, understandings of the spatial evolution of urban areas, and the analytical modeling of urban systems.

6 Discussions and Conclusion

The examples have emphasized the variety of indicators describing urban characteristics and changes available from earth observations. They include the mapping and monitoring of spatial, spectral, and temporal urban patterns in both the physical built up environment and vegetation. In general, remote sensing adds an inductive, bottom up perspective to understanding urban patterns and processes. It incorporates "real world" remote sensing-based measurements of urban form and dynamics rather than generalized consideration, as are commonly used in traditional spatial theories and models of urban spatial structure and change. Certainly, the patterns obtained from remote sensing data may represent an aggregate outcome of many different processes at work. Often it is difficult to disentangle the effects of the different variables and trends of interest. Thus, the remote pattern measurements have to be clearly structured to the operational scale of urban change processes. A conceptual attempt summarizing the case studies presented in this paper is shown in Fig. 7. The most elementary *pixel scale* reflects changes in urban material characteristics, e. g. aging processes reflected in spectral characteristics. The *land cover* level reflects dynamics in common urban land cover objects such us building constructions, expansion of roads, decreasing urban vegetation patches or similar changes. If land cover changes are aggregated to larger areas, they can reflect or lead to changes in urban *land use*. Examples are infill development and redevelopment, or evolving brownfields.

Urban land use dynamics are intrinsically linked with socio-economic, political, or demographic drivers (Knox 1994) and thus provide a useful platform for studying urban dynamic processes. On a coarser level, *urban areas* reflect an agglomeration of urban land uses usually arranged in distinct intra-urban patterns. Growing urban areas reflect spatio-temporal patterns of expanding urban land uses into rural areas. Urban growth of one particular city is usually directly link with changes in other urban agglomeration, e. g. gravity relationships or regional polarization within a system of cities. Linking remote sensing pattern measurements across scales strongly depends on the process of interest and remains a critical research question. But, earth observation may have the potential to establish such relationships. For example, a new urban development driven by population growth will basically be observed on all relevant scales. To conclude, the main argument of this paper is that urban remote sensing can add a significant new perspective to understand urban patterns and processes. Such potential has been widely neglected in the past. The remote sensing technology has proven oper-

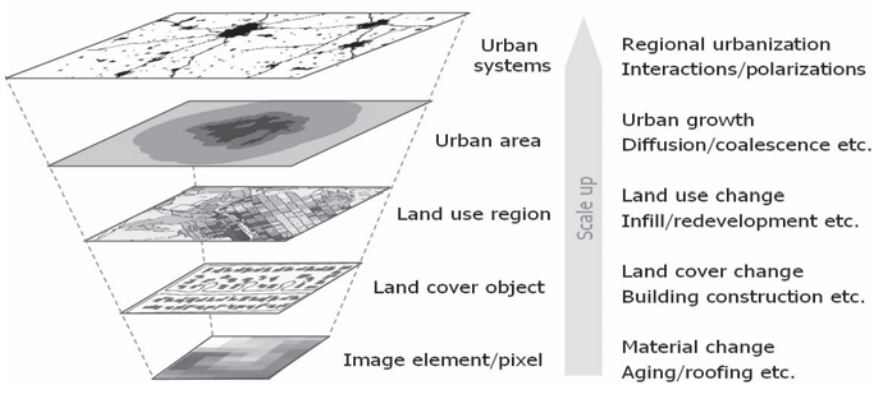

Fig. 7: Observing multi-scale dynamics for mapping and modeling of urban growth processes with remote sensing.

ational capabilities and many studies have provided mapping and monitoring products but rarely have asked the question of land change process behind observed patterns and dynamics. Remote sensing may provide the answers to questions asked in the early days of urban geography. Better theoretical understanding on the internal structures of cities, the link between urban form and socio-economic and demographic characteristics, and the spatio-temporal behavior of cities and urban systems are of particular importance for progress in the field urban geography. Remote sensing is not expected to address all questions but both traditional urban geographic research could benefit by being used in combination, with the traditional perspective helping to narrow down the possibilities suggested by the detailed analysis of urban form and their changes. Better process understanding and improved concepts will ultimately help in solving contemporary urban problems through providing information needed for sustained urban planning and management.

Acknowledgements

The author would like to acknowledge Keith C. Clarke, Helen Couclelis, Jeff Hemphill, Xiaohang Liu and Noah Goldstein, at the University of California Santa Barbara for their support of this research.

References

Barnsley, M.J. & Barr, S.L., 1997: A graph based structural pattern recognition system to infer urban land-use from fine spatial resolution land-cover data. – Computers, Environment and Urban Systems **21** (3/4): 209–225.

Dietzel, C., Herold, M., Hemphill, J.J. & Clarke, K.C., 2005: Spatio-temporal dynamics in California's Central Valley: Empirical links urban theory. – International Journal of Geographic Information Sciences **19** (2): 175–195.

Donnay, J.P., Barnsley, M.J. & Longley, P.A., 2001: Remote sensing and urban analysis. – In: Donnay, J.P., Barnsley, M.J. & Longley, P.A. (eds.): Remote sensing and urban analysis. – pp. 3–18, Taylor and Francis, London and New York.

Fotheringham, A.S., Brunsdon, C. & Charlton, M.E., 2002: Geographically Weighted Regression: The Analysis of Spatially Varying Relationships. – Wiley, Chichester.

Geoghegan, J., Wainger, L.A. & Bockstael, N.E., 1997: Spatial landscape indices in a hedonic framework: an ecological economics analysis using GIS. – Ecological Economics **23** (3): 251–264.

Herold, M., Clarke, K.C. & Scepan, J., 2002: Remote sensing and landscape metrics to describe structures and changes in urban landuse. – Environment and Planning (A) **34:** 1443–1458.

Herold, M., Liu, X. & Clarke, K.C., 2003a: Spatial metrics and image texture for mapping urban land use. – Photogrammetric, Engineering and Remote Sensing **69** (8): 991–1001.

Herold, M., Goldstein, N.C. & Clarke, K.C., 2003b: The spatiotemporal form of urban growth: measurement, analysis and modeling. – Remote Sensing of Environment **86:** 286–302.

Herold, M., Roberts, D., Gardner, M. & Dennison, P., 2004: Spectrometry for urban area remote sensing – Development and analysis of a spectral library from 350 to 2400 nm. – Remote Sensing of Environment **91** (3-4): 304–319.

Herold, M., Couclelis, H. & Clarke, K.C., 2005: The role of spatial metrics in the analysis and modeling of land use change. – Computers, Environment and Urban Systems **29** (4): 369–399.

Jensen, J.R. & Cowen, D.C., 1999: Remote sensing of urban/suburban infrastructure and socio-economic attributes. – Photogrammetric Engineering and Remote Sensing **65:** 611–622.

Knox, P.L., 1994: Urbanization: Introduction to urban Geography. – 436 p., Prentice Hall, New Jersey.

Liu, X., Clarke, K.-C. & Herold, M., 2006: Population density and image texture: a comparison study. – Photogrammetric Engineering and Remote Sensing **72** (2): 187–196.

Lo, C.P., 2004: Testing Urban Theories Using Remote Sensing. – GI Science and Remote Sensing **41** (2): 95–115.

Longley, P.A., 2002: Geographical information systems: Will developments in urban remote sensing and GIS lead to ''better' urban geography? – Progress in Human Geography **26:** 231–239.

Longley, P.A. & Mesev, V., 2000: On the measurement of urban form. – Environment and Planning (A) **32:** 473–488.

McGarigal, K., Cushman, S.A., Neel, M.C. & Ene, E., 2002: FRAGSTATS: Spatial Pattern

Analysis Program for Categorical Maps. URL: www.umass.edu/landeco/research/fragstats/fragstats.html.

O'Neill, R.V., Krummel, J.R., Gardner, R.H., Sugihara, G., Jackson, B., Deangelis, D.L., Milne, B.T., Turner, M.G., Zygmunt, B., Christensen, S.W., Dale, V.H. & Graham, R.L., 1988: Indices of landscape pattern. – Landscape Ecology **1**: 153–162.

Anschrift des Verfassers:

Dr. Martin Herold
Friedrich-Schiller-Universität Jena
Institut für Geographie
Löbdergraben 32, D-07743 Jena
e-mail: m.h@uni-jena.de

Manuskript eingereicht: März 2006
Angenommen: April 2006

Photogrammetrie • Fernerkundung • Geoinformation 4/2006, S. 277–286, 4 figs., 2 tabs.

Comparing Metropolitan Areas – A Transferable Object-Based Image Analysis Approach

ELISABETH SCHÖPFER, Salzburg & MATTHIAS S. MOELLER, Tempe, Arizona

Keywords: ASTER, land cover, land use, Las Vegas, object-based, Phoenix, remote sensing, transferable, urban

Abstract: Existing methods for the detection and mapping of land use/land cover (LULC) for urban areas are mainly based on a Maximum Likelihood statistical image analysis approach. These methods all have one thing in common: the user has to define and outline training samples, which are drawn in an interactive process manually by on screen digitizing. Spectral characteristics of these training samples will then be used in the classification process to define the spectral ranges of the desired classes. This process cannot be automated because the training samples have to be defined for each classification. This paper presents a reproducible classification algorithm based on image objects without any additional search for training samples. In the first step ASTER imagery of the metropolitan area Phoenix has been used for the development of the algorithm. In the second step the classification scheme was applied to another ASTER image data set of Las Vegas, located in a similar natural environment. The resulting classification on a medium scale level shows a reliable accuracy of 83.33 %.

Zusammenfassung: *Metropolregionen im Vergleich – ein übertragbarer objekt-basierter Ansatz der Bildanalyse*. Bestehende Methoden für die Erfassung und Kartierung von Landnutzung/Landbedeckung (LULC) für urbane Gebiete basieren hauptsächlich auf statistischen Bildanalysemethoden der größten Zugehörigkeitswahrscheinlichkeit (engl. *maximum likelihood*). Diese Methoden haben eine Sache gemeinsam: der Interpret muss zunächst Trainingsgebiete definieren, welche interaktiv vom Bildschirm abdigitalisiert werden. Die spektralen Eigenschaften dieser Trainingsgebiete werden dann im Klassifikationsprozess verwendet, um die spektrale Ausprägung der jeweiligen Klassen zu definieren, ein Prozess, der nicht automatisiert werden kann. In dieser Publikation wird ein reproduzierbarer Klassifikationsalgorithmus vorgestellt, der einzig auf der Analyse von Bildobjekten basiert, ohne die zusätzliche Definition von Trainingsgebieten. Zunächst wurde eine ASTER Szene der Region Phoenix für die Entwicklung dieses Algorithmus' verwendet. Im zweiten Schritt wurde das Klassifikationsschema auf eine andere ASTER Szene der Region Las Vegas übertragen, welche in einem ähnlichen Naturraum liegt. Die resultierende Klassifikation auf einer mittleren Maßstabsebene zeigt eine hohe Genauigkeit von 83.33 %.

1 Introduction

1.1 *Motivation*

Urban metropolitan areas are the regions on Earth that exhibit the most rapid changes and the fastest growth. Rapid development can be typically observed in areas where the surrounding space is not limited and land is cheap for purchase. The two metropolitan regions of Las Vegas, NV and Phoenix, AZ belong to these typical boom areas in the South West of the United States. The dynamic development and rapid expansion of these areas demands a detailed mapping of the newly constructed sites at least once a year.

1432-8364/06/2006/0277 $ 2.50

Both Las Vegas and Phoenix are included in the 100 cities project, which focuses on the intense and frequent monitoring of major cities worldwide. Remote sensing has become the key role in this project and provides a huge database with permanently updated imagery (http://elwood.la.asu.edu/grsl/UEM/). The 100 cities project is embedded in the framework of the Urban Environmental Monitoring project (UEM) located at Arizona State University. In this project ASTER (Advanced Spaceborne Thermal Emission and Reflection Radiometer) image data has been selected as a standard image because of its high spectral resolution in the mid to short wave infrared spectrum and the relatively high spatial resolution in the visible green, red and near infrared.

Based on recently acquired ASTER image data a robust and transferable algorithm for an automated detection and analysis of urban features, that is valid for these two natural regions (deserts), was developed. Major task was to establish a classification algorithm for one particular metropolitan urban area and to apply it to an ASTER image of a different urban area. This test was necessary to ensure that the newly developed algorithm can be applied – only with minor changes – to a different urban area located in a similar natural environment.

1.2 *Land use/land cover analysis of remotely sensed imagery*

This study applies an object-based image classification approach (Baatz & Schaepe 2000, Benz et al. 2004, Blaschke et al. 2000), since this method has been successfully applied on image data of different sensor types. The classification results for the Phoenix area lead to an increased accuracy compared to other methods based on a statistical spectral pixel by pixel analysis (Moeller 2005). Disturbed image recognition quality, especially the 'salt and pepper effect' known from common statistical approaches, is absent in the object-based classification result (Blaschke & Strobl 2001). One important task of this study is to apply the newly developed classification rules to satellite data from the same sensor acquired for another region with a similar natural environment. In this study, the Las Vegas area has been selected as the test site. The date of image acquisition for both sites has been chosen carefully to ensure that nature appears with a more or less identical phenology.

2 Study area and data sets used

2.1 *Study area*

The Las Vegas and the Phoenix metropolitan area are located in the western part of the U.S. (see Fig. 1). Both metropolitan areas belong to very similar natural environments, i. e. the desert. Both regions show more or less the same meteorological values, which are typical for an area with a minimum annual precipitation. Phoenix is embedded in the Sonoran desert, characterized by an annually unequally distributed and relatively low precipitation of 196 mm/year. Las Vegas is an even dryer place and in close proximity to the hottest place in the U.S., the Death Valley. It receives an annual precipitation of 114 mm/year (for the 30 year period from 1971–2000; NOAA 2005). The mean elevation of Phoenix is about 300 m above sea level and it is surrounded by some higher mountains with altitudes up to 700 m. Las Vegas is also located in a valley with an average elevation of 600 m above sea level and surrounded by high mountains with elevations up to 3500 m.

Natural land in the surroundings of both metropolitan areas is available almost without any limits making it comparatively cheap for real estate purposes. Developing of these new housing sites is easy and can be performed with minor costs. The only limiting and expensive factor so far is water supply. Water has to be directed over large distances to the Phoenix area. For the monitoring of the growth of these areas remotely sensed imagery are most suitable. This imagery is available since the early 1970s and has been used successfully for the monitoring the growth of Phoenix (Moel-

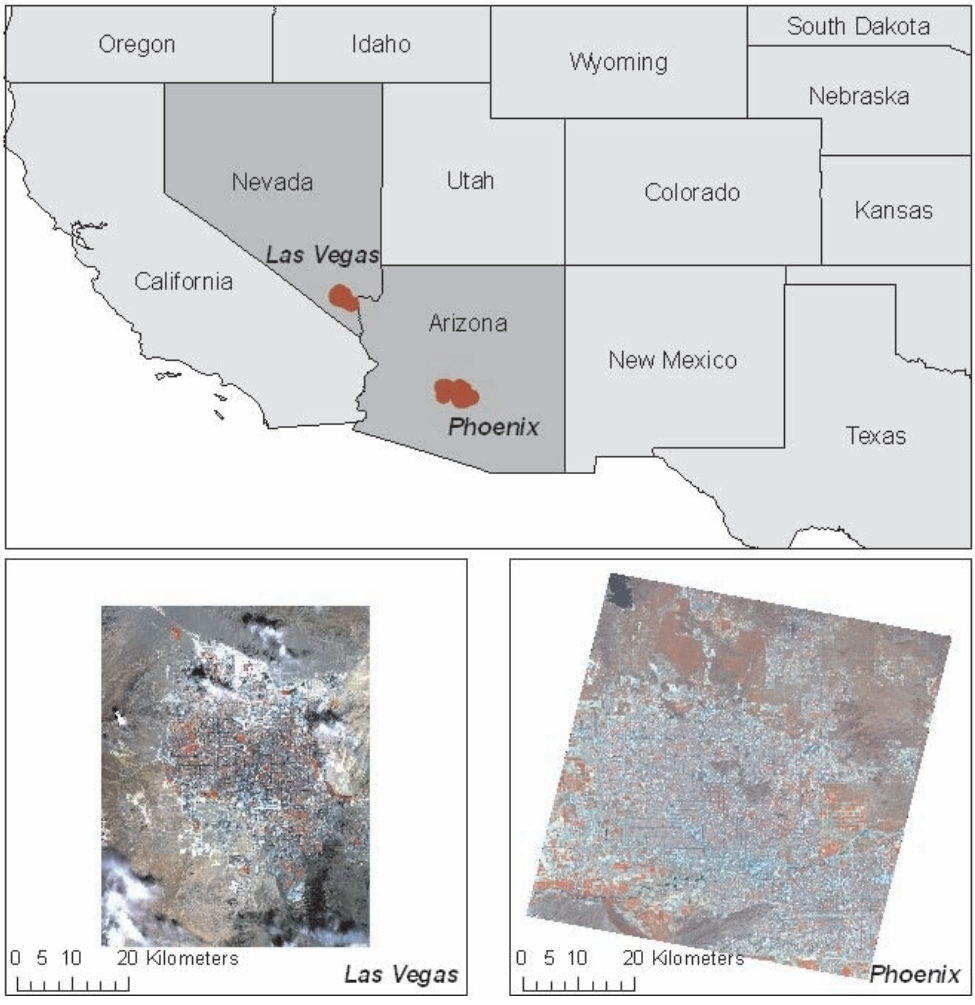

Fig. 1: Location of the two test sites in the Western States of the USA. The insets show the data used for Las Vegas and Phoenix.

LER 2005). The resulting time series of classified imagery can be analyzed in a spatial-temporal way for the detection of special growth pattern.

2.2 *Data*

The Landsat sensor typically provides remotely sensed imagery with a medium application scale (e. g. 1 : 50.000). Landsat has been proofed successfully for several Nation-wide studies (e. g. NLCD for USA, Corine for Europe). Since Landsat ETM (Enhanced Thematic Mapper) image data is affected by technical failure (the scan line corrector is permanently off), ASTER is the only operational sensor system for image data acquisition on a medium application scale. ASTER provides data with a medium spatial resolution in three wavelength regions, useful for investigating a wide range of urban processes. The high spatial resolution of ASTER in the visible to near infrared bands (15 m/pixel) permits detailed land cover classification of urban and peri-urban regions. Additionally it provides a

validated sensor calibration and image processing for worldwide locations. This calibration of image data is crucial since the extension and adoption of the newly developed algorithm to metropolitan areas all over the world is a major task. The long-term perspective of the 100 cities project is to map urban areas worldwide and to provide a reliable image data source as well as a consistent classification method.

For this study ASTER satellite data recorded April, 1st, 2005 for the Phoenix site and recorded May, 1st, 2005 for the Las Vegas region has been used. For Las Vegas two scenes had to be mosaiced since the area was covered by two adjacent images. Las Vegas comprises an area of approximately 48 km × 60 km, whereas Phoenix spans 60 km × 60 km (see Fig. 1). The data were preprocessed to a level 1b product. Due to an undisturbed atmosphere without any meteorological influences such as fog and clouds and in addition a very low absolute air humidity, an atmospheric correction was not found necessary.

3 Methods

3.1 *Segmentation*

Segmentation of images is an important research area and vast number of segmentation algorithms has been proposed over the past three decades (Freixenet et al. 2002). Recently, algorithms have been developed or were adopted for segmentation of remotely sensed imagery (Meinel & Neubert 2004). Remote sensing applications increasingly use image segmentations as a first step to derive image objects and subsequently process these relatively homogeneous objects rather than single pixels. These objects contain spatial and geometrical information and additionally provide relationships information between objects. These interrelations can improve the classification result in a way that is difficult to achieve using the pixel-based approaches. The object-based approach can be used for a semi-automated analysis for the majority of remote sensing applications. This study will demonstrate that classification schemes based on image objects are transferable between different scenes (Blaschke & Strobl 2001, Flanders et al. 2003, Benz et al. 2004, Schöpfer et al. 2005).

The segmentation algorithm used in this study is a region-based, local mutual best-fitting approach (Baatz & Schäpe 2000). This bottom up region merging technique is implemented in the commercial software eCognition (Benz et al. 2004). Initially each pixel forms one object or region. At each step a pair of image objects is merged into one larger object. Throughout this pairwise clustering process, the underlying optimization procedure minimizes the weighted heterogeneity nh of the resulting image objects, where n is the size of a segment and h an arbitrary definition of heterogeneity (Baatz & Schäpe 2000).

For the study of the metropolitan areas Phoenix and Las Vegas a sophisticated cognition network (Binnig et al. 2002) has been established to generate the class hierarchy (see Fig. 2). The developed system is based on classes which were proposed by Stefanov et al. (2001a, 2001b). The network controls the number of segmentation levels and the definition of classes. In this case study we used two classification levels, an approach called MSS/ORM (Burnett & Blaschke 2003).

Image segmentation was performed in three steps in order to obtain optimized image segments. First a fine level with a scale parameter of 10 has been calculated, followed by the second level with a higher weight on the compactness of the objects.

Tab. 1: Parameters of segmentation of the ASTER satellite data and the number of objects.

Level	Layers	Scale parameter	Color	Compactness	Number of objects
1	1, 2, 3	10	0.9	0.5	294020
2	1, 2, 3	25	0.9	0.8	54563
3	1, 2, 3	12	Spectral difference segmentation		26654

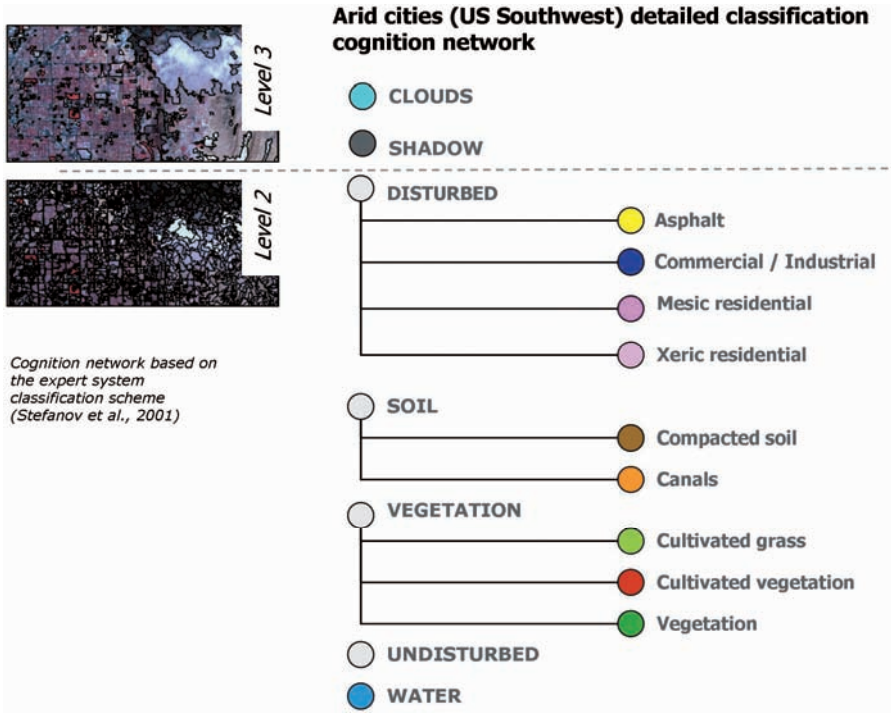

Fig. 2: Cognition network.

Finally spectral difference segmentation was used for the classification level (level 3, see Tab. 1). For the classification we focused on level 2 and 3.

3.2 *Object-based classification of the Phoenix test site*

The classes and their definitions have been given from the UEM project for the metropolitan area Phoenix (Stefanov et al. 2001a). Those classes have been set up for an expert classification scheme based on additional information, so called 'a priori knowledge' (see Tab. 2).

Several ancillary vector datasets were incorporated into the expert system model including water rights data, city and Native American reservation boundaries, and land use maps. Ancillary data provided additional useful information for the land cover classification (Stefanov et al. 2001b). This study does not use any kind of ancillary data. However, relationships among objects were utilized in order to fulfill the given class set. Thus different neighborhood relations between classes were defined as well as shape (form) parameters of objects. Only one class from the expert classification system (Stefanov et al. 2001a), *compacted soil (prior agricultural use)*, could not be adopted without utilizing ancillary data. Nevertheless, the approach presented in this paper might be used for analyzing satellite raw data and does not need any additional information.

The ASTER scene of the Phoenix area was used to develop a classification hierarchy that can be transferred to other scenes covering semi-arid environments. The developed classification scheme relies on spectral information rather than on structural features. The image data of Phoenix is absolutely cloud free and the classes *clouds* and *shadows* were therefore not necessary for this scene. They have to be introduced for the detection of these objects in the data set of the Las Vegas area only.

Tab. 2: Expert system class definitions.

Class Name	Properties
Cultivated vegetation	Actively photosynthesizing vegetation, with agricultural water rights
Cultivated grass	Actively photosynthesizing vegetation, in urban park areas
Vegetation	Actively photosynthesizing vegetation
Fluvial and lacustrine sediments (canals)	Mixed lithology gravels and soil associated with water transport features
Water	Standing or flowing water
Undisturbed	Undisturbed soil and native vegetation, bedrock outcrops
Compacted soil (prior agricultural use)	Disturbed soil with agricultural water rights
Compacted soil	Disturbed or bladed soil
Disturbed (commercial/industrial)	Mixed asphalt, concrete, soil, vegetation, and building materials, dense spatial texture
Disturbed (asphalt and concrete)	Mixed asphalt and concrete
Disturbed (mesic residential)	Built materials; vegetation cover greater than bare soil; dense spatial texture
Disturbed (xeric residential)	Built materials; vegetation cover less than bare soil; dense spatial texture

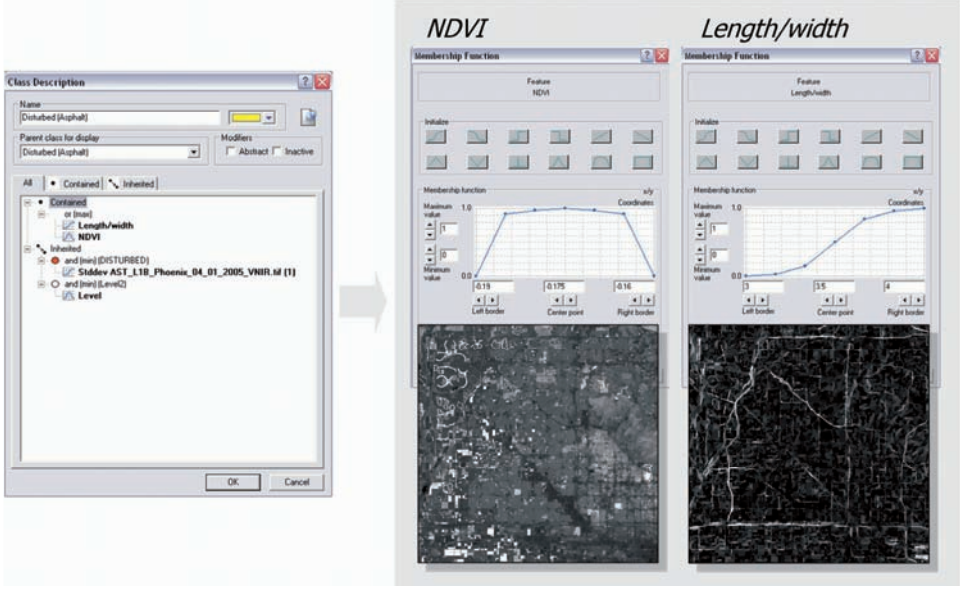

Fig. 3: Sample class definition.

In a first step the classes *clouds* and *shadows* have been classified in a higher level and used for the creation of a mask on the respective reporting level. Therefore a new feature has been calculated which is defined by the mean values of thermal band (4) divided by mean values of the thermal band (5). Additionally the size (sqm) has been considered for the classification of relevant objects. Water bodies and rivers were classified using red band mean values. Afterwards the *disturbed* and *undisturbed* areas were separated using the standard deviation of the green band. The disturbed areas were further subdivided into child classes utilizing the normalized difference vegetation index (NDVI). Different thresholds were defined to distinguish between *mesic residential* and *xeric residential areas*. The classes *commercial/industrial* and *asphalt* were separated using the NDVI and additionally the form feature length/width (see Fig. 3).

The NDVI was utilized also to detect vegetated areas, a class which has been split into subclasses *vegetation* and *cultivated land* by given thresholds for a certain area (sqkm) and a rectangular fit of the objects. Afterwards *cultivated grass* and *cultivated vegetation* could be classified by defining a new threshold for the NDVI. For the classification of *soil* a ratio of the standard deviation of the green and red band was used. The subclasses *canals* and *compacted soil* could be separated utilizing two class-related features named 'Rel. Border to *water* neighbor-objects' and 'Distance to *water* neighbor-objects (m)'.

3.3 *Transferability*

In order to test the transferability of the developed classification scheme to another image data set of a semi-arid environment the class hierarchy was exported. The workflow

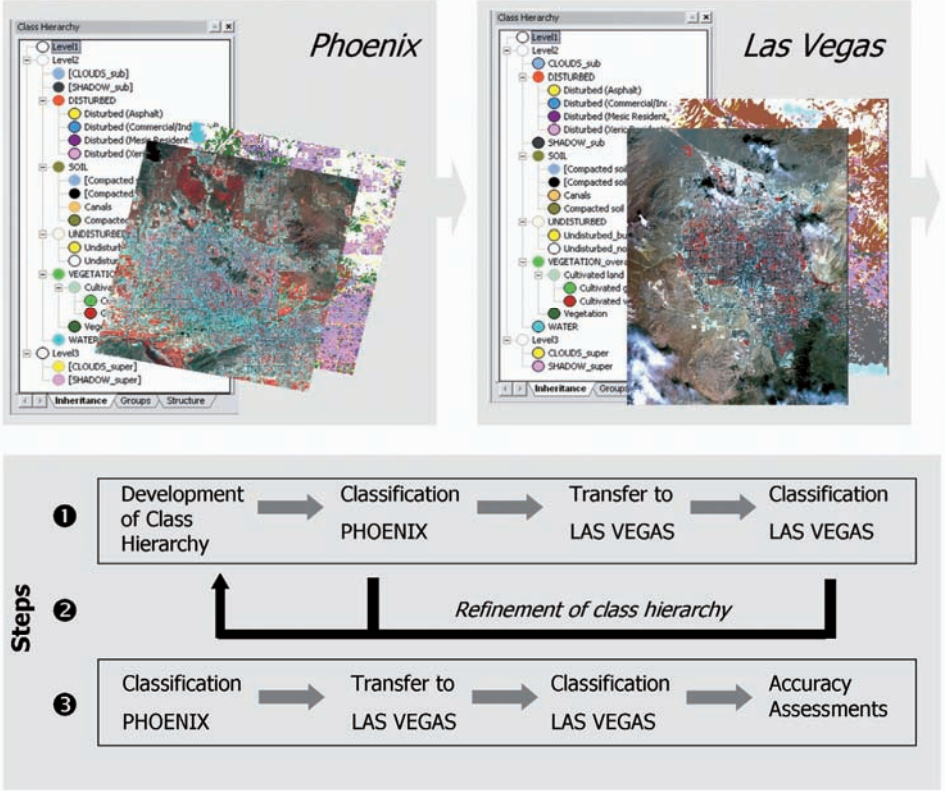

Fig. 4: Workflow of transferability between two scenes.

of the transferability between the two scenes can be seen in Fig. 4.

The ASTER image of Las Vegas was segmented using the same parameters described in chapter 3.1. In a first step ❶ the image was classified by importing the classification scheme and starting the classification process. To provide similar accuracy for the classification for both areas an iterative process has been started. The values defining membership function(s) of each class were tested and adapted and the final class hierarchy exported. The adjusted class hierarchy was then applied to the Phoenix data (step ❷) and the membership values were customized again and saved. This procedure has been repeated three times. In a last step ❸ the Phoenix data has been classified and the same class hierarchy directly transferred to the Las Vegas data set. At this time the values for defining membership functions of the classes were not adjusted in order to test the ability for an automated transferability of the class hierarchy.

4 Results and discussion

4.1 *Classification accuracy*

An automatically stratified random distribution of 195 points has been used for an accuracy assessment of the classification result. The reference values were based on visual interpretation of the spectral image data. The basic descriptive statistic is the overall accuracy, which is computed by dividing the total number of correctly classified pixels by the total number of reference pixels. The Kappa coefficient is calculated from the error matrix and is a value of the classification performance compared to the reference data. The coefficient also considers misclassified, as well as correctly classified, pixels. The classification of the Phoenix ASTER scene resulted in an overall accuracy rate of 84.24 % ($K^{\wedge} = 0.8268$). The accuracy of the transferred classification scheme applied to the Las Vegas image resulted in 83.33 % ($K^{\wedge} = 0.8148$).

4.2 *Usability and transferability*

When investigating the transferability of classification rules potentially influencing factors have to be considered. Leukert et al. (2004) listed the following items which may influence the transfer of knowledge-based classification rules: (1) date of image acquisition, (2) relief, (3) atmospheric impacts and (4) geographic region. The landscape and its topographic features appear in a broad variety and under different illumination effects. Consequently the high spectral variance, especially occurring in heterogeneous areas, such as urban areas, is represented in remote sensing imagery. Using an object-based approach might reduce the scattering by generalizing the landscape into meaningful homogenous objects. Thus the transferability of classification rule sets for a specific geographic region is still a challenging task, depending on the comparability of the image segments.

During the development of a transferable, flexible and transparent class hierarchy some difficulties were encountered. The accuracy of the classification result and the degree of transferability depends on the features used for the class descriptions. The most time-consuming task of the approach (apart from defining adequate scale parameters) is the development of a transferable class hierarchy. This research has demonstrated that form and shape properties of objects are stable parameters for class descriptions, whereas spectral properties appear to be slightly variable. Nevertheless, the NDVI could be transferred with only minor adaptations. Finally it could be demonstrated that the used rules sets lead to similar overall accuracies for both scenes.

The efficiency of image analysis and image processing regarding the usability and reusability of rule sets has also been tested. The target classes and the classification procedure itself can be reproduced by any user without the necessity of defining new training areas. The software used for this study allows an exchange of the developed object class descriptions. This portability of the embedded class definition may improve

flexibility, cooperation and exchange between project partners.

ASTER images combined with a knowledge-based classification approach are suitable for an automated workflow of scenes belonging to similar natural environments.

5 Outlook

The research presented here is part of the 100 cities project. A major task of this project is to develop standardized and transferable methods that permit a reliable and reproducible comparison of different urban areas. The transferability of the developed classification approach could significantly improve this comparison based entirely on satellite remote sensing imagery. The next step in the 100 cities project will be to determine key cities that represent specific natural environments around the globe. Standardized classification schemes will be developed for each key city, which can then be transferred to cities of the same natural environment. The ASTER sensor could demonstrate its high potential for urban mapping on a medium application scale level.

Acknowledgements

We thank Phil Christensen, Regents Professor and the Ed and Helen Korrick Professor in the Department of Geological Science at Arizona State University and PI of the UEM project, for his support. Special thanks go to Chris Eisinger, Research Assistant in the Department of Geological Sciences, Arizona State University, for providing the pre-processing of ASTER data, for critical statements and stimulating discussions. This research was carried out partly under the NASA funded Urban Environmental Monitoring (UEM) 100 cities project at Arizona State University.

References

Baatz, M. & Schaepe, A., 2000: Multiresolution Segmentation: an optimization approach for high quality multi-scale image segmentation. – In: Strobl, J. et al. (Eds.): Angewandte Geographische Informationsverarbeitung XII. Beiträge zum AGIT-Symposium Salzburg 2000, Karlsruhe, Wichmann, pp. 12–23.

Benz, U., Hofmann, P., Willhauck, G., Lingenfelder, I. & Heynen, M., 2004: Multi-resolution, object-oriented fuzzy analysis of remote sensing data for GIS-ready information. – ISPRS Journal of Photogrammetry & Remote Sensing **58:** 239–258.

Blaschke, T. & Strobl, J., 2001: What's wrong with pixels? Some recent developments interfacing remote sensing and GIS. – GIS Zeitschrift für Geoinformationssysteme **6**: 12–17.

Blaschke, T., Lang, S., Lorup, E., Strobl, J. & Zeil, P., 2000: Object-oriented image processing in an integrated GIS/remote sensing environment and perspectives for environmental applications. – In: Cremers, A. & Greve, K. (Eds.): Umweltinformation für Planung, Politik und Oeffentlichkeit/Environmental Information for Planning, Politics and the Public. – Vol. **2:** 555–570, Metropolis Verlag, Marburg.

Burnett, C. & Blaschke, T., 2003: A multi-scale segmentation/object relationship modelling methodology for landscape analysis. – Ecological Modelling **168** (3): 233–249.

Freixenet, J., Muñoz, X., Raba, D., Martí, J., & Cufí, X., 2002: Yet Another Survey on Image Segmentation: Region and Boundary Information Integration. – ECCV **3:** 408–422.

Leukert, K., Darwish, A. & Reinhardt, W., 2004: Transferability of Knowledge-Based Classification Rules. – International Archives of Photogrammetry and Remote Sensing (IAPRS), Vol. XXXV, (Part B4).

Meinel, G. & Neubert, M., 2004: A Comparison of segmentation programs for high resolution remote sensing data. – International Archives of the ISPRS, XXXV, Part B, Commision 4, 1097–1105.

Moeller, M., 2005: Remote Sensing for the Monitoring of Urban Growth Patterns. – The International Archives of the Photogrammetry, Remote Sensing and Spatial Information Sciences, Vol. XXXVI – 8/W27, on CD, ISSN 1682–1777.

Schöpfer, E., Lang, S. & Blaschke, T., 2005: A „Green Index" incorporating remote sensing and citizen's perception of green space. – International Archives of Photogrammetry, Remote Sensing and spatial information sciences, Vol. No. XXXVII-5/W1, Tempe, AZ, 1–6.

Stefanov, W.L., Ramsey, M.S. & Christensen, P.R., 2001a: Monitoring the urban environment: An expert system approach to land cover

classification of semiarid to arid urban centers. – Remote Sensing of Environment **77** (2): 173–185.

Stefanov, W.L., Christensen, P.R. & Ramsey, M.S., 2001b: Remote sensing of urban ecology at regional and global scales: Results from the Central Arizona-Phoenix LTER Site and Aster Urban Environmental Monitoring Program. Remote Sensing of Urban Areas/Fernerkundung in urbanen Räumen. – Regensburger Geographische Schriften **35:** 313–321.

Internet References

NOAA 2005: http://www.wrh.noaa.gov/vef/climate/page1.php

US Census Bureau 2005: http://factfinder.census.gov

Addresses of the authors:

Dr. Elisabeth Schöpfer
Centre for Geoinformatics (Z_GIS)
Salzburg University, Austria
Schillerstrasse 30, A-5020 Salzburg
Tel.: +43-662-8044-5266, Fax: -8044-5260
e-mail: elisabeth.schoepfer@sbg.ac.at

Dr. Matthias S. Moeller
Arizona State University (ASU)
Global Institute of Sustainability (GIOS)
c/o Institute of Geography
University of Bonn
Meckenheimer Allee 166, D-53115 Bonn,
Tel.: +49-228-73-3526, Fax: -228-73-5607
e-mail: matthias.moeller@asu.edu

Manuskript eingereicht: März 2006
Angenommen: April 2006

Photogrammetrie • Fernerkundung • Geoinformation 4/2006, S. 287–296, 10 figs., 2 tabs.

The Utilization of Image Texture Measures in Urban Change Detection

K. Wayne Forsythe, Toronto & Nigel M. Waters, Calgary, Canada

Keywords: Remote sensing, image texture, urban change, pansharpening, unsupervised classification, image differencing

Abstract: Image texture is increasingly being integrated into classification procedures using remotely sensed data. This research examined the utility of texture measures when integrated within established approaches for monitoring urban development. Landsat-7 satellite data for the years 1999 and 2002 were enhanced through a pansharpening process to provide 15 metre spatial resolution multispectral data. The images were acquired within the same approximate yearly time frame to help minimize seasonal vegetation differences and the effects of varying sun positions. Texture proved valuable in accounting for and distinguishing varying degrees of ''greenness'' in the imagery and the dissimilarity option was useful in locating recently excavated land. The measures were also helpful in separating agricultural fields from urban features. An increase of 3 % in overall classification accuracy was realized when texture information was included as a classification variable. An integrated unsupervised classification/image differencing change detection process with a combination of inputs including texture, principal components, and the Normalized Difference Vegetation Index (NDVI) provided enhanced classification results and allowed for the estimation of urban expansion rates (4.62 square kilometres per year for the 1999–2002 period).

Zusammenfassung: *Die Verwendung von Image Texturwerten in der Stadtentwicklungsanalyse*. Texturwerte werden zunehmend für Satellitenbild-Klassifikationsverfahren verwendet. Dieser Artikel überprüft die Nützlichkeit von Texturwerten und integriert sie innerhalb einer herkömmlichen städtischen Entwicklungsüberwachungsanalyse. Landsat-7 Daten wurden für die Jahre 1999 und 2002 durch ein ,,pansharpening'' bearbeitet, um die Multispektraldaten auf 15 Meter in der räumlichen Auflösung zu verbessern. Die Bilder wurden etwa zur gleichen Jahreszeit aufgezeichnet, um saisonale Vegetationsunterschiede und die Effekte bei der Veränderung der Sonnenposition herabzusetzen. Die Textur von Objekten war wertvoll in der Erkennung unterschiedlicher Grün-Abstufungen in den Bildern, und die ,,dissimilarity'' Option war nützlich, um kürzlich gerodetes Land zu lokalisieren. Die Maßnahmen waren auch hilfreich bei der Trennung von landwirtschaftlichen Flächen und städtischen Strukturen. Eine Zunahme von 3 % der gesamten Klassifizierungsgenauigkeit konnte festgestellt werden, da Texturwerte in die Klassifikationsverfahren eingeschlossen sind. Es wurde versucht, mehrere Parameter in die Klassifikation zu integrieren, wie die Textur, die Hauptkomponenten und der normalisierte Vegetationsindex (NDVI), welche schlussendlich bessere Klassifizierungsergebnisse hervorgebracht haben. Die Untersuchungen führten zu dem Resultat, dass sich die Fläche der Stadt im Untersuchungszeitraum um jährlich 4,62 km^2 vergrößert.

Introduction

Research into texture measures has mostly focused on which statistics and window sizes provide the biggest gains in feature extraction, as well as ways in which texture bands can be combined with spectral data to increase classification accuracy. Traditionally, texture features are combined with or integrated into classification procedures

1432-8364/06/2006/0287 $ 2.50

(Karathanassi et al. 2000, Marceau et al. 1990, Pesaresi 2000, Pusissant et al. 2005, Shaban & Dikshit 2001, Tatem et al. 2004, Zhang et al. 2003). Tatem et al. (2004) utilized texture and found that a "superresolution" classification produced higher accuracies, but involved increased computational expense. In studying CO_2 emissions in Copenhagen, Soegaard & Møller-Jensen (2003) used a grey level co-occurrence matrix combined with a parallelepiped classification to define urban areas. In this case, only a few pixels had their texture statistics calculated, and each parallelepiped was assumed to be texturally homogeneous and assigned the value of pixels it encompassed. It has also been found that using at least three different texture bands, combined with spectral data, produced the highest gains in classification accuracy (Zhang et al. 2003).

Remote sensing methods are very effective in the analysis of urban change (Forsythe 2004, Hostert & Diermayer 2003, Masek et al. 2000, Ridd & Liu 1998). The use of fused or sharpened data for urban applications is also well-documented (Forsythe 2004, Steinnocher 1997, Zhang 2002, Zhang 2004). In this research, a combined unsupervised classification/image differencing change detection process that includes texture measures is utilized to examine urban growth.

Study Area

Calgary, Alberta is the fastest growing major metropolitan area in Canada (Statistics

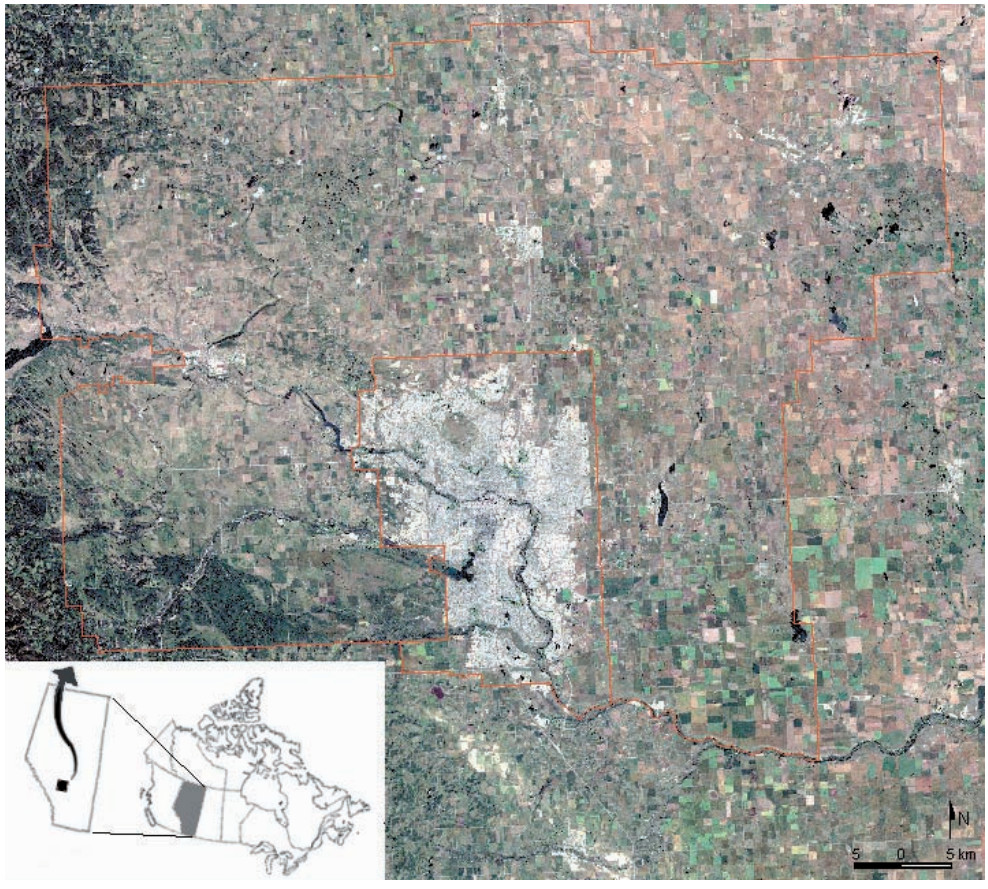

Fig. 1: Calgary Census Metropolitan Area (boundaries in red).

Canada 2005). The Census Metropolitan Area (CMA) – (Fig. 1) contains the smaller communities of Cochrane and Airdrie which are also developing rapidly. In addition, surrounding communities such as Okotoks and Strathmore are growing in part due to the economic prosperity that Calgary is currently experiencing. Two distinct growth phases can be identified from census data for Calgary over the last 30 years. During the 1970's, the population grew by over 50% from 400000 in 1971 to 625000 in 1981. From the mid-1990's onward, large annual increases in population occurred, indicating, in part, a shift from a natural resource based economy to a more diversified financial system.

Data

Landsat 7 Enhanced Thematic Mapper Plus (ETM+) imagery was acquired, ortho-rectified (NAD83-GRS1980 UTM Zone 11 projection), and subset (to the city limits of Calgary) for the dates of July 9, 1999 (Fig. 2) and August 18, 2002 (Fig. 3).

The images were the best available in terms of being "cloud free" and the dates encompass the same approximate yearly time frame to help minimize seasonal vegetation differences and the effects of varying sun positions. It is however quite apparent from the large areas of "green" in the 1999 data, that moister conditions existed at the time of image acquisition in 1999 compared to 2002.

Methods and Analysis

To enhance urban features within the data and assist with boundary delineation, the PANSHARP algorithm (as implemented in the PCI Geomatica software) was used to upgrade the spatial resolution of the images from 30 to 15 metres. This process eliminates problems (such as the destruction of data spectral characteristics, colour distortion, and operator and data set dependence) that can occur during the data fusion or sharpening process (Zhang 2002). A more detailed discussion of the process can be found in Zhang (2004).

Image classification has been successfully used to distinguish urban expansion from land cover changes that occur due to other factors such as agricultural practices (For-

Fig. 2: Landsat 7 subset image – July 9, 1999 (Path 42, Row 24).

Fig. 3: Landsat 7 subset image – August 18, 2002 (Path 42, Row 24, shifted 20% south).

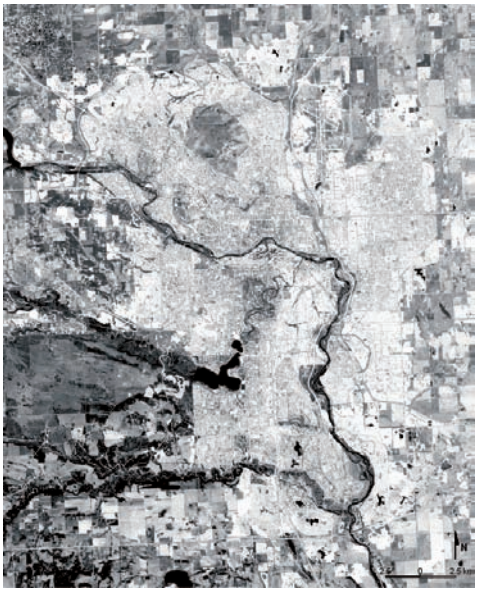

Fig. 4: Mean Texture.

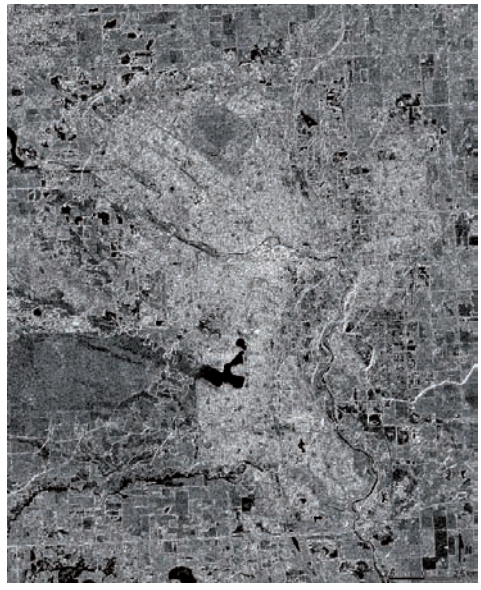

Fig. 5: Dissimilarity Texture (black areas on the urban fringe indicate excavated land).

SYTHE 2004, MASEK et al. 2000). Previous studies (DU 2005, FORSYTHE 2004, MASEK et al. 2000, SHABAN & DIKSHIT 2001, YEH & LI 2001) have shown that a number of features derived from the original satellite bands can be useful in distinguishing classes. DE KOK et al. (2003), FORSYTHE (2004), and SHABAN & DIKSHIT (2001) found that texture measures were a great asset for urban change detection. Of the many options that are available, mean, dissimilarity, contrast, and homogeneity texture measures were generated with both 3×3 and 7×7 windows using band 2 of the ETM+ data. These parameters were chosen based on the authors' previous urban change detection research and results reported in the literature (DE KOK et al. 2003, FORSYTHE 2004, SHABAN & DIKSHIT 2001, STEINNOCHER 1997). The 3×3 results were clearly superior to the 7×7 results in terms of the amount of detail that could be discerned, especially in areas where urban growth had occurred. Mean texture measures (Fig. 4) delineated urban built-up areas very well, and distinguished urban and agricultural features having similar spectral characteristics. Dissimilarity (Fig. 5) detailed newly excavated areas in remarkable detail, while homogeneity was somewhat less successful in locating these areas. Contrast was the least successful of the texture options which does not correspond with the results of PESARESI (2000) who found that the contrast measure was especially well-suited to discerning the differences between built and non-built environments.

Determining the optimal window size and texture statistics is still a process requiring many trials. While it has been found that the window size used is overwhelmingly responsible for the homogeneity and accuracy of a texture class (MARCEAU et al. 1990), there is no one best size. This is because such an optimal size depends on the spatial resolution of the image and the land use being captured (PESARESI 2000). Windows must be large enough to encompass the whole of the texture pattern, but small enough not to include more than one (PESARESI 2000, PUSISSANT et al. 2005). Traditionally, large window sizes, ranging from 31×31 to 40×40 to 51×51, have been recommended (KARATHANASSI et al. 2000, PESARESI 2000).

However, some researchers have found that with higher spatial resolution images, smaller window sizes must be used due to the greater variability seen in urban areas. In these cases, a window size of 7×7 was recommended (Pusissant et al. 2005, Zhang

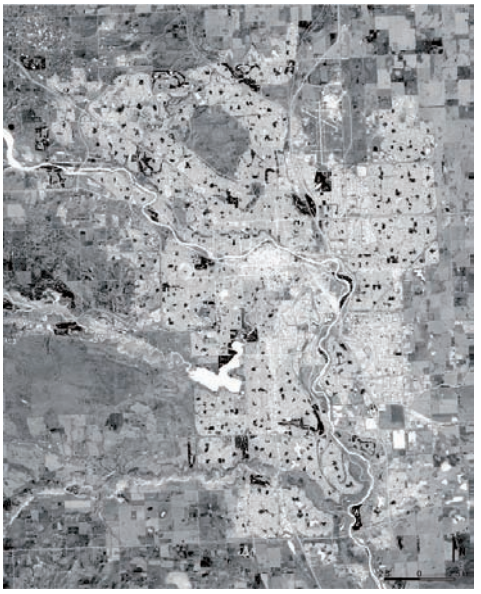

Fig. 6: Principal Component 2 (small black areas within the city limits are parks with larger black areas representing golf courses and other large manicured green areas).

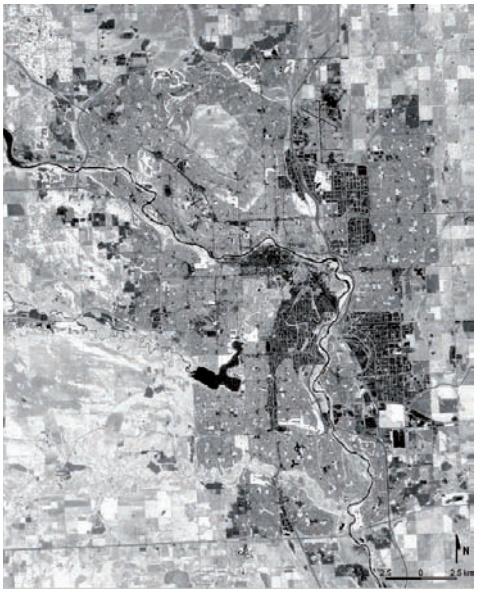

Fig. 7: NDVI (black areas within the city limits represent industrial and manufacturing land uses with black areas on the fringe indicating excavated land).

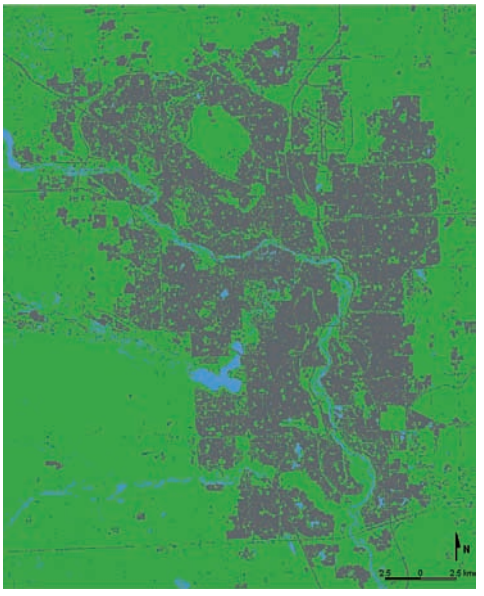

Fig. 8: Aggregate 2002 Classification (green = greenspace, grey = built, blue = water).

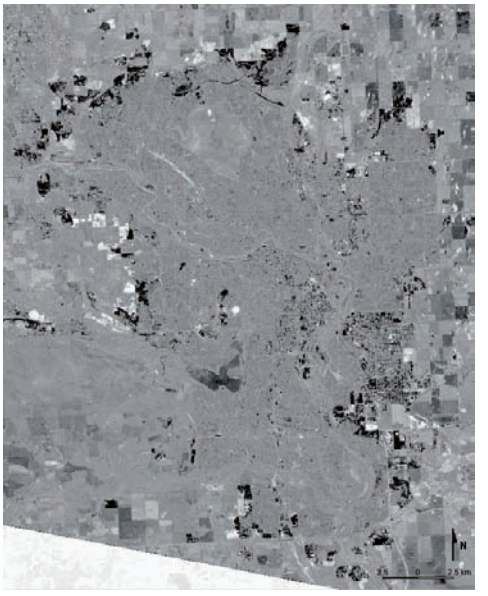

Fig. 9: 2002 Band 2 – 1999 Band 2.

et al. 2003), but this was found to be unsuitable for the imagery used and objectives of this research.

Similar problems have been encountered in determining which of the texture statistics derived from the matrices should be used. Depending on the land cover, certain measures will provide more or less accuracy (Pesaresi 2000, Shaban & Dikshit 2001, Zhang et al. 2003). No one measure provides the best results, so a combination may be a better solution. However, the mean measure (Du 2005, Zhang et al. 2003) and contrast measure (Pesaresi 2000, Shaban & Dikshit 2001) stand out as two of the best for urban applications.

In addition to texture, Principal Components and a Normalized Difference Vegetation Index (NDVI) were generated as inputs for the classification procedures in a process similar to that utilized by Du (2005), Forsythe (2004) and Masek et al. (2000). Principal Component 2 (Fig. 6) was effective in distinguishing urban green areas including parks and golf courses. NDVI (Fig. 7) was useful for distinguishing urban industrial/manufacturing and newly excavated areas from residential districts.

Two distinct classification procedures were performed. One did not include texture, while the other had mean texture added as an additional classification input. Fig. 8 represents the aggregate classification results that were derived using the six Landsat bands (1, 2, 3, 4, 5, 7), mean texture, principal component 2, and NDVI. These data were then combined with the results of image differencing operations (Fig. 9) using band2 (2002 band 2 minus 1999 band 2). The overall classification accuracy for the three classes (greenspace, built, and water) was 88 % (Kappa 0.75) compared to 85.3 % (Kappa 0.69) when texture measures were not included (full accuracy statistics are presented in Tab. 1 and 2).

Some interesting features in the difference image include white areas generally representing excavated areas where previous agricultural or forested land has been replaced by land being prepared for building and darker (blacker) areas mainly representing areas where housing developments have replaced excavated land (Forsythe 2003).

The use of an unsupervised classification layer as an agricultural mask was necessary to complete the data analyses. It can be seen in from the large black/grey square/rectangle agricultural fields in Fig. 9 that these areas have also changed (due to crop rotation or harvesting) in addition to the urban areas that were either newly developed (or redeveloped) and excavated. Image texture

Tab. 1a: Accuracy Statistics for Classification with Texture Measures.
Overall Accuracy: 88 % – 95 % Confidence Interval (82.47 % – 93.53 %).
Overall Kappa Statistic: 0.75 % – Overall Kappa Variance: −0.10 %.

Class Name	Producer's Accuracy	95 % Confidence Interval	User's Accuracy	95 % Confidence Interval	Kappa Statistic
Greenspace	95.56 %	(90.74 % 100.37 %)	86.87 %	(79.71 % 94.03 %)	0.67
Built	76.27 %	(64.57 % 87.97 %)	91.84 %	(83.15 % 100.52 %)	0.87
Water	100.00 %	(50.00 % 150.00 %)	50.00 %	(−44.30 % 144.30 %)	0.50

Tab. 1b: Accuracy Statistics – Error (Confusion) Matrix.

Classified Data	Reference Data Greenspace	Built	Water	Totals
Greenspace	86	13	0	99
Built	4	45	0	49
Water	0	1	1	2
Totals	90	59	1	150

Tab. 2a: Accuracy Statistics for Classification with No Texture Measures.
Overall Accuracy: 85.33% – 95% Confidence Interval (79.34% – 91.33%).
Overall Kappa Statistic: 0.69% – Overall Kappa Variance: −0.04%

Class Name	Producer's Accuracy	95% Confidence Interval	User's Accuracy	95% Confidence Interval	Kappa Statistic
Greenspace	94.32%	(88.91% 99.72%)	83.84%	(76.08% 91.60%)	0.61
Built	72.13%	(60.06% 84.20%)	89.80%	(80.30% 99.29%)	0.83
Water	100.00%	(50.00% 150.00%)	50.00%	(−44.30% 144.30%)	0.50

Tab. 2b: Accuracy Statistics – Error (Confusion) Matrix.

Classified Data	Reference Data Greenspace	Built	Water	Totals
Greenspace	83	16	0	99
Built	5	44	0	49
Water	0	1	1	2
Totals	88	61	1	150

(as noted above) was very useful when included in the unsupervised classification procedures. It helped to discriminate between the urban and agricultural areas where spectral signatures were similar compared with when it was not included as a classification input variable. The aggregate classifications consisting of urban, greenspace, and water were developed from 64 original unsupervised K-means classes. This allowed for small features that may have caused classification problems (i.e. aggregated into the incorrect class when fewer original K-means classes were used) to be clearly separated and delineated. They were then assigned to the appropriate aggregate class.

ArcGIS software was used to combine the difference and unsupervised classification images and to calculate areas. Fig. 10 illustrates the overall urban change that occurred during the 1999–2002 period. A total of 13.86 square kilometres was identified as new urban development over the three year period (an average was 4.62 square kilometres per year). A small cloud in the middle of the 2002 image has introduced some error into the final result and some omission errors can be found in the southern part of the image in addition to some commission errors to the east of the city (related to the a lack of water in low-lying areas in the 2002 image compared to the 1999 data). Overall, the results are very good with changed urban areas well represented and the excavated and newly developed areas clearly delineated.

Conclusion

Image texture provided for an increased level of accuracy when it was included as an input in classification procedures. A 3×3 window was found to improve the delineation of urban features as compared to the 7×7 option. The mean measure was useful in distinguishing urban from agricultural areas, while the dissimilarity option was very proficient in locating excavated areas of the urban fringe.

A combined approach including image differencing and unsupervised classification allowed for the measurement of urban development. The pansharpened images enabled finer detail to be distinguished (including excavated vs. newly built land) than is possible with coarser resolution data. Calgary is a rapidly expanding urban centre. The use of additional parameters (especially image texture) that can be generated from image data proved particularly effective in determining urban growth. Although the

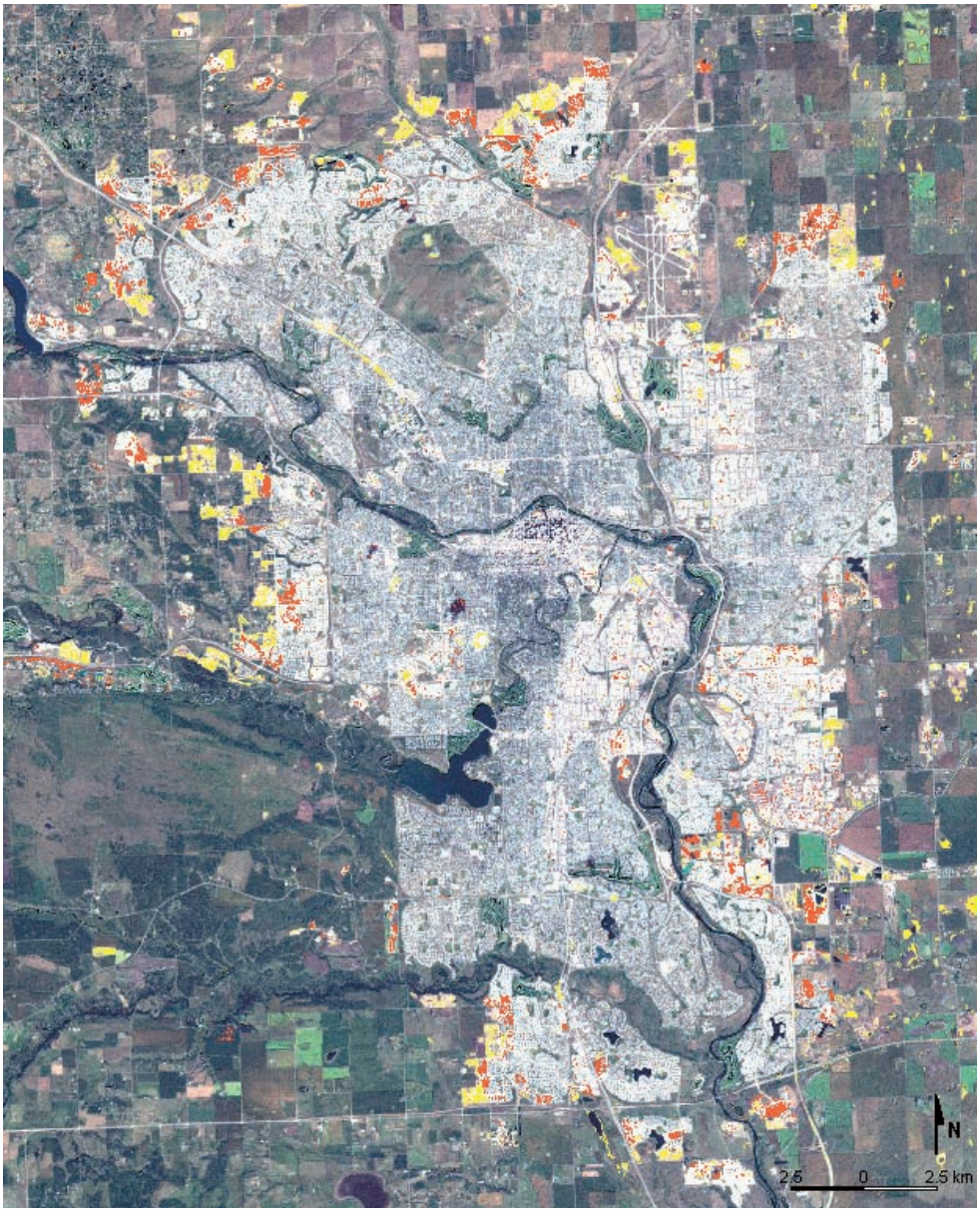

Fig. 10: Overall Urban Change from 1999 to 2002 (Yellow: excavated land replaces vegetation; Red: developed land replaces excavated land; background image Landsat 2002 Bands 3, 2, 1).

images were acquired during the same season (year to year), it was necessary to compensate for differences in greenness to obtain suitable urban classification results. The use of texture measures was very advantageous as they provided additional information to assist in classification procedures and define boundaries between various land cover features.

References

De Kok, R., Wever, T. & Fockelmann, R., 2003: Automatic procedures for large-area mapping applied on urban environment. – The International Archives of the Photogrammetry, Remote Sensing and Spatial Information Sciences (CD-ROM), Vol. XXXIV-7/W9. Proceedings of the 4th International Symposium Remote Sensing of Urban Areas. Regensburg, Germany, June 27–29, 2003. pp. 41–45. (CD-ROM). ISSN 1682–1777

Du, P., 2005: Urban Change Detection and Analysis in the Greater Toronto Area from 1972 to 2004 using Remote Sensing and GIS. – Unpublished M.S. A. Research Paper. Department of Geography, Ryerson University. Toronto, Ontario, Canada.

Forsythe, K.W., 2003: Monitoring "Megacity" Urban Development Pansharpened Landsat 7 Results for Toronto, Ontario, Canada. – The International Archives of the Photogrammetry, Remote Sensing and Spatial Information Sciences (CD-ROM), Vol. XXXIV-7/W9. Proceedings of the 4th International Symposium Remote Sensing of Urban Areas. Regensburg, Germany, June 27–29, 2003. pp. 60–65. ISSN 1682–1777

Forsythe, K.W., 2004: Pansharpened Landsat 7 Imagery for Improved Urban Area Classification. – Geomatica **58** (1): 23–31.

Hostert, P. & Diermayer, E., 2003. Employing Landsat MSS, TM and ETM+ for Mapping 3 Decades of Urban Change in Berlin, Germany. – The International Archives of the Photogrammetry, Remote Sensing and Spatial Information Sciences (CD-ROM), Vol. XXXIV-7/W9. Proceedings of the 4th International Symposium Remote Sensing of Urban Areas. Regensburg, Germany, June 27–29, 2003. pp. 225–228. (CDROM). ISSN 1682–1777

Jensen, J.R., 2004: Introductory Digital Image Processing: A Remote Sensing Perspective. – 3rd Ed., 526 pp., Prentice Hall, Upper Saddle River, New Jersey.

Karathanassi, V., C.H. Iossifidis & D. Rokos, 2000: A Texture-Based Classification Method for Classifying Built Areas According to their Density. – International Journal of Remote Sensing **21** (9): 1807–1823.

Marceau, D.J., Howarth, P.J., Dubois, J.M. & Gratton, D.J., 1990: Evaluation of the Grey-Level Co-Occurrence Matrix Method for Landcover Classification Using SPOT Imagery. – IEEE Transactions on Geoscience and Remote Sensing **28** (4): 513–519.

Masek, J.G., Lindsay, F.E. & Goward, S.N., 2000: Dynamics of Urban Growth in Washington D.C. Metropolitan Area 1973–1996 from Landsat Observations. – International Journal of Remote Sensing **21** (18): 3473–3486.

Pesaresi, M., 2000: Texture Analysis for Urban Pattern Recognition Using Fine-Resolution Panchromatic Satellite Imagery. – Geographical and Environmental Modelling **4** (1): 43–63.

Pusissant, A., Hirsch, J. & Weber, C., 2005: The Utility of Texture Analysis to Improve Per-Pixel Classification for High to Very High Spatial Resolution Imagery. – International Journal of Remote Sensing **26** (4): 733–745.

Ridd, M.K. & Liu, J., 1998: A Comparison of Four Algorithms for Change Detection in an Urban Environment. – Remote Sensing of the Environment **63:** 95–100.

Shaban, M.A. & Dikshit, O., 2001: Improvement of classification in urban areas by the use of textural features: the case study of Lucknow City, Uttar Pradesh. – International Journal of Remote Sensing **22** (4): 565–593.

Soegaard, H. & Møller-Jensen, L., 2003: Towards a Spatial CO_2 Budget of a Metropolitan Region Based on Textural Image Classification and Flux Measurements. – Remote Sensing of Environment **87** (2-3): 283–294.

Statistics Canada, 2005: http://www.statscan. ca (accessed 30 Dec. 2005)

Steinnocher, K., 1997: Texturanalyse zur Detektion von Siedlungsgebieten in hoch auflösenden panchromatischen Satellitenbilddaten. – Proceedings of the 9th Symposium for Applied Geographic Information Processing (Angewandte Geographische Informationsverarbeitung IX), AGIT '97. July 2–4, 1997. Salzburg, Austria. pp. 143–152.

Tatem, A.J., Abdisalan, M.N. & Hay, S.I., 2004: Defining approaches to settlement mapping for public health management in Kenya using medium spatial resolution satellite imagery. – Remote Sensing of Environment **93** (1-2): 42–52.

Yeh, A.G. & Li, X., 2001: Measurement and Monitoring of Urban Sprawl in Rapidly Growing Region Using Entropy. – Photogrammetric Engineering & Remote Sensing **67** (1): 83–89.

Zhang, Q., Wang, J., Gong, P. & Shi, P., 2003: Study of Urban Spatial Patterns From SPOT Panchromatic Imagery Using Textural Analysis. – International Journal of Remote Sensing **24** (21): 4627–4645.

Zhang, Y., 2002: A New Automatic Approach for Effectively Fusing Landsat 7 as well as IKONOS Images. – Proceedings of the IEEE/

IGARSS'02. Toronto, Canada. June 24–28, 2002. (CD-ROM).

ZHANG, Y., 2004: Understanding Image Fusion. – Photogrammetric Engineering & Remote Sensing June 2004: 657–661.

Addresses of the Authors:

K. WAYNE FORSYTHE, Ph.D., Assoc. Prof.
Department of Geography
Program in Geographic Analysis
Ryerson University, 350 Victoria Street
Toronto, Ontario, Canada M5B 2K3
e-mail: forsythe@geography.ryerson.ca

NIGEL M. WATERS, Ph.D., Prof.
Department of Geography
University of Calgary
2500 University Drive N.W.
Calgary, Alberta, Canada T2N 1N4
e-mail: nwaters@ucalgary.ca

Manuskript eingereicht: März 2006
Angenommen: Mai 2006

Photogrammetrie • Fernerkundung • Geoinformation 4/2006, S. 297–302, 2 figs.

Urban Land Use Data for the Telecommunications Industry

Regine Richter, Ulla Weingart, Tobias Wever, Munich & Ulrike Kähny, Düsseldorf

Keywords: Remote Sensing, Telecommunication Industry, UMTS, urban land use, urban clutter data, EuroMaps

Abstract: Universal Mobile Telecommunications System (UMTS) is the new third generation telecommunication standard. UMTS stands mainly for a fast data transfer and complex multimedia applications. In order to offer specific UMTS services for special user groups and localities, such as trade fairs, the telecommunications industry uses high resolution urban land use (clutter) data that provides information about urban density as well as a variety of utilization categories. The urban clutter data set covers the whole of Germany and provides 24 urban density and urban use classes, with a minimum object size of 0.5–2 ha, depending on the object class.

The data was produced on the basis of "EuroMaps", a high resolution satellite image mosaic of Germany. The natural colour mosaic is based on up-to-date IRS-1C/D data; the high resolution (5-m on the ground) as well as the high positional accuracy (RMSE 90 % < 12 m) of the image data, in combination with their homogeneity, make EuroMaps well suited for large area mapping in the field of urban development.

Visual interpretation techniques supported by special mapping software, designed for streamlining the production, were applied to map the urban areas in detail. The whole production took one year.

Generally, the urban geometries can be used for several applications. For example, statistics about municipal or regional population density, as well as construction and industrial sites, can be derived from the data. The regional reference of the information and manifold regional statistics and analysis can easily be derived by overlay with ancillary information.

Zusammenfassung: *Städtische Landnutzungsdaten für die Telekommunikationsindustrie*. Universal Mobile Telecommunications System (UMTS) ist der Standard der so genannten dritten Generation der Telekommunikation. UMTS bietet einen schnellen Datentransfer, der für komplexe Multimedia-Anwendungen erforderlich ist. Die Anbieter von Telekommunikationsdiensten setzten für die Planung ihrer UMTS Funknetze hoch auflösende Landnutzungsdaten ein, die Aufschluss über die städtische Bebauungsdichte und andere nützliche Kategorien geben. Dieser Landnutzungsdatensatz liegt flächendeckend für die Bundesrepublik vor und enthält 24 Bebauungsdichteklassen mit einer minimalen Objektgröße von 0,5–2 ha, in Abhängigkeit von der jeweiligen Objektklasse.

Diese Landnutzungsdaten wurden aus dem hoch auflösenden Bilddatenmosaik „EuroMaps" abgeleitet. Dieser Datensatz basiert auf Echtfarben Satellitenbilddaten des Sensors IRS-1C/1D mit einer sehr hohen räumlichen Auflösung von 5 m. In Kombination mit einer Lagegenauigkeit (RMSE 90 % < 12 m) sind diese Bilddaten für das urbane Monitoring bestens geeignet. Der Datensatz wurde visuell mit einer speziellen Software ausgewertet, um so urbane Nutzungen detailliert kartieren zu können.

Prinzipiell können die kartierten Objekte für unterschiedliche Anwendungen genutzt werden, beispielsweise für die Analyse der Bevölkerungsdichte, für Bebauungsplanung und auch für die Ermittlung der Verteilung von Industrieanlagen. Mit Hilfe zusätzlicher Information aus bestehenden GIS Datensätzen können auf Basis der Landnutzungskartierung weitere regionale Statistiken erstellt werden.

1432-8364/06/2006/0297 $ 1.50

Introduction

With the recent unequalled success story of mobile telecommunications technology, service network operators have been undertaken enormous investment for the network infrastructure in order to improve the quality and availability of telecommunication services in general and also to provide specific services.

The high costs and the lack of available radio frequencies require an effective planning and modelling of radio propagation, especially when considering the rapid growth of network size and number of users. The number of services in the third generation Universal Mobile Telecommunication System – UMTS – is substantially higher than with GSM. Increased system complexity and others parameters actually reinforce the demand for effective network planning. For instance, one of the fundamental characteristics of UMTS is that the coverage range is intrinsically linked to the capacity of the system: more traffic carried by a cell results in a smaller the coverage area for the cell.

Background

E-Plus Mobilfunk GmbH & Co. KG, a German mobile network operator, runs an area-wide digital, mobile network for the whole of Germany. Generally, digital, spatially-oriented land cover/land use data (Clutter data) and radiowave propagation models are the basis for its macrocellular radio network planning, which ensures an area-wide supply with accompanying good quality by optimizing the available frequencies as well as antenna positions and characteristics.

Besides physical parameters, strategic ones also play a major role in the planning of mobile networks. While an optimal network quality has to be ensured in those places where demand is high, inevitable interferences have to be placed in areas where they influence the telecommunication services as little as possible or not at all. Also, sparsely populated

Base Data

Satellite Data

The requirements concerning data actuality and a minimum object size of 0.5–2 ha, depending on the object class, required the use of high resolution satellite data for the classification of urban areas. This applies especially to urban density classes which are assigned mainly on the basis of textural context.

With "EuroMaps", a common product development of GAF AG and Euromap GmbH, a high resolution natural colour satellite image mosaic from Germany is available based on up-to-date IRS-1C/D data. The high resolution (5-m on the ground) and the high positional accuracy (RMSE 90% < 12 m) of the image data, in combination with their homogeneity, make Euro-Maps very well suited for large area mapping in general and particularly in the field of urban deve-lopment.

Ancillary Data

- Municipal Data: Generally statistical data (e. g. population data) are based on municipal data. These data were therefore merged with the derived built-up areas to ensure compatibility/consistency of clutter data with ancillary data.
- In order to delineate industry, trade and service classes, geographically linked company data and addresses were included in the classification. The data comprised information about location, number of employees and the trade branch.
- For refining operations, topographic maps with a scale of 1: 25.000 and city plans were included in the data interpretation. Both sets of ancillary data were essential for the delineation of the classes "large" and "small scale industry", "trade and service enterprises".

Technical Approach

In most cases, built-up areas of municipalities consist of different delineated zones where one specific housing type is predomi-

nant in each zone. Using these housing types built-up areas can be classified into several categories and subcategories on the basis of high resolution satellite and ancillary data.

The complete vector coverage of built-up areas in Germany consists of 24 different classes with the following main categories:

- Building Density (e. g., Detached Housing, Housing Blocks, Industrial Areas),
- Storeys (e. g., Single/Multiple Family Housing, High-rise Buildings),
- Special Classes (e. g., Railway Stations, Hospitals, Trade Centres, Airports etc.).

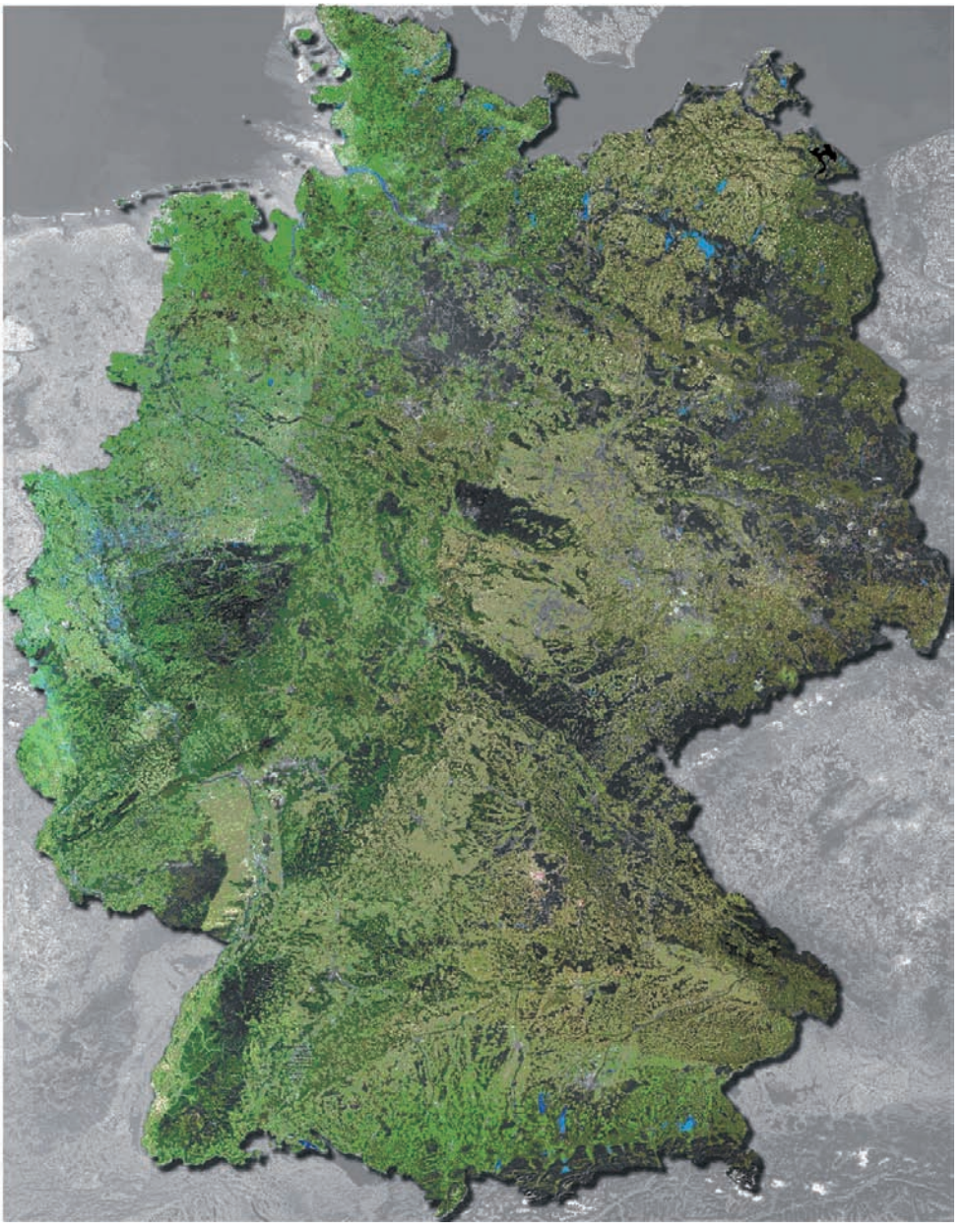

Fig. 1: Euro-Maps – high resolution satellite image mosaic of Germany.

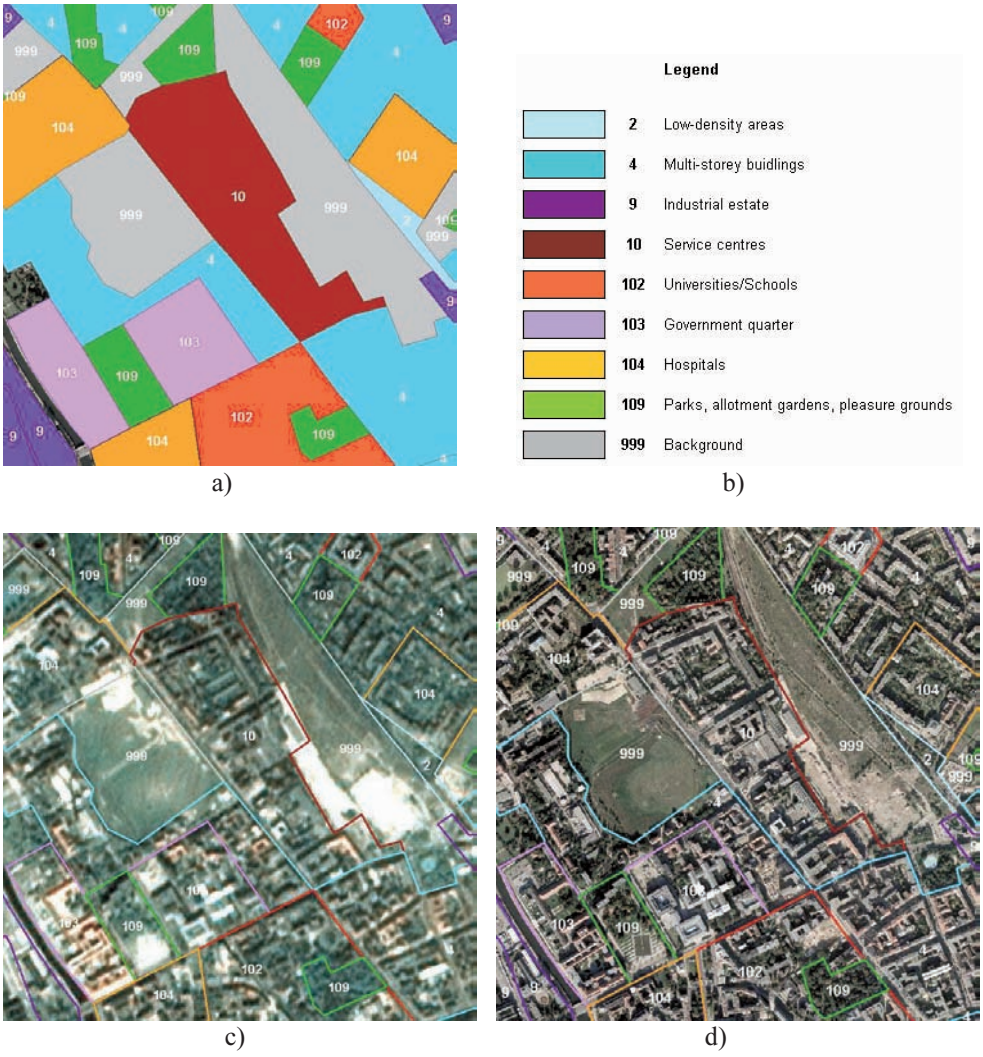

Fig. 2: Berlin example from the country-wide urban clutter data.
a) Urban classification
b) Legend
c) Subset of high resolution satellite image mosaic of Germany – EuroMaps (5 m)
d) Subset of orthoimage (0.4 m) used for verification

The delineation of urban classes was realized via visual interpretation and on-screen digitizing techniques. The interpretation was supported by a dedicated proprietary software (GeoFIS) designed to streamline the production, has been applied to map the urban areas in detail in order to ensure fast processing and reliable attributing. GeoFIS works in a two-window mode to enable the visualisation of at last two information layers. The GIS functionality also allows the display of ancillary vector data such as municipal boundaries or previously derived classification results. The vector module of GeoFIS enables a multifunctional handling of the polygons such as dissection, connection and merging and avoidance of intersections. GeoFIS is connected with an MSAc-

cess database that is updated and expanded continuously during the mapping exercise.

Because the built-up areas are developed in a very diverse regional manner the delineation of urban classes was carried out step by step for each federal state to ensure homogeneity of the data set over the whole of Germany. Normally, the boundaries of the built-up areas were drawn along the streets. In cases with very wide streets, stream courses or other linear elements the boundary was placed in the middle of the linear object.

The quality and consistency of GAF clutter data are among the highest commercially available and are based on longstanding experience, streamlined technology, robust extraction techniques and approved quality assurance procedures.

Verification

The verification of the urban clutter data set for the whole of Germany was performed by the client E-Plus Mobilfunk GmbH & Co. KG, a German mobile network operator. The performance was determined as being better than the required 95% for the class delineation and the positional accuracy (standard deviation) was better than 15 m and thus fully compliant with the required specification.

The verification exercise was performed randomly using the above mentioned ancillary data and was for some specific areas based on very high resolution orthophotos (0.4 m).

Conclusion

The vector coverage of built-up areas is a unique urban land use data set covering the whole of Germany. It consists of 24 different urban classes outlining different settlement geometries and densities as well as special urban zones such as trade fairs or industrial areas. At the moment no other land use data set available on the market offers a comparable country-wide mapping accuracy with a minimum object size between 0.5–2 ha (depending on the urban object class).

The product serves E-Plus Mobilfunk GmbH & Co. KG mainly for strategic network planning to ensure an optimal network quality in those places with high/increased demand and to serve special user groups and localities with specific services. Due to the great success of the urban clutter data set in physical and strategic planning of mobile networks, E-Plus Mobilfunk GmbH & Co. KG is planning a continuous updating of the urban clutter data set.

The exclusive availability of "EuroMaps", a high resolution satellite image mosaic of Germany and neighbouring countries, was the ultimate precondition for the generation of this product at reasonable costs. The high resolution (5-m on the ground) as well as the high positional accuracy (RMSE 90% < 12 m) of the image data, in combination with their homogeneity, make EuroMaps well suited for a wide range of tasks in the fields of thematic planning, mapping and visualization up to a scale of 1:20,000. The orthorectified product consists of approx. 400 single images (Multispectral/PAN Merges) resulting in the above mentioned country-wide satellite image mosaic "EuroMaps". Euro-Maps will be updated regularly by up-to-date satellite data to ensure a reliable and actual data basis.

The high resolution urban clutter data set and country-wide satellite image mosaic Euro-Maps can be used for many planning and mapping purposes. Distribution of both data sets is made by GAF AG.

Anschriften der Autoren:

Dipl.-Geogr. Regine Richter
e-mail: richter@gaf.de

Dipl.-Geol. Ulla Weingart
e-mail: weingart@gaf.de

Dr. rer. nat. Tobias Wever
e-mail: wever@gaf.de
GAF AG, Gesellschaft für Angewandte Fernerkundung und Informationssysteme
Arnulfstr. 197, D-80634 München

Dipl.-Ing. Ulrike Kähny
e-mail: ulrike.kaehny@eplus.de
E-Plus Mobilfunk GmbH & Co. KG
E-Plus Platz, D-40468 Düsseldorf

Manuskript eingereicht: März 2006
Angenommen: April 2006

Photogrammetrie • Fernerkundung • Geoinformation 4/2006, S. 303–314, 10 figs., 3 tabs.

Comparison of DSM Generation Methods on IKONOS Images

Thomas Krauß, Manfred Lehner, Peter Reinartz, Weßling & Uwe Stilla, München

Keywords: GeoInformatics, VHR data, Stereo Data, DSM generation, dynamic programming

Abstract: In this article two methods for an almost fully automatic generation of digital surface models (DSM) from Ikonos stereo data are described and limitations are analyzed. An important critical parameter for the derivation of DSM is the convergence angle of the stereo pair. Impacts of this value are shown and discussed.

Zusammenfassung: *Vergleich von DSM-Erstellungsmethoden auf Basis von IKONOS-Stereobildern*. In diesem Beitrag werden zwei Methoden für die nahezu vollautomatische Erzeugung digitaler Oberflächenmodelle (digital surface models, DSMs) beschrieben und analysiert. Ein wichtiger kritischer Parameter für die Gewinnung digitaler Oberflächenmodelle ist der Konvergenzwinkel der beiden Stereo-Aufnahmen. Der Einfluss dieses Parameters wird untersucht.

1 Introduction

Digital surface models (DSM) and three dimensional city models are important for many applications. Beside of maps, urban planning and information systems stereo data become essential in the case of catastrophes like earth quakes or floodings or in case of civil defense applications because they show the degree and the extent of destruction much more clearly than single images. An automatic interpretation of stereo images regarding exact location and height information will lead to fast change detection capabilities.

For this reason a system which is able to generate fully automatically DSMs and even 3D-city models from VHR satellite imagery like Ikonos is of great value for many applications. Since the intended purpose is to provide such models very quickly e. g. in disaster situations there are some requirements. A main point is that the information has to be gained in a short time for any possible acquisition area on the earth surface. Such constraints lead to the usage of stereo images from very high resolution (VHR) satellites from which the high resolution urban DSM can be derived. Beside this it is not possible to rely on locally available information like cadastral data or data of street networks in most developing countries. The models have to be generated fast with a reasonable accuracy for relatively large urban regions.

Two methods for an approach to a fully automatic generation of a DSM are described and limitations are analyzed. One critical parameter for the derivation of a DSM is the convergence angle of the stereo pair. Based on Ikonos stereo pairs with different convergence angles the impact of this value is examined and effects on the accuracy of the two methods are shown and discussed.

Three dimensional city models

Currently there exists a broad variety of methods for city modeling. These methods are mostly based on cadastral data, aerial images, aerial and terrestrial laser scanner

1432-8364/06/2006/0303 $ 3.00

data, terrestrial photographs and much more. The modeling integrates data from several of these sources in often intense manual work to the urban models (CyberCity 2006, 3D Geo 2006).

For example CyberCity uses a semi-automatic extraction of 3D-point-clouds on a photogrammetric workstation. From these points the roofs are generated and the walls are built by projection of the roofs to the digital terrain model or directly from cadastral data. The textures of roofs and walls are finally extracted by projection of the models into the aerial photos. As stated by CyberCity a good operator is able to extract up to 500 roof parts per day.

In our approach a big limitation is the missing availability of several data sources. To create models for a selected urban area of the world in a short time it is often only possible to obtain very few high resolution satellite images of the area.

Subject of this work is to develop a system which creates urban models only from a minimum of two high resolution stereo satellite images. Such images are provided at the moment e. g. by Space Imaging (Ikonos, SpaceImaging 2006) with a ground resolution of about 1 meter pan and 4 m multispectral or Digital Globe (QuickBird, 60 cm panchromatic and 2.4 m multispectral).
In the near future many more high resolution optical satellites are due to go into operation like WorldView I (2006) and II (2008) offering half-meter panchromatic and 1.4 to 1.8 m multispectral resolution (DigitalGlobe 2006).

Methods and algorithms

Area based matching algorithms depend on comparing similar areas of a matching window. But areas with steep slopes and large convergence angles lead to problems with occlusion where such area based matching fails.

One requirement for a good algorithm for generating DSMs in urban areas is therefore a good handling of geometric changes (a roof appearing wide in one and narrow in the other image) and occlusions (walls only seen in one image).

By visual interpretation of a stereo image pair, objects like houses, trees and cars can be interpreted easily. Also the human recognition masks out inconsistent areas as occlusions automatically. Hidden features in one and the other image vanish when looking at the stereoscopic image and the brain recognizes a fairly good 3D image with almost perfect height information.

Therefore an algorithm was searched which maps corresponding lines of the image pair one to the other. This restriction to lines only can be introduced in a first approch if we stick to epipolar geometry of the images.

A possible solution was found in an approach called "dynamic time warping" based on dynamic programming which is well known in speech recognition (Ney 1982, Sakoe & Chiba 1978, Itakura 1975). Recorded samples of words rarely fit to actual spoken words. A system has to match the recorded voice with learned words. To achieve this all samples are fragmented in overlapping short parts of which a spectral characteristic is memorized. The same procedure is applied to the voice input. As speech is varying in duration such sequences seldom fit together. But a simple linear stretch in time is not applicable because words are not uniformly stretched. Vowels are stretched more whereas consonants mostly keep the same length.

Due to the fact that the requirements are very comparable – warp two sequences of values to each other – this approach seems to be suitable. Similar algorithms are already used in the meantime also in computer vision (van Meerbergen et al. 2002, Hirschmüller 2005).

2 Description of the DSM generation methods

2.1 *Hierarchical intensitiy based matching (''method A'')*

Hierarchical intensity based matching as implemented into XDibias image processing system of DLR consists of two major steps.

In a first step the matching process uses a resolution pyramid (Lehner & Gill 1992, Kornus et al. 2000) to cope even with large stereo image distortions stemming from carrier movement and terrain. Large local parallaxes can be handled without knowledge of exterior orientation which is often not available with sufficient accuracy. The selection of pattern windows is based on the Foerstner interest operator (Foerstner & Guelch 1987) which is applied to one of the stereo partners. For selection of search areas in the other stereo partner(s) local affine transformations are estimated based on already available tie points in the neighborhood from a coarser level of the image pyramid.

Tie points with an accuracy of one pixel are located via the maximum of the normalized correlation coefficients computed by sliding the pattern area all over the search area. These approximate coordinates of tie points are refined to sub-pixel accuracy by local least squares matching (LSM). The number of tie points found and their final sub-pixel accuracy achieved depend mainly on image similarity and decrease with increasing stereo angles or time gaps between imaging. The software was originally devised for along-track 3-line stereo imaging as utilized by stereo scanners MEOSS and MOMS operated by DLR.

Normally, the procedure can be executed fully automatically and results in a rather sparse set of tie points well suited for introduction into bundle adjustment and as an excellent source of seed points for further densification via region growing in the second step. For example in the Munich Ikonos case there are only 1% tie points or 0.6% in Athens area when the totally available number of pixels is taken as reference.

The second step uses the region growing concept first published by Otto & Chau (1989) based on the implementation of the Technical University of Munich (TUM) (Heipke et al. 1996). It combines LSM with a strategy for local propagation of initial conditions of LSM.

Various methods for blunder reduction are used for both steps of the matching:

- Threshold for correlation coefficient
- 2-directional matching and threshold on resulting shifts of the coordinates
- Threshold on residuals in image space from forward intersection based on the rigorous modeling of the imaging process or on rational polynomial functions (RPC).

In areas of low contrast the propagation of affine transformation parameters for LSM in region growing leads to high rates of blunders. In order to avoid intrusion into homogeneous image areas (e. g. roof planes without structure) the extracted image chips are subject to low thresholds on variance and roundness of the Foerstner interest operator. This and the many occlusions found in densely built-up areas imaged with a large stereo angle create lots of insurmountable barriers for region growing. Thus for this type of stereo imagery the massive number of seed points provided by the matching in step one turns out to be essential for the success of the region growing.

The numbers of tie points found and their sub-pixel accuracy is highly dependent on the stereo angle. A large stereo angle and thus a large base to height ratio b/h leads to poorer numbers of tie points and to lower accuracy in LSM via increasing dissimilarity of correctly extracted image chips. Thus, a large b/h cannot be recommended for stereo imaging of city areas. This contradicts the normal imaging practice for Ikonos and QuickBird stereo acquisitions. Tab. 1 gives the percentages of tie points from the two matching steps for the Munich and Athens test areas.

Tab. 1: Percentages of tie points in relation to interest operator points (original image resolution of image pyramid) and total number of pixels in image (region growing).

Test area	Stereo angle (degrees)	b/h ratio	Percentage of tie points	
			Base: interest op.points	Base: total pixels
Munich	9.95°	0.17	86%	84%
Athens	30.28°	0.54	46%	41%

Tab. 2: Mean correlation coefficient c from LSM and standard deviation sigma of residuals in RPC forward intersection (after blunder reduction).

Area	c	sigma [pixel]
Munich	0.90	0.137
Athens	0.78	0.175

In a first approximation the standard deviation of stereo height measurement is proportional to the quotient of the standard deviation of the image coordinates from matching and the base to height ratio. Thus, a smaller b/h can be compensated by improved matching accuracy. This effect can be seen in Tab. 2 for our test areas where the smaller b/h seems to be even more than compensated by better matching conditions. Thus, in case of small stereo angles more tie points with overall better accuracy can be determined in densely built-up areas resulting in a better DSM.

The tie point determination described above does not require epipolar geometry. The method described in the next chapter is depending on epipolar geometry. For VHR satellite imagery software has been developed to derive quasi epipolar images using algorithms given in Morgan (2004). For standard stereo configurations Ikonos images can be ordered already in epipolar geometry from SpaceImaging. With the newly developed software epipolar images can be generated also for multi-temporal stereo pairs and non-standard Ikonos stereo imaging conditions as for Munich test case.

In order to compute a DSM from the tie point cloud from matching the object space coordinates of the tie points are computed by forward intersection based on the rigorous modeling of the imaging process or on RPC. If ground control points are available they are used in bundle adjustment or correction of RPC. The irregular 3D point cloud is transformed into a regular DSM grid by using the triangulation and interpolation as described in Hoja et al. (2005).

2.2 *Dynamic line warping (''method B'')*

The images are assumed to be available as a stereo pair with parallaxes in image line direction (epipolar images, horizontal epipolar lines). Creating a dense digital surface model (DSM) from such image pairs is based on finding corresponding image parts in each of the two images and calculating a local height of an image feature out of the relative displacement of the locations of this feature in the two images (parallaxes).

Because of the assumption of epipolar images there exist only horizontal parallaxes and no vertical shifts between the two images. This allows reducing the problem ''find correlations of image parts between two images'' to only ''find correlations in corresponding lines of the images''. Each line of an image is represented as a profile of gray values as shown in figure 1 top and bottom respectively.

Such sequences have to be mapped on each other stretching and compressing parts to achieve an optimal local fit. To achieve this the ''dynamic time warp'' algorithm used in speech recognition was implemented to warp image lines one to the other (Krauß et al. 2005).

The method used in speech recognition (Ney 1982) calculates spectral characteristics for short overlapping parts of the audio samples and distances between each of these parts and uses dynamic programming to receive a so called ''minimal total distance'' for the given sample with the compared sample of the dictionary. Only this minimum total distance is used further for determining the most probable sequence of words.

For explanation of the method let's take as an example two sequences of values I and I' as $I^T = (1\ 0\ 2\ 1\ 0)$ and $I'^T = (0\ 1\ 0\ 2\ 1)$. The distance-matrix $M_{i,j}$ will then be calculated as $M_{i,j} = |I_i - I'_j|$ thus

$$M = \begin{pmatrix} 1 & 0 & 1 & 1 & 0 \\ 0 & 1 & 0 & 2 & 1 \\ 2 & 1 & 2 & 0 & 1 \\ 1 & 0 & 1 & 1 & 0 \\ 0 & 1 & 0 & 2 & 1 \end{pmatrix}$$

In the next step the rows and columns are cumulated to a matrix D filling the first line and column according to

$$D_{1,j} = \sum_{k=1}^{j} M_{1,k}, \qquad D_{i,1} = \sum_{k=1}^{j} M_{k,1}$$

and the rest of the matrix $D_{i,j}(i,j > 1)$ as

$$D_{ij} = M_{ij} + \min\{D_{i-1,j}, D_{i,j-1}, D_{i-1,j-1}\}$$

yielding D in the example from above:

$$D = \begin{pmatrix} \mathbf{1} & \mathbf{1} & 2 & 3 & 3 \\ 1 & 2 & \mathbf{1} & 3 & 4 \\ 3 & 2 & 3 & \mathbf{1} & 2 \\ 4 & 2 & 3 & 2 & \mathbf{1} \\ 4 & 3 & 2 & 4 & \mathbf{2} \end{pmatrix}$$

In this Matrix D the overall distance is defined as the rightmost bottom element – in the example 2. This is a measure for all needed shifting, stretching and squeezing operations for one sequence to fit onto the other. In speech recognition it's sufficient finding the dictionary sample with the smallest minimal total distance to the given voice input. But beneath this minimal total distance a so called "minimal path" can be defined. This path connects the endpoints of the compared sequences in a manner describing what parts of one sequence has to be shifted, stretched or squeezed to fit on the other. From this minimal path the searched parallaxes can be extracted. Starting from the rightmost bottom element going back always using the smallest possible next neighbour to the top, left or top-left gives the minimal path (marked above in bold).

For the implementation of the algorithm we first have to define a "distance". In the case of a direct comparison of the sequences of gray values of the two epipolar images this can be in a first approach the absolute value of the gray value distance.

Calculating the matrix, picking a small area of the result and showing the extracted correlations between the input gray value profiles yields Fig. 1. As can be seen well areas with different widths in the profiles are correctly mapped to each other.

A perfectly diagonal line as minimal path represents no relative displacements between the two profiles. All deviations from this line indicate the searched parallaxes. If this minimal path is represented by pairs of coordinates $\mu_k = (i,j)_k$ it's possible to fit a parabola through $D_{i-1,j+1}$, $D_{i,j}$ and $D_{i+1,j-1}$ to calculate the parallaxes as the minimum of this parabola in subpixel accuracy.

Using small window areas of diameter ω around every line position for calculating the distance $M_{i,j}$ gives better results but introduces on the other hand smoothing effects as resulting from area based methods. The distance $M_{i,j}$ of line y with images $I_{x,y}$ and $I'_{x,y}$ and window size ω is then calculated as

$$M_{i,j} = \sum_{\lambda=-\lfloor\omega/2\rfloor}^{\omega-\lfloor\omega/2\rfloor-1} \sum_{\mu=-\lfloor\omega/2\rfloor}^{\omega-\lfloor\omega/2\rfloor-1} |I_{i+\lambda,y+\mu} - I'_{j+\lambda,y+\mu}|$$

Afterwards a vertical median filter of size 3 is applied to reduce line streaking and blunders resulting from the line by line correlation. For acceleration of processing time a maximum correlation window size can be chosen. Outside of this distance from the main diagonal the matrix M simply gets filled with a maximum distance value instead of the calculated distance.

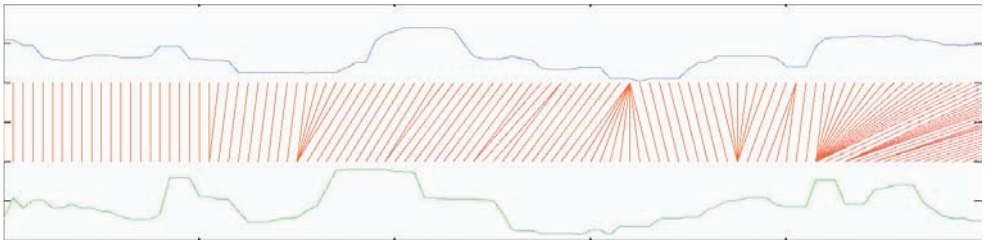

Fig. 1: Found correlations between the two input gray value profiles (top and bottom of graphic).

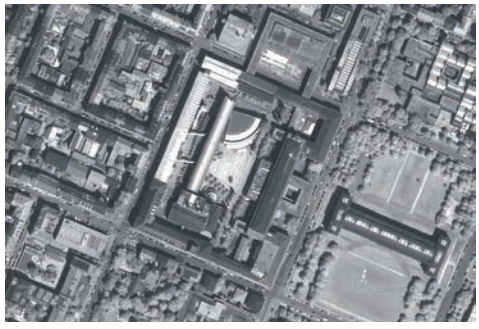

Fig. 2: Ikonos image of test area ''Munich TUM'' (600 m × 400 m).

3 Image and reference data

For experiments the following Ikonos data sets provided by Space Imaging were used:

- Munich acquired 2005-07-15, 10:28 GMT, level 1A images (only corrected for radiometry and inner orientation) with a ground resolution of 83 cm and declination angles of $+9.25^\circ$ and -4.45°
- Athens acquired 2004-07-24, 9:24 GMT, level 1B image pair (epipolar) with a ground resolution of 88 cm and declination angles of -19.99° and $+13.17^\circ$

Apart from these high resolution satellite imagery a set of laser scanner data from the region around the Technical University in Munich was available as reference data.

The high resolution Ikonos satellite imagery is accompanied by rational polynomial coefficients (RPCs) for every image. These coefficients are used to transform geographical coordinates longitude X, latitude Y and ellipsoid height Z to image coordinates $(x, y)^T$ by division of two polynoms with 20 coefficients each (Jacobsen et al. 2005, Grodecki et al. 2004).

The Munich scene is a non-standard Ikonos stereo acquisition with a small stereo angle of about only 10°. SpaceImaging provided the radiometrically corrected images with RPC. After applying the area based matching (image pyramid) tie points were available for transformation of the image pair into epipolar geometry (all parallaxes in column direction).

The Athens scene was acquired as a so called ''Ikonos standard stereo pair'' which stands for an exposure with declination angles of about 10° to 20° each in one orbit and delivery as epipolar images (actual stereo angle was 30.28°).

The images given in Fig. 3 contain the same clippings from the Ikonos stereo pair as the DSMs in Fig. 4. As can be seen the blocks of houses mostly contain narrow courtyards in the center. These courtyards are about 8 to 10 m wide whereas the houses

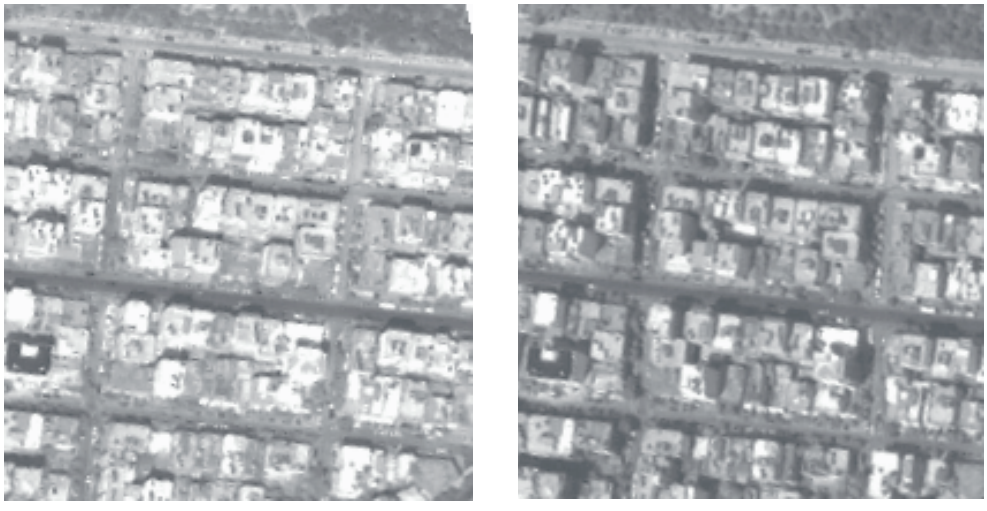

Fig. 3: Sections (250 m × 250 m) of the stereo pair test area ''Athens''.

are about 15 m and the streets are about 12 m wide.

4 Application of the methods to the test data

4.1 *Test data set Athens*

The first example is the test data set "Athens" as shown in Fig. 3. Applying first the classical hierarchical algorithm (referred as A in the following) gives as a result the DSM shown in Fig. 4, left.

Applying the dynamic programming algorithm (method B) with a window size $\omega = 3$ yields Fig. 4, right.

The DSM in Fig. 4, left generated with the classical hierarchical algorithm (A) shows no large blunders but a much more smooth DSM whereas the DSM calculated with the dynamic programming (method B, Fig. 4, right) shows sharp edges but many blunders and streaking in epipolar direction because of no linkage between the calculation of every epipolar line. As can be seen method B shows much more details especially at sharp ridges than method A but generates also more blunders.

As can be seen in Fig. 4 method A smoothes out most of the smaller courtyards because of the window size of 13×13 pixels used in region growing. The streets in this area are, however, wide enough to be found by method A. Method B on the other hand reveals sharp edges from top to bottom reproducing buildings, courtyards and streets much more clearly whereas the line streaking effects leading to blurry edges can be seen left to right – in epipolar direction.

4.2 *Test data set Munich*

Applying method A to the Munich scene shown in Fig. 2 yields the DSM shown in Fig. 5 and 6 left.

As can be seen the results are obviously better than in the Athens scene. Small courtyards are better resolved than in the previous test case. However comparing Fig. 5, left with the reference laser DSM (Fig. 7) shows some blurring at the edges of the buildings and smoothed out regions on the main building of the university.

After transforming the Munich scenes locally to epipolar geometry using some tie points the dynamic programming algorithm is applied to the area around the technical university with a window size of 3 (Fig. 5, right) and the analogous clipping in Fig. 6 on the right side.

Comparing the two DSMs generated by method A and B and the laser DSM reveils the differences as can be seen in Fig. 5 to 7.

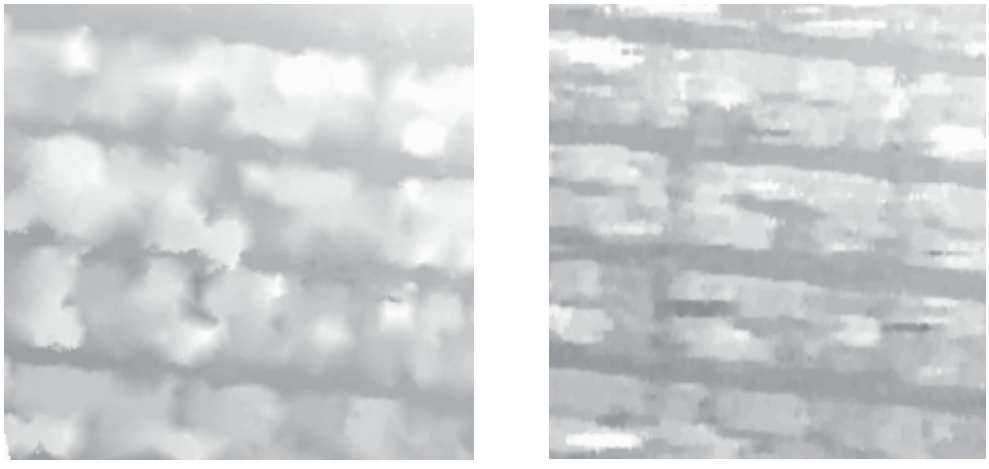

Fig. 4: Details of DSMs of the test area "Athens" (Fig. 3) generated by hierarchical intensity based matching (method A, left) and by dynamic line warping (method B, right).

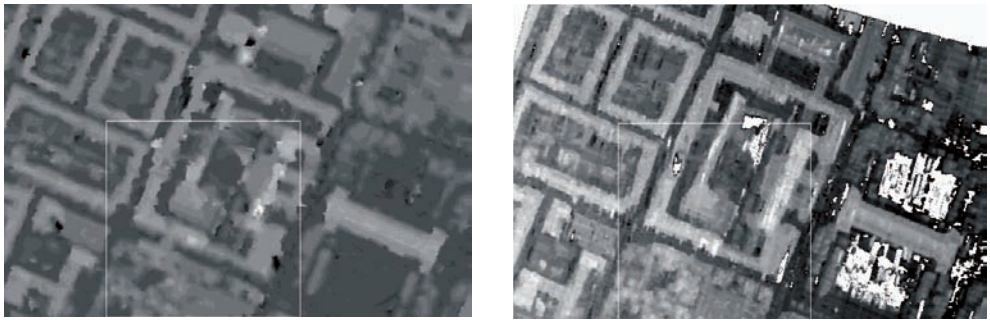

Fig. 5: DSM generated by applying the hierarchical intensity based matching of method A (left) to the Munich scene Fig. 2, right: DSM calculated with method B.

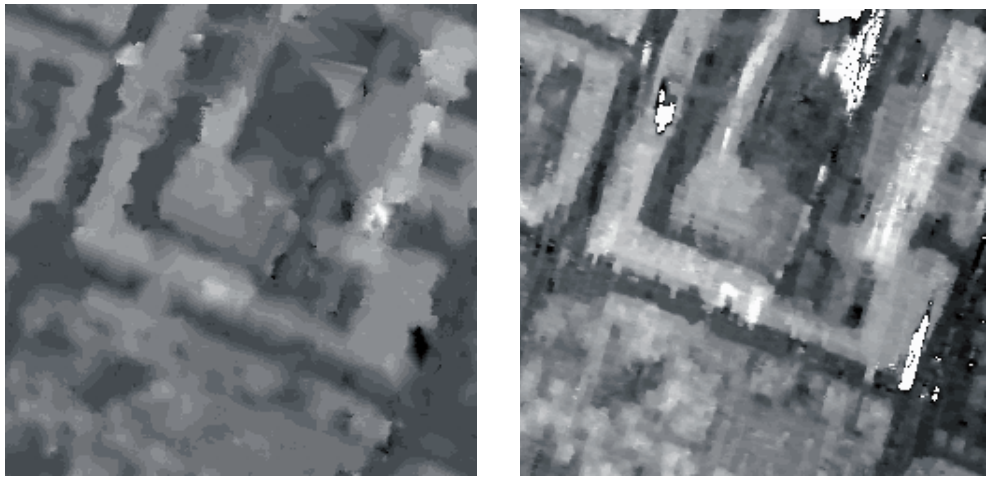

Fig. 6: Clips from Fig. 5, 250 m × 250 m, left method A, right method B.

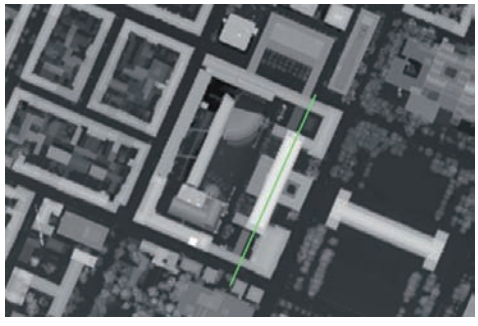

Fig. 7: DSM of test area ''Munich, TUM'' (Fig. 2) generated from Laser scanning data. The green line shows the location of the profile depicted in Fig. 9.

Fig. 7 shows the laser DSM used as reference data for comparison of the generated DSMs from the Ikonos images.

The DSM generated by method B shows much less smoothing than the one generated with method A but on the other hand more blunders as can be seen for example in the grass area near the Old Pinakothek and streaking effects in epipolar direction (top to bottom).

Fig. 8: Masks created manually showing buildings (left), streets, grass and soil (middle) and trees (right).

The edges of the buildings are more straight in epipolar direction with method B than with method A but cross epipolar direction more jagged than with method A due to the line streaking effects. So the tower of the university in the middle of the southern buildings gets nearly wiped out with method B due to the streaking where on the other hand the rim of the western building and the ridge of the main building is badly reproduced by method A.

5 Quality assessment of the generated DSMs

5.1 *Masking*

For assessment of the generated DSMs the test area is divided into three classes, namely:

- buildings
- streets, grass and soil
- trees

Masks for these areas were manually created (see Fig. 8).

Statistics and histograms were calculated for every class. Tab. 3 shows the mean heights h and standard deviation σ for each of the masked areas and each DSM case.

Tab. 3 shows that both methods estimate the heights of buildings in reference to the laser DSM about 2.5 m too low and the level of streets and soil about 1.5 m too high. This is due to a smoothing of the walls as can be seen also in the profile in Fig. 9 which raises on the one hand street levels in proximity to steep walls and lowers building heights near rims of the buildings on the other hand. The standard deviations of the differences certifies method A better results than method B especially in building areas.

Method B shows an overestimation of tree heights in comparison to the laser DSM and method A of about 4 m. The laser DSM is a composit of flight campaigns in April and November 2003 with sparse foliage and all fetched 3D points averaged. Thus the heights in the laser DSM should be lower than the DSMs generated from the july Ikonos imagery. As shown in Reinartz et al. (2005) forest and tree heights are often underestimated by optical stereo evaluation using method A.

Tab. 3: Mean heights h and standard deviation sigma in meters for the three masks applied to laser-DSM and DSMs generated by method A and B. The last two lines show the difference DSMs between the DSM of method A and the laser DSM and DSM B and the laser DSM.

	Buildings		Streets		Trees	
Channel	h	σ	h	σ	h	σ
Laser DSM	530.34	6.21	517.48	4.49	522.25	4.17
Method A	527.85	6.72	519.14	6.41	523.18	5.52
Method B	527.97	8.13	518.84	7.33	526.18	6.14
A − Laser	−2.49	3.49	1.66	5.56	0.92	4.68
B − Laser	−2.37	5.11	1.36	5.95	3.92	4.46

5.2 *Profiles*

As another method for visualization of the quality of two DSMs profiles are chosen. Fig. 9 shows a profile cut from south to north along the main building of the university starting at a tree south of the street and stretching over the campus through the street north as drawn into Fig. 7.

The first peak denotes a tree south of the street. The second peak is the first (southern) building, after a small courtyard follows the gable of the main building, a second yard and the northern building. Since the southern and northern buildings are cut across the roof slope can be seen.

Looking at the steep walls of the buildings a smoothing as shown in Fig. 9 on the right building can be seen. Analyzing the slope shows that the width of an object is almost correct at a height of about 80% and smoothes out about 4 to 5 meter at the bottom of a building.

In this case of the Munich scene no significant differences in smoothing out steep walls between method A and B can be seen. However both methods are not satisfactory enough because of large errors e. g. on the main building arising from missing tie points in method A or height errors in the first courtyard with method B arising from streaking effects in epipolar direction.

Looking at profiles across buildings in the Athens case gives another view as can be seen in Fig. 10.

The profile show a clear difference in the smoothing out of steep walls in comparison to the munich scene profiles above. Especially in Fig. 10 complete courtyards are missing due to non existing tie points because of the large convergence angle of this stereo pair.

The quality of the DSM generated by method B shows no such big degradation under increasing convergence angles as method A. Here also streets, courtyards and steep walls still remain visible and get reproduced reasonably good as can be proved by visual check of the DSMs from Fig. 4 with the original imagery in Fig. 3.

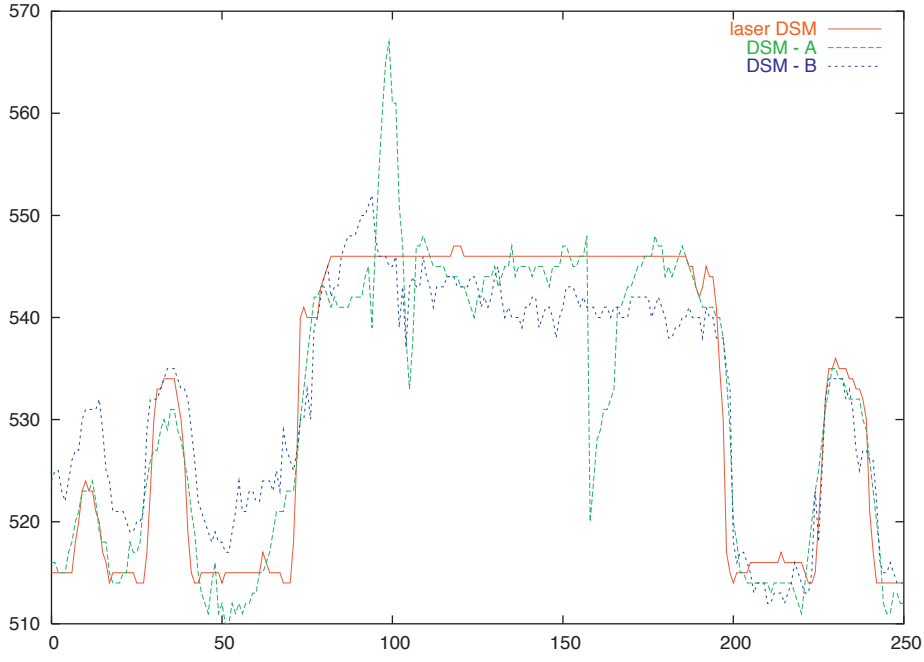

Fig. 9: Profiles of the DSMs generated by method A and B for test area ''Munich, TUM'' (all units in meter). The location of the profile is shown in Fig. 7.

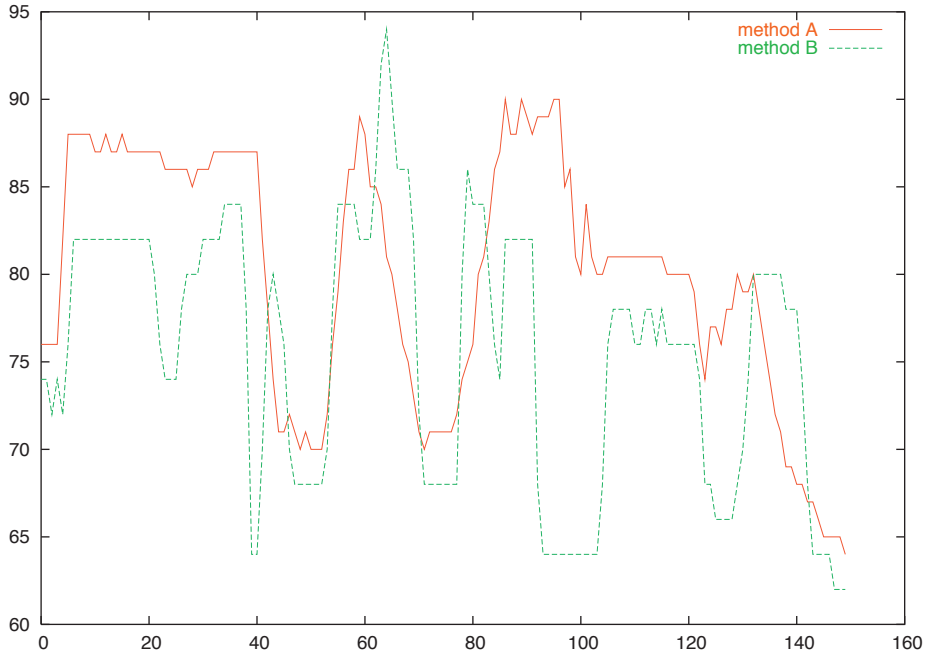

Fig. 10: Profile from center of Fig. 4 showing higher buildings with narrow courtyards.

6 Discussion

Comparing the DSMs generated by the two methods for the two test scenes shows pros and cons for both methods. So method A relies heavily on finding good tie points in the first step since the region growing can't proceed to large areas in urban scenes due to occlusion and other effects. But missing tie points result in a smoothing out and therefore no straight and sharp edges.

Method B on the other hand suffers in the herein presented algorithm much from streaking effects and large blunders in meadows.

But comparing the profiles of the DSMs of the Munich scene with the Athens scene shows clearly an effect of the larger convergence angle in the Athens case. While method B achieves almost the same character of the DSM as in the Munich case with a relatively small convergence angle the DSM quality of method A drops significantly due to more missing important tie points and therefore a smoothing out of much more small details like streets or courtyards.

Further work will be needed to reduce the streaking between lines through interconnection of the epipolar lines in the DSM generation with method B. Also analyzing and eliminating large blunders in grass areas possibly due to BRDF effects have to be implemented.

References

3D Geo, 2006: http://www.landxplorer.net/. (accessed 02/2006)

CyberCity, 2006: http://www.cybercity.tv/. (accessed 02/2006)

DigitalGlobe, 2006: http://www.digitalglobe.com/about/imaging.shtml. (accessed 02/2006)

SpaceImaging, 2006: http://www.spaceimaging.com/. (accessed 02/2006)

Foerstner, W. & Guelch, E., 1987: A Fast Operator for Detection and Precise Location of Distinct Points, Corners and Centres of Circular Features. – ISPRS Intercommission Workshop, Interlaken.

Grodecki, J., Dial, G. & Lutes, J., 2004: Mathematical Model for 3D feature extraction from multiple satellite images described by RPCs. – ASPRS Annual Conference Procee-dings, Denver, Colorado

Heipke, C., Kornus, W. & Pfannenstein, A., 1996: The evaluation of MEOSS airborne 3-line scanner imagery – processing chain and results. – Photogrammetric Engineering and Remote Sensing **62** (3): 293–299.

Hirschmüller, H., 2005: Accurate and efficient stereo processing by semi-global matching and mutual information. – IEEE Conference on Computer Vision and Pattern Recognition (CVPR).

Hoja, D., Reinartz, P. & Lehner, M., 2005: DSM generation from high resolution satellite imagery using additional information contained in existing DSM. – International Archives of the Photogrammetry, Remote Sensing and Spa-tial Information Sciences **36** (1/W3). ISPRS Workshop, Hannover

Itakura, F., 1975: Minimum prediction residual principle applied to speech recognition. – IEEE Trans. Acoust. Speech signal process ASSP **23:** 67–72.

Jacobsen, K., Büyüksalih, G. & Topan, H., 2005: Geometric Models for the orientation of high resolution optical satellite sensors. – International Archives of the Photogrammetry, Remote Sensing and Spatial Information Sciences **36** (1/W3). ISPRS Workshop, Hannover.

Kornus, W., Lehner, M. & Schroeder, M., 2000: Geometric inflight calibration by block adjustment using MOMS-2P 3-line-imagery of three intersecting stereo-strips. SFPT (Société Française de Photogrammétrie et Télédétection) **159:** 42–54.

Krauß, T., Reinartz, P., Lehner, M., Schroeder, M. & Stilla, U., 2005: DEM Generation from Very High Resolution Stereo Satellite Data in Urban Areas Using Dynamic Program-ming. – International Archives of the Photogrammetry, Remote Sensing and Spatial Information Sciences **36** (1/W3).

Lehner, M. & Gill, R., 1992: Semi-automatic derivation of digital elevation models from stereoscopic 3-line scanner data. – ISPRS 29 (B4): 68–75.

Morgan, M., 2004: Epipolar Resampling of Linear Array Scanner Scenes. – PhD thesis, University of Calgary, Canada. UCGE Reports Nr. 20193.

Ney, H., 1982: Dynamic programming as a technique for pattern recognition. – Proc. 6th Int. Conf. Pattern Recognition, pp. 1119–1125.

Otto, G. & Chau, T., 1989: Region growing algorithm for matching of terrain images. – Image and vision computing **7** (2): 83–94.

Reinartz, P., Müller, R., Hoja, D., Lehner, M. & Schroeder, M., 2005: Comparison and Fusion of DEM derived from SPOT-5 HRS and SRTM Data and Estimation of Forest Heights. – Proc. EARSeL workshop Special Interest Group 3D Remote Sensing, pp. 10 on CD-ROM

Sakoe, H. & Chiba, S., 1978: Dynamic programming algorithm optimization for spoken word recognition. – IEEE Trans. Acoust. Speech signal process, ASSP **26:** 43–49.

van Meerbergen, G., Vergauwen, M., Pollefeys, M. & van Gool, L., 2002: A hierarchical symmetric stereo algorithm using dynamic programming. – International Journal of Computer Vision **47** (1/2/3): 275–285.

Addresses of the authors:

Dipl.-Phys. Thomas Krauß,
e-mail: thomas.krauss@dlr.de

Dr. Manfred Lehner
e-mail: manfred.lehner@dlr.de

Dr. Peter Reinartz
e-mail: peter.reinartz@dlr.de

German Aerospace Center (DLR)
Remote Sensing Technology Institute
PO Box 1116, D-82230 Weßling, Germany

Prof. Dr. Uwe Stilla
e-mail: stilla@bv.tu-muenchen.de

Photogrammetry and Remote Sensing
Technische Universität München
Arcisstrasse 21, D-80333 München

Manuskript eingereicht: März 2006
Angenommen: April 2006

Photogrammetrie • Fernerkundung • Geoinformation 4/2006, S. 315–325, 11 figs., 1 tab.

Detection of Vehicle Queues in QuickBird Imagery of City Areas

Jens Leitloff, Stefan Hinz & Uwe Stilla, München

Keywords: Remote Sensing, urban, feature extraction, edge detection, optical satellite imagery, QuickBird

Summary: There is an increasing demand in traffic monitoring of densely populated urban areas. Fixed installed sensors like induction loops, bridge sensors and cameras only acquire traffic flow in a limited area. To complement these systems, our approach uses satellite images for detecting vehicle queues on the entire road network.

In satellite imagery single vehicles are merged to either dark or bright ribbons if they stand in a row. Therefore they can hardly be separated, since they show no detectable features like windshields or shadows. To decrease the number of misdetections it is necessary to use a priori information of road location and direction from GIS to exclude non-relevant areas for the queue detection algorithm.

Initial hypotheses for the queues can be extracted as lines which represent the centers of the queues. We then exploit the fact that vehicle queues show a repetitive pattern. This pattern is also observably in the width profile of queues which can be derived from the gradient amplitude image. Variations of the width profile are analyzed for discrimination of single vehicles within a queue and an algorithm to robustly estimate the contrast of single vehicles is used for verification. We show results obtained from panchromatic QuickBird imagery covering a part of a complex inner city area and discuss the numerical evaluation of the results.

Zusammenfassung: *Erkennung von Fahrzeugreihen in QuickBird-Bildern von Stadtgebieten.* Durch das weiterhin wachsende Verkehrsaufkommen in urbanen Gebieten besteht ein verstärkter Bedarf nach intelligenter Verkehrsüberwachung und -beeinflussung. Die Erfassung der dafür benötigten Daten erfolgt hauptsächlich durch fest installierte Sensoren, wie Induktionsschleifen oder Brückenkameras. Da diese Systeme nur einen Teil des Straßennetzes abdecken, wird in der vorliegenden Arbeit ein Ansatz zur Erkennung von Fahrzeugreihen aus optischen Satellitenbildern vorgestellt. Die dadurch flächendeckend gewonnenen Daten können als Ergänzung zu vorhandenen Verkehrsmodellen genutzt werden.

Um eine möglichst geringe Fehlerrate bei der Fahrzeugerkennung zu erhalten, werden GIS Daten als zusätzliche Information verwendet. Nicht relevante Bildregionen können hierdurch ausgeschlossen werden.

Da Fahrzeugenreihen in Satellitenbildern aufgrund der geringen Auflösung als zusammenhängende Linien abgebildet werden, erfolgt als erster Schritt deren Erfassung durch Linienextraktion. Im Anschluss wird die Breite der extrahierten Linien im Gradientenbild bestimmt. Durch Analyse der Variation der Breite, welche sich wiederholende Muster zeigt, können anschließend Hypothesen für einzelne Fahrzeuge extrahiert werden. Zur Verifikation der gefundenen Hypothesen wird deren Kontrast zur Straßenoberfläche verwendet.

Es werden Ergebnisse aus der Prozessierung eines innerstädtischen QuickBird Bildes und deren Evaluierung gezeigt.

1 Introduction

1.1 *Motivation*

There is an increasing demand in traffic monitoring of densely populated areas. The traffic flow on main roads can partially be acquired by fixed installed sensors like induction loops, bridge sensors and stationary cameras. Usually traffic on smaller roads – which represent the main part of urban road networks – is rarely collected and informa-

1432-8364/06/2006/0315 $ 2.75

tion about on-road parked vehicles is not captured. Wide-area images of the entire road network can complement these selectively acquired data. New optical sensor systems on satellites provide images with 1-meter resolution or better, e. g. Ikonos and QuickBird, make this kind of imagery available. Hence new applications like traffic monitoring and vehicle detection from these images have achieved considerable attention on international conferences, e. g. (Bamler & Chiu 2005, Heipke et al. 2005, Stilla et al. 2005). The presented approach focuses on the detection of single vehicles by extraction of vehicle queues from satellite imagery.

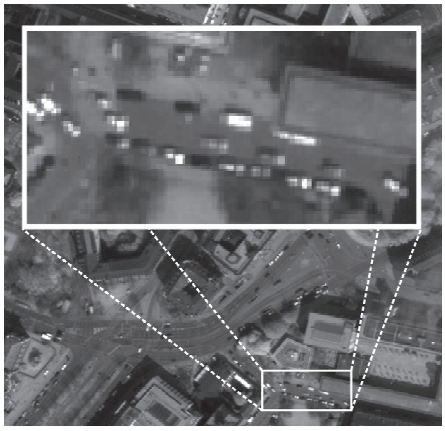

Fig. 1: Vehicles in satellite imagery (Quick-Bird). GSD = 0.6 m.

1.2 *Related work*

Depending on the used sensors and the resolution of the imagery different approaches (Stilla et al. 2004) have been developed in the past. The extraction of vehicles from images with resolution about 0.15 m is widely tested and delivers good results in many situations. These approaches either use implicit or explicit vehicle models (Hinz 2003). The appearance-based, implicit model uses example images of vehicles to derive gray-value or texture features and their statistics assembled in vectors. These vectors are used as reference to test computed feature vectors from image regions. Since the implicit model classification uses example images the extraction results depend strongly on the choice of representative images.

Approaches using an explicit model describe vehicles in 2D or 3D by filter or wire-frame representations. The model is then matched „top-down" to the image or extracted image features are grouped „bottom-up" to create structures similar to the model. A vehicle will be declared as detected, if there is sufficient support of the model found in the image. These attempts deliver comparable or even better results than approaches using implicit models but are hardly applicable to satellite imagery where vehicles appear as blobs without any prominent sub-structures (see Fig. 1).

Three different methods for vehicle detection from simulated satellite imagery of highway scenes are tested in (Sharma 2002). The gradient based method and the method using Bayesian Background Transformation (BBT) deliver the best number of vehicle counts compared to ground truth. Since the number of false detections is lower using BBT, this method is more reliable. A third method using Principal Component Analysis (PCA) gives inconsistent performance depending on the noise level of the image. Furthermore, the method gives the lowest vehicle count. A manually created background image is mandatory for the PCA and BBT method, which requires extensive interactive work. Consequently, the approach can hardly be generalized and is limited to images of the same scene. Gerhardinger et al. (2005) use the commercial software *Features Analyst*® to implement an iterative learning approach by analyzing the spectral signature and the spatial context. The authors report that good results can be achieved using a very accurate road GIS, which was only available through manual digitalization. An encouraging approach for single vehicle detection is presented in (Jin & Davis 2004). First, they use morphologic filtering for a rough distinction between vehicle pixels and non-target pixels, though being similar to vehicles. Then a morphological shared-weight neural network is used for extraction. The approach

achieves good performance values under the condition that vehicles appear isolated. The approach is not designed for vehicle queues or traffic jams (Jin & Davis 2004).

The latter approaches are designed for a resolution coarser than 0.5 m and limit their search space to roads and parking lots using GIS information. By this, the number of false alarms is significantly decreased.

In dense traffic situations, traffic jams or parking lots, car groupings show quite evident regularities (see e. g. Fig. 1). Exploiting the knowledge about these repeating occurrences and the fact that cars rarely occur isolated is also referred to as global modeling in the field of vehicle detection. Vehicle hypotheses extracted by a neural network classifier (Ruskoné et al. 1996) or a "spot detector" (Michaelsen & Stilla 2001) are collinearly grouped into queues while isolated vehicle hypotheses are rejected. Hinz & Stilla (2006) use a differential geometric blob detector for initial extraction followed by a modified Hough transform for accumulating global evidence for car hypotheses. Since these grouping schemes select hypotheses but do not add new hypotheses, these approaches need an over-segmentation as initial result. They are designed for medium resolution images of approximately 0.5 m GSD.

When high resolution imagery is available a more promising strategy is to focus on reliable hypotheses for single vehicles first and complete the extraction afterwards by searching for missing vehicles in gaps of a queue using a less constrained vehicle model (Hinz 2003). By this, not only queues but also isolated cars can be extracted as long as they belong to the set of reliable hypotheses.

One of the few approaches focusing directly on vehicle queues – in particular military convoys – is presented in Burlina et al. (1997). They extract repetitive, regular object configurations based on their spectral signature. The search space is limited to roads and parking lots using accurate GIS-information in their approach. This seems necessary since the spectrum will be heavily distorted, if adjacent objects gain much in

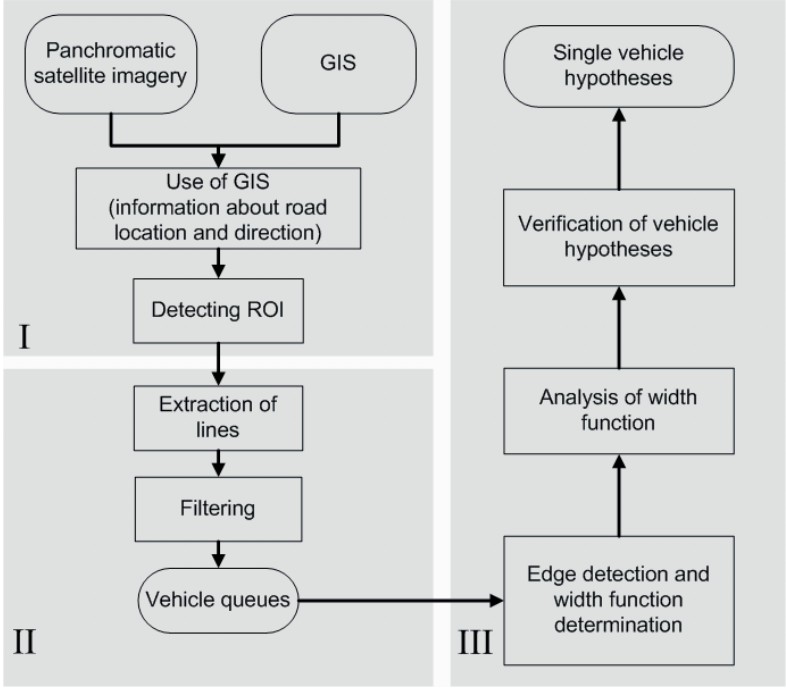

Fig. 2: Processing steps.

influence – even if the spectrum is computed for quite small image patches.

1.3 *System Overview*

Fig. 2 shows the overall design of the presented approach which is separated into three processing stages. In the pre-processing stage (Fig. 2 I) data from a GIS are used to determine Regions of Interest (ROI) in the panchromatic satellite imagery.

Afterwards we use a differential geometric approach to extract initial hypotheses of the queues as lines (Fig. 2 II). From these hypotheses ''single vehicles'' (Fig. 2 III) are determined by analyzing the width profile of the queues calculated from the gradient image. The analysis strategy is ''coarse-to-fine'', i. e. hypotheses generation is based on coarse and global information while for verification and refinement details and context information is utilized.

For testing we have selected a section of a complex inner city area captured by panchromatic QuickBird imagery. This presented work is just the first implementation of a module from a more comprehensive vehicle detection approach for complex urban scenes, which will combine global and local vehicle features for extraction. Hence, the primary objective of this work is to test robust algorithms with high correctness, while less emphasis is put on the achieved completeness.

2 Detection

In section 2.1 the used model will be presented. Section 2.2 describes the extraction of vehicle queues using sophisticated line extraction. Then a number of attributes are calculated (section 2.3). Finally, the attributes are analyzed and checked for consistency to verify or falsify single vehicle hypotheses (section 2.4).

2.1 *Vehicle Queue Model*

Generally, a vehicle queue is defined as ribbon with distinct symmetries along and across its local orientation. Basically, the model is similar to that defined in (Hinz 2003); though, since this model is originally designed for aerial images, a number of modifications regarding the significance of different features have been applied.

A vehicle queue

- must have sufficient length, bounded width and low curvature;

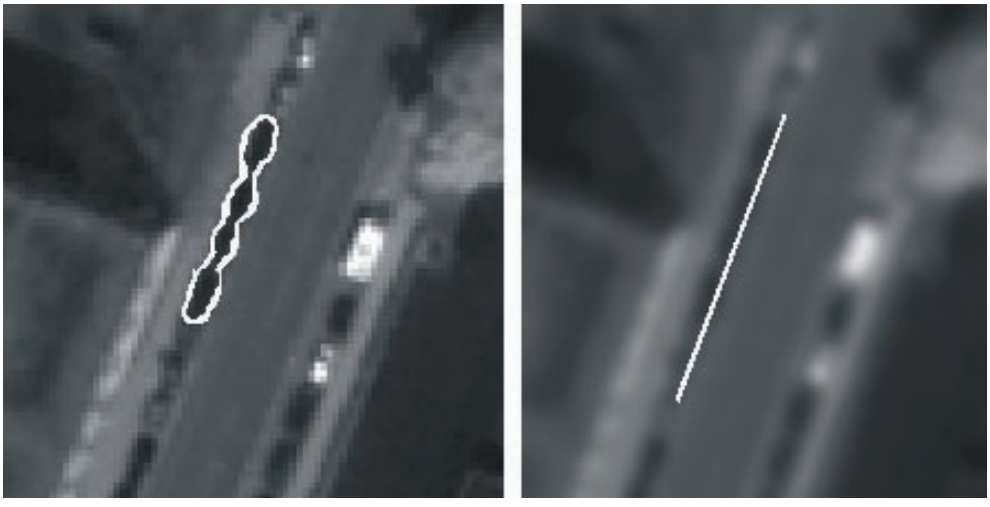

(a) (b)

Fig. 3: Queue model. a) original image, b) smoothed image.

- shows a repetitive pattern along the medial axis, both in contrast and width (Fig. 3a), while length and width of the individual replica correspond to vehicle dimensions;
- collapses to a line in Gaussian scale space, i. e. when smoothing the image accordingly (Fig. 3b).

Please, note that this queue model differs from the above mentioned approaches in a way that – in particular through the scale-space description – the queue is modeled as a unique structure and not just as a composite of its underlying, smaller elements. At first glance, this seems of less importance. Still, it provides the basis for detecting a queue hypothesis as a whole (even though at a coarser scale) rather than constructing it from smaller elements. Thereby global knowledge can be incorporated from the very beginning of extraction.

2.2 *Vehicle Queue Hypotheses*

Since many of the involved image processing algorithms depend on the contrast of the queues, image enhancement seems to be useful. In our case the gray value ranges which contain less information (e. g. over-exposed areas) are cut off. In doing so the image is scaled from the originally 11 bit to 10 bit.

For exploitation of a-priori road information, Regions of Interest (RoI) are derived from road axes of GIS data. Within these areas the vehicle detection is performed. Please notice that the assumption about the road width is vague, because the accuracy of road map data is approx. 2 m.

For generating first hypotheses, line extraction is carried out by applying the differential geometric approach of Steger (1998). This algorithm is primarily based on the computation of the second image derivatives, i. e. the local curvatures of the image function. Parameters for the line extraction are chosen corresponding to vehicle geometry (vehicle width: w) and radiometry (expected contrast to road), i. e. the corresponding scale parameter for line extraction has to be chosen as

$$\sigma = \frac{w}{2\sqrt{3}}$$

where σ defines the smoothing factor, calculated from the maximum expected width (e. g. $w = 2.5$ meter).

In addition, the line extraction algorithm is supported by morphologic filtering with a directional rectangular structuring element oriented along the particular road segment. In doing so the queues are enhanced and substructures in bright cars are almost completely removed. The relaxed parameter settings lead to a huge number of false hypotheses but also return nearly all promising hypotheses for vehicle queues. Fig. 5 shows results for the extraction of bright (cyan) and dark (white) lines. However, since the line extraction requires a minimum amount of contrast between vehicles and the road surface, gray vehicles cannot be extracted reliably, because they hardly emerge from their surroundings.

Bright and dark lines are extracted separately. They are connected if they fulfill distance and collinearity criteria. In the given data a maximum distance of one vehicle length must not be exceeded. Furthermore, the merging of parallel lines would lead to significant positional errors and is therefore prevented. The final processing steps consist of geometric smoothing by polygonal approximation and resampling (Ramer 1972), and testing all resulting lines against a minimum length threshold and a maximum direction difference to the road.

2.3 *Determination of Vehicle Queues' Width*

The width determination is done by detection of vehicle sides in the gradient image. The algorithm starts at the first point of a line and processes consecutively all following points of the line. A profile perpendicular to the line direction is spanned in each point. Afterwards the gray value in the gradient image is calculated by bilinear interpolation, thus, deriving the gradient amplitude function of the profile. The maximum

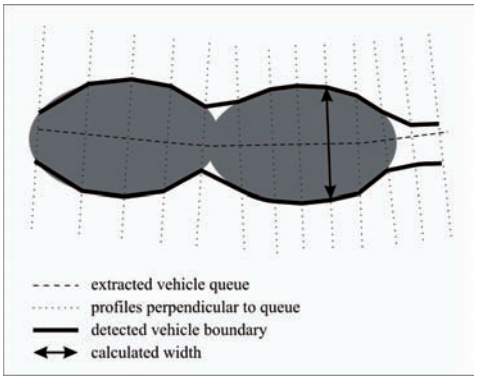

Fig. 4: Concept of queue width determination.

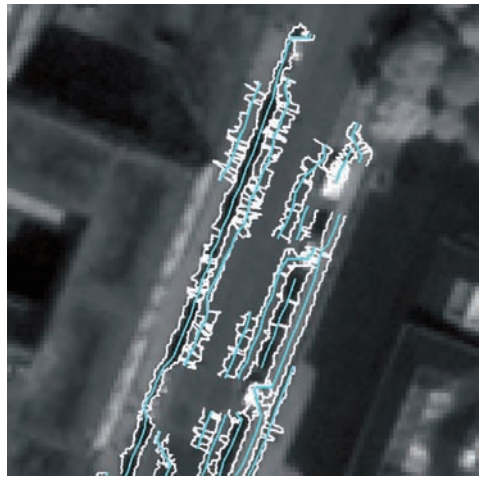

Fig. 5: Width extracted from gradient image: Extracted edges (white), queues' contrelines (cyan).

value on either side of the vehicle queue is supposed to correspond with the vehicle boundary. The distance between the two maximum values is calculated with sub-pixel accuracy and gives the queue width. If no maximum is found the gaps are closed by linear interpolation after width determination. Fig. 4 illustrates the algorithm for width calculation and Fig. 5 shows the result of width extraction.

One can see that most edges correspond to vehicle sides. However, since the gradient image has quite weak contrast, edge extraction delivers also some irregularities, i. e. noisy boundaries. Therefore smoothing of the extracted edges is useful to reduce the number of outliers.

Usually the irregularities are caused by other strong edges nearby the vehicle queue. In future implementations we intend to detect such outliers by a more sophisticated shape analysis of the boundary functions.

2.4 *Separating queues into single vehicles*

To find single vehicles, we use the knowledge that vehicle queues are characterized by significant repetitive patterns caused by gaps between single vehicles. This means that the extracted width function also shows significant variations (Fig. 6). Maximum values in this function approximately are assumed to represent the centres of single vehicles and minimum values represent gaps between two vehicles in the queue.

The following parameters are used:

v_{min} ... minimum length of a single vehicle and search interval
v_{max} ... maximum length of a single vehicle and search interval
l_{min} ... position of the minimum width within search interval
l_{max} ... position of the maximum width within search interval
d ... distance between l_{min} and l_{max}

A vehicle hypothesis is generated if the following condition is fulfilled:

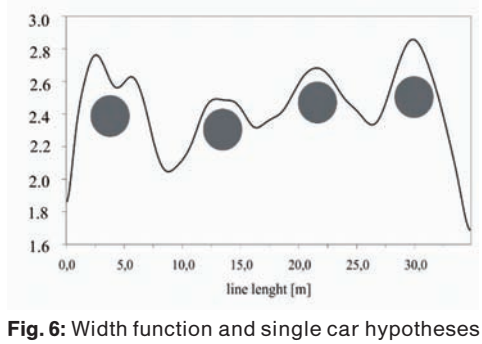

Fig. 6: Width function and single car hypotheses (cricles).

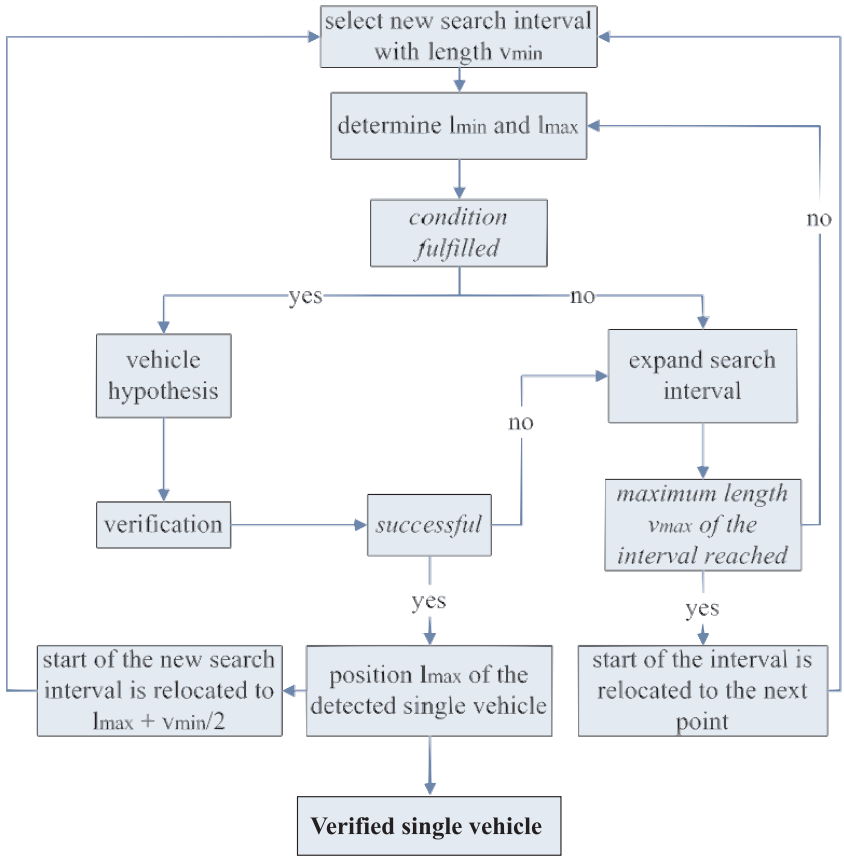

Fig. 7: Concepts of width functions' analysis.

$$\frac{v_{min}}{2} \leq d \leq \frac{v_{max}}{2}$$

Fig. 7 shows the flow chart of the width analysis scheme. Essentially, this algorithm tries to find local maxima and minima in the noisy width function and place the vehicle positions in such a way that vehicle hypotheses do not overlap.

It is possible that more than one hypothesis is found for a vehicle. This is caused by two or more maxima in the width function within the vehicle. Therefore we control the space between two hypotheses not to fall below a certain minimum distance. If more than one hypothesis is found, the hypothesis with the highest maxima in the width function will be verified.

After a hypothesis has been generated we use the contrast of the vehicle and the adjacent road surface for a simple verification. Here the difference of the median gray values of the inner and the outer region is calculated (see Fig. 8).

3 Results

The performance of the implemented approach has been tested on panchromatic QuickBird data with approx. 60 cm GSD. The results of the approach were evaluated concerning the criteria "correctness" and "completeness". They are defined as follows:

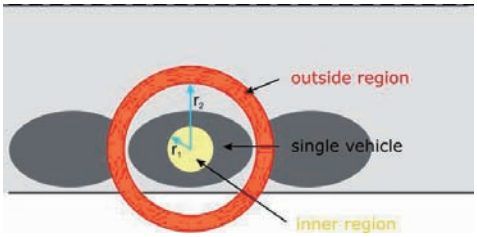

Fig. 8: Verification.

$$\text{correctness} = \frac{TP}{TP + FP}$$

$$\text{completeness} = \frac{TP}{TP + FN}$$

with TP true positives
FP false positives
FN false negatives

The measures refer to single vehicles, i. e. true positives are correctly extracted vehicles, false positives are misdetections, and false negatives are missed vehicles with respect to the reference data. Fig. 9 shows examples of extracted vehicles. The cyan crosses are verified detected vehicles (TP) and the white crosses are misdetections (FP). Tab. 1 summarizes the evaluation depending on the four types of reference data included:

a) all vehicles
b) only bright and dark vehicles, i. e. without gray vehicles
c) only bright vehicles
d) only dark vehicles

Gray vehicles have been excluded from the reference in b) since they almost show no contrast to their surroundings. It has to be mentioned that the acquisition of reference data for some vehicles is certainly not free of errors. Even a human observer is sometimes not able to identify all vehicles in an image scene with high confidence. Therefore our reference data can only be treated as a very good approximation of real "ground-truth".

As mentioned in the beginning we are focussing on high correctness rather than completeness, since we want to test the algorithms' reliability in terms of providing seed points for completing the result. Hence, the correctness of about 76 % is a promising result and underlines the importance of the analysis of the width functions – especially if we consider that only a very simple verification method is used at the moment. Concerning the completeness we obtain varying results. As supposed the line extraction and the verification works much better for dark vehicles, since more dark vehicles are grouped in queues. Despite of these promising correctness values, a maximum completeness of 48.2 % underlines the necessity of further improvements.

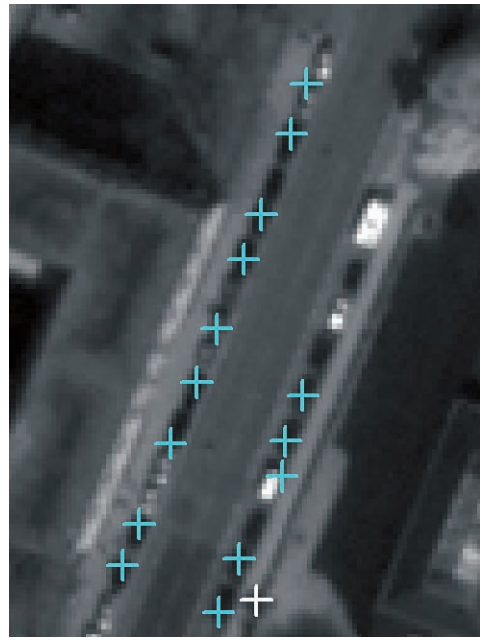

Fig. 9: Extracted single vehicles: Correct extractions (cyan), misdetections (white).

Tab. 1: Evaluation of the line and width analysis.

	Reference data			
	(a)	(b)	(c)	(d)
Completeness [%]	34.1	40.3	22.2	48.2
Correctness [%]	76.0	72.3	71.1	73.1

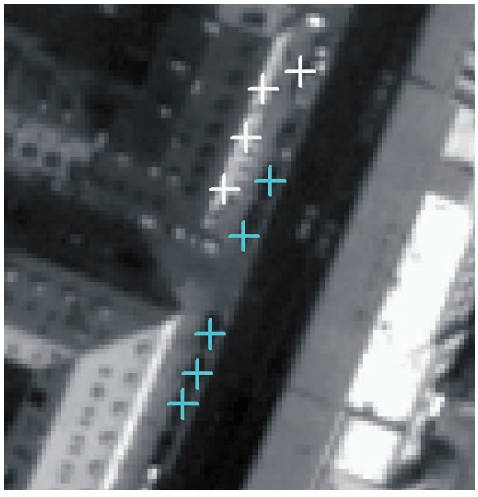

Fig. 10: Extracted single vehicles: Correct extraction (cyan), misdetections (white).

Concerning this weak completeness, one has to keep in mind that not all vehicles are contained in queues and, furthermore, that the line extraction does not extract all existing queues.

There are also a number of misdetections, in particular when objects similar to vehicles are at side-walks (see e. g. Fig. 10). Such failures could be overcome, for instance, when analysing neighbourhood relations of extracted vehicles more in-depth. A constellation as achieved for the right queue in Fig. 9 is very unlikely to happen; five vehicles are almost perfectly aligned in a row while one isolated vehicle is located on the "wrong" side of this row. Incorporating this kind of reasoning into the approach would allow furthering reducing the misdetection rate.

The numerical assessment of the results obtained when applying the approach to a large, complex urban scene confirms the discussion above (see Fig. 11). Despite the weak completeness, the good correctness of the eventually extracted vehicles allows to serve as starting point for searching additional vehicles. Therefore the next steps of implementation will include the search for isolated vehicles using the information from the previously queue detection. Preliminary investigations using a differential blob detector (Hinz 2005) for accomplishing this task have already been undertaken.

Concluding the discussion, vehicles with good or even medium contrast to the road surface can be extracted very accurate. Furthermore, the results show that the analysis of width is able to extract single vehicles from queues with high correctness. Still, the completeness of the overall extraction is relatively low, since only queues can be extracted but no isolated vehicles. The results clearly show that the approach is promising but further improvements are necessary.

4 Summary

We presented an approach for vehicle queue detection from panchromatic QuickBird imagery of urban scenes. For this purpose we use differential geometric line extraction applied in ROIs selected from a GIS and extract the width of the detected vehicle queues. The analysis of these width functions allows to extracting single vehicles with high correctness. As dark vehicles grouped in queues show better contrast the results for completeness and correctness are better than the results for bright vehicles. Gray vehicles have not been extracted. Nonetheless, the approach implemented so far has to be seen as a first step of a more complex system for space-borne vehicle detection. However, the fast computation makes the approach even now applicable as additional verification for other prior detection.

A reference database for several images is already set-up. In future works the parameters for line extraction as well as the verification will be obtained from the statistical analysis of this database. Furthermore the manually digitized road data of the GIS are supposed to be replaced by a national core database (ATKIS).

Acknowledgement

The shown images include material © [2004] DigitalGlobe, Inc. ALL RIGHTS RESERVED. This work was done within the TUM-DLR Joint Research Lab (JRL) [http://

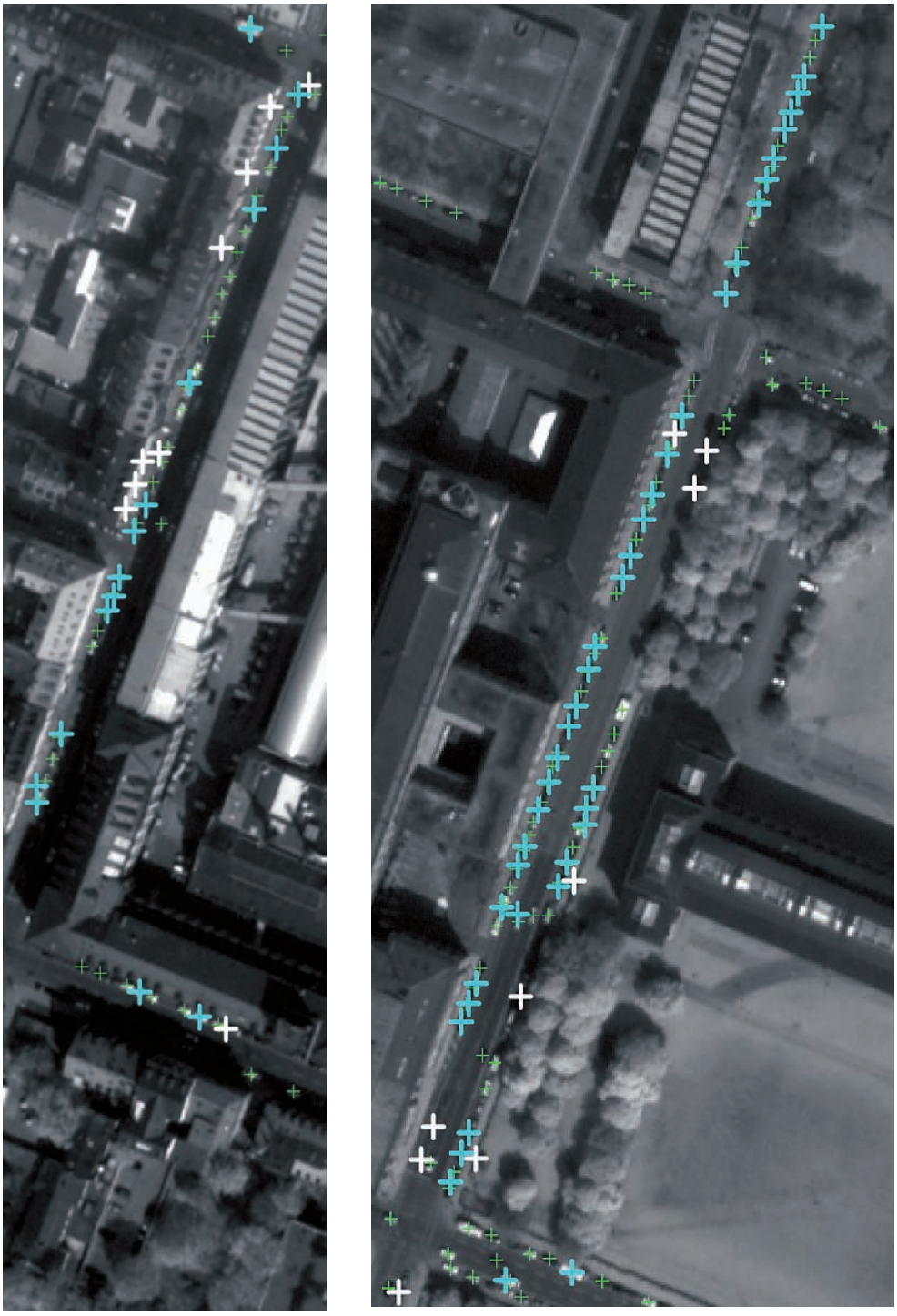

Fig. 11: Results for a large urban area: Correct extractions (cyan), misdetections (white), missing extractions (green).

www.ipk.bv.tum.de/jrl] which is funded by Helmholtz Gemeinschaft.

References

Bamler, R. & Chiu, S., 2005: Spaceborne traffic monitoring from SAR and optical data (Jointly Organized with ISPRS WG III/5). – Session at IGARSS'05 (on CD)

Burlina, P., Chellappa, R. & Lin, C., 1997: A Spectral attentional mechanism tuned to object configurations. – IEEE Transactions on Image Processing **6**: 1117–1128.

Gerhardinger, A., Ehrlich, D. & Pesaresi, M., 2005: Vehicle detection from very high resolution satellite imagery. – In: Stilla, U., Rottensteiner F. & Hinz. S. (Eds.): CMRT05, International Archives of Photogrammetry, Remote Sensing and Spatial Information Sciences **36** (Part 3/W24): 83–88.

Heipke, C., Jacobsen, K. & Gerke, M. (Eds.), 2005: High-resolution earth imaging for geospatial information. – International Archives of Photogrammetry and Remote Sensing **36**, Part 1 W3 (on CD).

Hinz, S., 2003: Integrating local and global features for vehicle detection in high resolution aerial imagery. – International Archives of Photogrammetry, Remote Sensing and Spatial Information Sciences **34** (Part 3/W8): 119–124.

Hinz, S., 2005: Fast and subpixel precise blob detection and attribution. – Proceedings of ICIP 05, Sept. 11–14, 2005, Genua.

Hinz, S. & Stilla, U., 2006: Car detection in aerial thermal images by local and global evidence accumulation. – Pattern Recognition Letters **27:** 308–315.

Jin, X. & Davis, C.H., 2004: Vector-guided vehicle detection from high-resolution satellite imagery. – Proc. IEEE International Geoscience and Remote Sensing Symposium (IGARSS '04), Vol. **2**: 1095–1098.

Michaelsen, E. & Stilla, U., 2001: Estimating urban activity on high-resolution thermal image sequences aided by large scale vector maps. – Proc. IEEE/ISPRS Joint Workshop on Remote Sensing and Data Fusion over Urban Areas, 25–29.

Ramer, U., (1972): An iterative procedure for the polygonal approximation of plane curves. – Computer Graphics and Image Processing **1**: 244–256.

Ruskoné, R., Guiges, L., Airault, S. & Jamet, O., 1996: Vehicle detection on aerial images: A structural approach. – In: Kropatsch, G. (Eds.): Proc. 13th International Conference on Pattern Recognition (ICPR'96), Vol. 3, IEEE Computer Society Press, 900–903.

Sharma, G., 2002: Vehicle detection and classification in 1-m resolution imagery. – MSc Thesis, Ohio State University, Columbus, USA-OH.

Steger, C., 1998: An Unbiased Detector of Curvilinear Structures. – IEEE Transactions on Pattern Analysis and Machine Intelligence **20** (2): 113–125.

Stilla, U., Michaelsen, E., Soergel, U., Hinz, S. & Ender, J., 2004: Airborne monitoring of vehicle activity in urban areas. – International Archives of Photogrammetry, Remote Sensing and Spatial Information Sciences **35** (Part B3): 973–979.

Stilla, U., Rottensteiner, F. & Hinz. S. (Eds.), 2005: Object Extraction for 3D City Models, Road Databases, and Traffic Monitoring – Concepts, Algorithms, and Evaluation (CMRT05). – Int. Archives of Photogrammetry, Remote Sensing and Spatial Information Sciences **36** (Part 3/W24).

Addresses of the authors:

Dipl.-Ing. Jens Leitloff
Photogrammetry and Remote Sensing
Technische Universität München
Arcisstrasse 21, D-80333 München
e-mail: jens.leitloff@tum.de

Dr.-Ing. Stefan Hinz
Remote Sensing Technology
Technische Universität München
Arcisstrasse 21, D-80333 München
e-mail: Stefan.Hinz@bv.tu-muenchen.de

Prof. Dr.-Ing. Uwe Stilla
Photogrammetry and Remote Sensing
Technische Universität München
Arcisstrasse 21, D-80333 München
e-mail: stilla@bv.tu-muenchen.de

Manuskript eingereicht: März 2006
Angenommen: Mai 2006

VAKAT

Photogrammetrie • Fernerkundung • Geoinformation 4/2006, S. 327–337, 6 figs., 2 tabs.

Modeling Ephemeral Settlements Using VHSR Image Data and 3D Visualization – the Example of Goz Amer Refugee Camp in Chad

STEFAN LANG, DIRK TIEDE, Salzburg & FERDINAND HOFER, Washington DC

Keywords: Remote Sensing, modeling ephemeral settlements, VHSR Image, 3D Visualization, refugee camp in Chad

Abstract: Crisis situations in the aftermath of man-made or natural disasters lead to increasing volumes of internally displaced people and refugees. The recent crisis in Darfur for example has mobilized more than 800,000 people, about one fourth of them being accommodated in refugee camps in Eastern Chad. More permanent camps, like Goz Amer, have converted to ephemeral settlements over time, but even there aid agencies report on limited knowledge concerning the actual number of inhabitants and changes due to reallocations. This paper demonstrates that full usability of very high spatial resolution (VHSR) data for rapid information delivery relies on well-established workflows for the transformation of raw image data into ready-to-use information. On prototype level this workflow couples automated analysis of high-resolution image data with GIS-based visualization techniques. Extracted dwellings and habitation structures are used as proxies for an estimation of camp inhabitants. The provision of a geo-referenced, pseudo-realistic 3D-scenario is considered an effective means for coordinated humanitarian aid delivery. For the study on Goz Amer camp, a 3.1 km^2 subset of a QuickBird scene has been pan-sharpened and resampled to a 0.6 m ground resolution. Sobel-filtering created an edge-enhanced product, which was segmented in a fine scale representing relevant dwelling structures at best. By means of rule-based classification and fuzzy operators the segments were assigned to different dwelling types (including orientation of main axis), fences/walls, bare soil/sand, single trees, and vegetation. Accuracy assessment was done using a visually interpreted reference layer, focusing on tents. The number of extracted tents (2,263) was multiplied by an estimated factor of average family size, considering a specified level of uncertainty. An overall number of 20,362 camp inmates was calculated. This number can be spatially disag-

Zusammenfassung: *Modellierung temporärer Siedlungen mittels höchstauflösender Fernerkundungsdaten und 3D Visualisierung – am Beispiel des Flüchtlingslagers Goz Amer im Tschad.* Ausgelöst durch Krisensituationen nimmt weltweit die Zahl der Binnenflüchtlinge und Grenzflüchtlinge zu. Die aktuelle Krise in Darfur beispielsweise hat mehr als 800,000 Menschen mobilisiert, wovon ungefähr ein Viertel in Flüchtlingslagern im östlichen Tschad untergebracht ist. Permanentere Lager wie Goz Amer können aufgrund der stabileren Struktur als vorübergehende Siedlungen aufgefasst werden. Selbst dort herrscht aber bei den Hilfskräften und -organisationen nur begrenztes Wissen hinsichtlich der tatsächlichen Zahl der Bewohner und der Dynamik durch Umverteilungen zwischen den Lagern. Diese Studie zeigt auf, wie räumlich höchstaufgelöste (VHSR) Daten für eine rasche Bereitstellung relevanter Informationsanlieferung mittels eines Workflows eingesetzt werden können. Auf Prototypniveau verknüpft dieser die automatisierte Analyse höchstauflösender Bilddaten mit GIS-gestützten Visualisierungstechniken. Extrahierte Zelte werden zusammen mit anderen Wohnstrukturen (Hütten, Zäune) als Indikatoren für eine Schätzung der Lagereinwohner verwendet. Die Erstellung und Vermittlung eines georeferenzierten, pseudo-realistischen 3D-Scenarios wird als ein wirkungsvolles Mittel für koordinierte humanitäre Hilfsaktionen betrachtet. Für die Studie wurde ein 3,1 km^2 großes Subset einer QuickBird Satellitenbildszene pan-geschärft und auf 0,6 m resampelt. Durch Sobel-Filterung wurde anschließend ein kantengeschärftes Produkt erzeugt, das in einer feinen Skala segmentiert wurde, um relevante Strukturen optimal wiederzugeben. Mittels regelbasierter Klassifikation und Fuzzy-Operatoren wurden die Bildsegmente unterschiedlichen Behausungstypen zugeordnet, d. h. Zelte (einschließlich Lagebestimmung der Hauptmittelli-

1432-8364/06/2006/0327 $ 2.75

gregated by applying a regular (here: 50 m * 50 m) grid or using administrative camp units. Finally, utilizing a library of 3D-symbols and ancillary digital elevation data, a 3D scene was generated providing a pseudo-realistic impression of the overall situation and setting of the camp.

nie), Hütten und Zäune. Darüber hinaus wurden grobe Landbedeckungsklassen im Camp ausgewiesen, also offener Boden bzw. Sand, größere Einzelbäume und Vegetation. Die Genauigkeitsabschätzung erfolgte über einen Vergleich mit einer visuell interpretierten Datengrundlage. Dabei wurde das Augenmerk vor allem auf die extrahierten Zelte gelegt. Die 2263 extrahierten Zelte wurden mit einem aus Literaturangaben geschätzten Faktor multipliziert, wodurch auf die Gesamtzahl der Lagerbewohner geschlossen werden konnte. Diese beläuft sich auf 20362 Bewohner. Die Gesamtzahl kann räumlich mithilfe eines regelmäßigen Raster oder administrativen Lagereinheiten disaggregiert werden. Schließlich wurde eine Bibliothek mit 3D-Symbolen erzeugt und mithilfe eines digitalen Geländemodells (DGM) eine 3D Szene erstellt, die einen pseudo-realistischen Eindruck der gesamten Situation vermittelt.

Introduction

In many places of the world, but with an emphasis in Central and Eastern Africa, man-made disasters such as civil wars or other aggressions against the civil population have mobilized large numbers of affected people. The ongoing crisis in the Darfur region (Western Sudan) has caused more than 800,000 people to leave their homes and villages (Caritas 2004) and is considered one of the most disastrous humanitarian catastrophes recorded recently.

The Darfur crisis

Sudan, a federal state consisting of 26 states since 1994, is the largest country in Africa covering an area of 2.5 million km^2 and stretching between 4° to 22° N and 22° to 38° E, respectively. The Nile river system is the predominant surface water system; 64 % of the Nile river basin is located in Sudan, which makes up four fifths of the countries total area. Effects of climate change on sub-Saharan ecosystems have caused an extension of arid zones and have developed a further potential for the destabilization of the traditional economic structure. Sudan's population is 34.3 million (2004) with an annual growth rate of 2.2 % (FAO). The population distribution shows a great imbalance in accordance with climate conditions. Exceptions to this trend are the areas of confluence of White Nile and Blue Nile (Khartoum) and the area of confluence of Main Nile and Atbara River. Economically, factors of spatial disparities contribute to the imbalance between Khartoum and the South: the distribution of resources and political power, industrial infrastructure, and transport facilities. In Darfur, population concentration is above the average, especially south of 15°N. The Darfuri can be divided into the local, non-Arab indigenous inhabitants of the region and the peoples of Arab descent. Internal southward shifts to this area have put pressure on sedentary farmers of the more humid areas. The Darfur crises can be regarded as a manifestation of the Sudan crises on Darfurian territory. Possible driving forces are generally the same ones as in the North-South conflict whereas the existence of oil deposits in the war-stroke areas of Darfur is presently not proved. The geographical situation of Darfur is a landlocked position with poor road-infrastructure and large distances to navigable rivers. This position acts as barrier for Sudan as a

resource provider. The transfer from resource-based to ethnic-based argumentation is founded in the hardening of the ethnic divide, which begins to act once a conflict has started.

In addition, the southern Sudanese regions claim equality of political power on the national level. They request an economic development on equal terms of the Sudan country. Some of these North-South-type conflicts do not take place in southern Sudan nevertheless they can be regarded as proxy wars, such as in the case of the Darfur conflict which has been ongoing for the last decades with changing intensity and geographic extent. More than three million people live in camps as internally displaced persons (IDPs), or had crossed the Chadian border for staying there as refugees (Reeves 2005). It has become complex due to the centralization of power in Khartoum and the involvement of south Sudanese rebels in the 1990ies entering the Darfurian region. In spite of the high revenues of Sudan's oil-industry, agriculture remains the most important and likewise, the most vulnerable branch of the country's economy. The deterioration of the existing agricultural potential has an impact on food supply and poverty in general. The land reform in 1994 had probably the strongest impact on the relationship between the periphery and the Khartoum based central government.

VHSR imagery and a workflow for information delivery to aid support

The co-ordination of targeted relief support from international organisations like the United Nations High Commissariat for Refugees (UNHCR), the World Food Programme (WFP) or FAO requires, as one of the most crucial prerequisites, exact and spatially disaggregated numbers of affected people (Ehrlich et al. 2004). This includes up-to-date knowledge about the population living in refugee camps. But even if the number of camp inmates was recorded initially, internal reorganisations and inter-camp re-allocations of refugees may change the overall picture in the short-term. Means are needed for rapid information update, preferably utilizing automated and repeatable procedures different from manual counting or listings (FAO, oral communication). In principle, satellite remote sensing data and adequate analysis techniques fulfil these criteria, though with constraints. Harvey (2002) points out three important aspects why population estimation based on satellite imagery is still a challenging task. First no direct link exists between population and reflectance characteristics as in land cover mapping. Secondly, a qualitative variable like land cover is more readily classifiable across the entire image than a quantitative one. Thirdly ground truth information for population estimation is usually available on aggregated levels only. Four approaches for population estimation from remote sensing data are given by Lo, 1986, (cited in Harvey 2002): the first, counting of dwellings, has been a domain of visual image interpretation for a long time. The second, measurement of urbanised areas, uses allometric mapping and relates population to the size of city footprints. It also includes other indicative methods such as nightlight mapping. The third, measurement of areas of land use types, uses statistical links between population figures and land-use (dasymetric mapping). The fourth, automated digital image analysis returns to a more direct population mapping by automating dwellings counts. Today the availability of very high spatial resolution (VHSR) data along with automated analysis techniques may move the latter a significant step forward. For a general overview on current and potential use of satellite imagery with regard to UN humanitarian organizations and their operations see Bjorgo 2002. Even with full operational processing and analysis of high-resolution image data the question arises: may satellite remote sensing really contribute to gain a better picture on how population structure of a refugee camp is composed and which dynamics occur there?

Within the EU-Network of Excellence GMOSS (Global Monitoring for Security and Stability) a workflow for high-standard information transformation and delivery

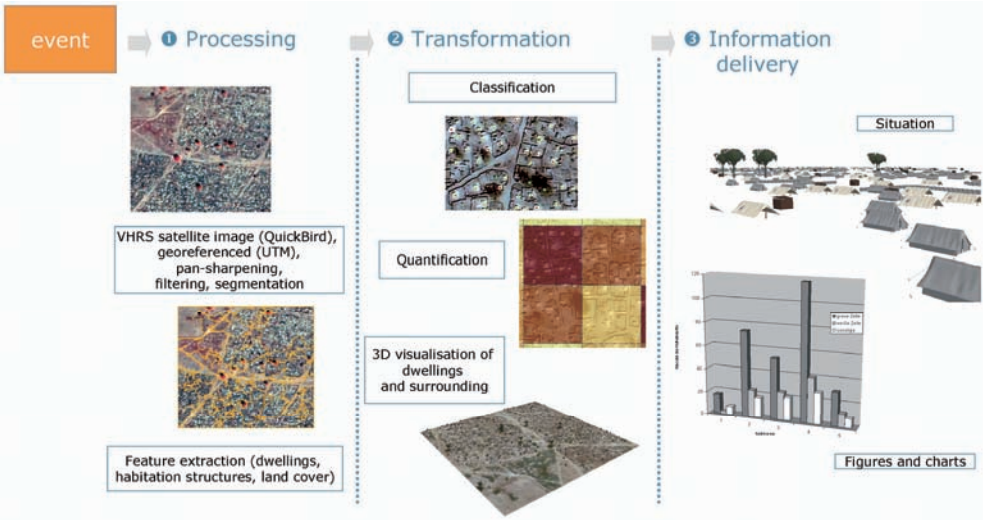

Fig. 1: Triggered by a certain event or crisis situation very high spatial resolution satellite data is acquired. These are pre-processed, geo-referenced and integrated using a global reference tool. Extraction of dwellings and other population-relevant features is performed using object-based image analysis. Based on photographs and descriptions from the specific setting, a library of different dwelling types is composed. Such 3D features are then placed on the locations derived by automated image classification.

has been established. The workflow builds upon a sequence of automated image analysis and visualisation techniques for modelling population-relevant features. It aims at transforming imaged scenes to ready-to-use and policy-relevant information. As illustrated in Fig. 1, the workflow includes the entire chain of pre-processing, feature extraction, classification, quantification and pseudo-realistic 3D visualisation. The latter provides a pseudo-realistic representation of the situation, complemented by existing or derived ancillary data sets like a digital elevation model (DEM) or a coarse-scaled land cover set. Delivering a complete picture of the very situation and the respective crisis area, including figures and charts, it may directly support relief actions or other fine-scale operations.

Case study Goz Amer

The Goz Amer camp

During recent aggressions in the Darfur region, about 150,000 refugees crossed the border to Chad (Welthungerhilfe 2004). To date, about two third of those people live in one of the refugee camps established and maintained in the Eastern Chad (Caritas 2004). The camp Goz Amer (see Fig. 2) is situated about 100 km west of the Chadian/Sudanese border. The total amount of refugees registered at the UNHCR was 18,341 (UNHCR Camp statistic of August 2004).

An apparently regular and stable pattern of tents and other pertaining structures (like fences or huts) justifies the term 'ephemeral settlements' as a metaphor for the semi-permanent character of the camps. Although only a minority of the camps are planned and designed from the government, the term 'informal settlements' may be misleading in this context; rather emphasizes the lack of juridical justification of dwelling structures.

Data sources and pre-processing

From an 11bit QuickBird scene, recorded in December 2004 and comprising an area of 64.4 km^2, a subset was created showing

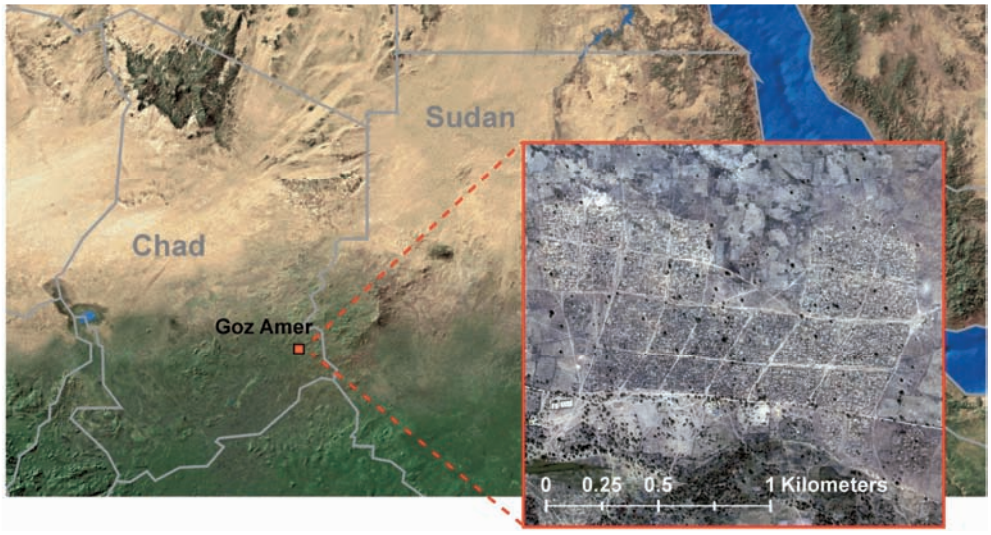

Fig. 2: The Sudanese refugee camp Goz Amer, Eastern Chad.

the Goz Amer camp and the near surroundings with a total area of 3.1 km^2. The scene was pre-registered in UTM-34N (WGS-84). Resolution merge led to a ground spatial distance of 0.6 m. Pan-sharpening was done according to Liu (2000) using an image fusion model implemented in the software package Erdas Imagine 8.7. The method maintains original spectral values to a large extent (> 90 %) and enables deriving detailed information of small structured and high homogeneous areas. A 3*3 Sobel filter matrix was used for edge detection and enhancement. This was done on the resolution-merged blue channel as proposed by Lang & Tiede (2005). The additional information content of the Sobel filtered image layer was required for delineating linear objects during segmentation. Image segmentation itself was done using a region-based, local mutual best fitting approach (Baatz & Schaepe 2000) as implemented in the software eCognition 4. We applied two scale levels for targeting different size-constraint categories of dwelling structures (see Tab. 1).

Tab. 1: Segmentation settings (L = Level, SP = scale parameter, SW = shape weighting, CPW = compactness weighting).

L	SP	SW	CPW	Remarks
2	25	0.2	0.8	bright medium-sized shelters and big shelters well segmented
1	15	0.2	0.5	dark small shelters well segmented

Class definition and classification

Classes of concern within the camp area are known: the primary idea was to determine tents, huts and other habitation structures. Owing to this, in a knowledge-driven approach, an appropriate model was established, which supports extracting the expected object types. We used a rule-based production system with specific descriptive features and fuzzy rules (see Tab. 2). We differentiated between inheritance hierarchy and semantic hierarchy, the first addressing the inheritance of class descriptions from parent to child classes; the second referring to the logical coherence among different classes.

Objects of interest were extracted as single objects. Therefore the number of image ob-

Tab. 2: Class definition containing inheritance and semantic grouping, features and rules, class area and percentage of total area.

Class name	*Inheritance (◘ parent/⊡ child); semantic grouping (O parent/⊙ child); single class (◇)*	*Features/rules (⌘= membership to, ⬥ = mean value of, D = density, B = brightness, C = compactness, % = relative border length to)*	*Class area (ha)/% of total (3.1 km²)*
Bare soil total	O of *bare soil* and *bare soil shadow*		
Bare soil	⊙ of *bare soil total*	⌘ all other classes < 0.2	131.1/43.4
Bare soil shadow	⊙ *bare soil total* ⊡ of *shadow*	% *Single trees shadow* [0.4–0.5]	–
Fences	◇	**B** [350–340]; **D** [0.65–1.3] ⌘ [0.1–1]; ⬥ Sobel [30–50]	5.7/1.9
Shadow	◘ of *bare soil shadow* and *tree* (shadow)	**B** [220–390]	–
Single trees total	O of *single trees* and *tree* (shadow)	–	–
Single trees	⊙ of *single trees total*	NDVI [0.24–0.29]	11.3/3.7
Tree (shadow)	⊙ of *single tress total* ⊡ of *shadow*	% *Single trees* neighb. [0.3–0.8]	–-
Tents bright total	O of *tents bright and tents bright border*		
Tents bright	⊙ of *tents bright total*	⬥ Blue layer [360–370]	1.5/0.5
Tents bright border	⊙ of *tents bright total*	**C** [1.5–1.7]; ⌘ [0.1–1] **%***Tents bright* neighb.[0.35–0.6]	-
Traditional shelter	◇	Area [3–20 (m²)] ; **B** [300–400] **C** [1–1.5] % *Tents bright* neighbours [0]	1.9 / 0.7
Vegetation outspread	◇	NDVI [1.35–2.55] ∧[0.03–0.04] ratio NIR [0.24–0.25]	126.2 / 41.8

jects directly corresponds with the actual number of dwellings or habitation structures. This especially applies for 2,263 objects of the class *Tents bright* (i. e. UNHCR tents of 12 to 20 m^2) and 2,640 objects of the class *Traditional shelter* (i. e. self made, straw covered huts of 4 to 24 m^2).

Accuracy assessment

Accuracy assessment using ground truth information is usually hampered in crisis situation. We therefore created a reference data set by visual interpretation and manually digitizing relevant dwelling structures. In order to represent a sufficient part of the whole camp a grid of 100 m cell-size was superimposed on the whole scene (Fig. 3). 70 out of 280 cells were randomly selected and used to digitize tents and shelters, represented as mid-points. Altogether, 80 % of these were extracted correctly (point-in-polygon). More specifically for *Tents bright* the following applies: out of 790 manually digitized *Tents bright* mid-points, 235 were not contained by a classified *Tents bright* polygon. This corresponds to a producer accuracy of 70.3 %. By a buffer of 1.2 m (two pixels) the amount of misclassified tents could be corrected by 74 tents. Under this condition,

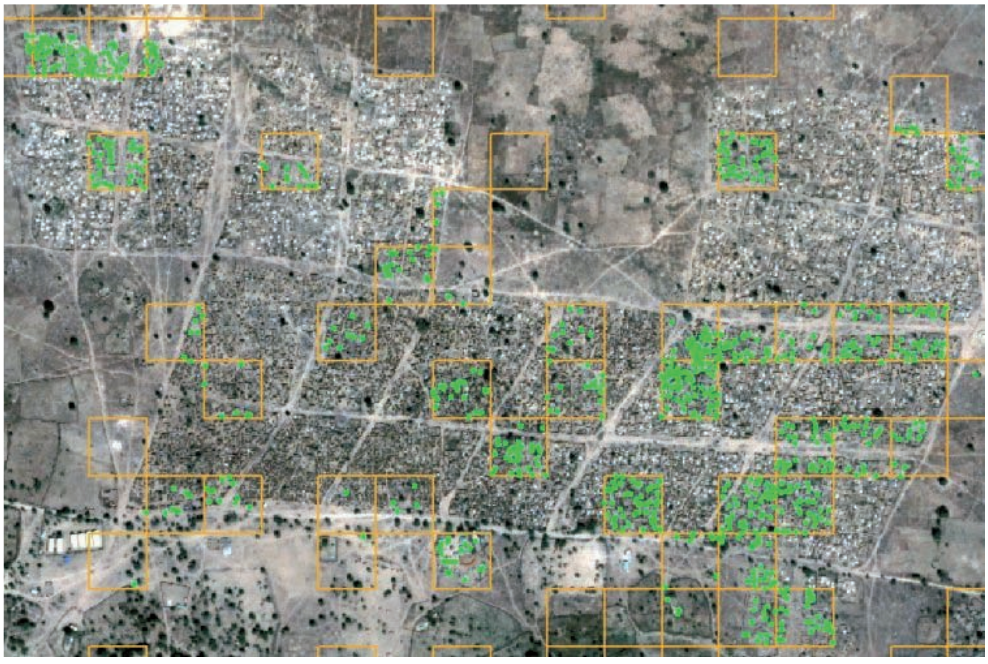

Fig. 3: Accuracy assessment in 70 random cells. Green dots indicate manually digitized tents (790 altogether).

producer accuracy bright tents increases to 79.6%.

Estimation of camp population

Appropriate and quick population estimation based on extracted objects is feasible. The proposed metric is based on an assessment with the help of eyewitness of an IDP-Camp in Darfur (oral communication with T. SPIELBÜCHLER). One assumption, also backed by photographs on web pages, is the use of traditional dark shelters for cooking and staying during daytime only; they are neither used nor suitable for sleeping. Consequently, they give a clue for the estimation process but are not directly related to the number of inmates. A cautious estimation projecting the number of the extracted bright tents by a factor of an average family size provides a realistic, though inexact, number of inmates. A factor of 1.2 (i. e. 20% according to the producer's accuracy) results in a total number of bright tents of 2,715. Assuming that the average West-Darfurian family has between seven and eight family members[1] this would account to a total number of 20,362.5 camp inmates (i. e. 2,715 times 7.5). This value slightly overestimates the real number of around 18,500 at that time.

Spatial (dis-)aggregation of camp population

Since information about population is spatial explicit (i. e. available on the tent level), the overall amount of camp inmates can be aggregated or disaggregated to any spatial subunits of the camp. This may be administrative subdivisions for management related tasks or a regular grid of e. g. 50 m * 50 m cells for analytical purposes. Fig. 4 shows an example of the latter for analysing population densities in a subset of the camp.

[1] http://www.Sudanreeves.org (accessed: 11/2005)

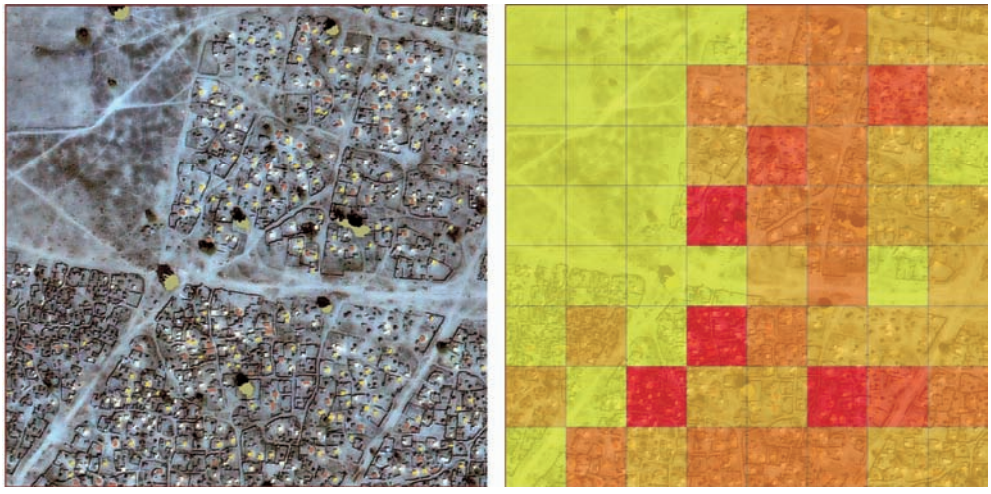

Fig. 4: Extracted dwellings (left) and population densities in a 50 m * 50 m cell grid (right).

Data integration and pseudo-realistic 3D visualization

Visualization of the derived information can be a benefit to the local administration of refugee camps. It also provides rescue teams an overview about the situation they may expect there. Pseudo-realistic 3D visualisation reveals a better impression with more self explaining information, especially to people who are not experienced in reading maps. The workflow discussed above offers the possibility for a gapless chain of information extraction, information delivery and 2D/3D visualization. Fig. 5 gives an overview about the required steps for data integration and visualization. This was conducted using the ArcGIS Extension 3D Analyst supporting data integration and visualization while simultaneously providing GIS analysis functions. Information extracted from the image data comprises: (1) relevant dwelling structures exported as anchor points (i. e. centroids of the extracted objects), which hold attribute information about the dwelling type and main direction (orientation); (2) linear fence structures as centrelines of fence objects; (3) land cover classification (bare soil, vegetated areas, single trees). A 3D symbol library containing three main dwelling types (i. e. large/small tents, traditional shelters) has been constructed in Autodesk 3D Studio Max using image material of the camp. Terrain height information was obtained from SRTM (Shuttle Radar Topography Mission) data.

The resulting scene is a real-time visualisation enabling the users to change between different perspectives, navigate in the third dimension and easily create and export prerendered animations. The use of a 3D symbol library adapted to the current situation gives a much better impression than using wildcard symbols for different dwelling types. Due to the small amount of dwellings types in this example, the effort for creating such a symbol library is limited. Further improvement of the pseudo-realistic impression could be reached by automatically adjusting the symbols. This was done by using the main direction of the extracted dwelling object and attaching this information as an attribute to the anchor point layer. Once created, the 3D scene is not the end of the line: It is a flexible model to change easily data sources, integrate new or updated information and enables the use of GIS analysis functions, e. g. surface analysis, spatial queries, viewshed analysis etc.

The whole scene has been transferred to a globe environment (here: ArcGlobe),

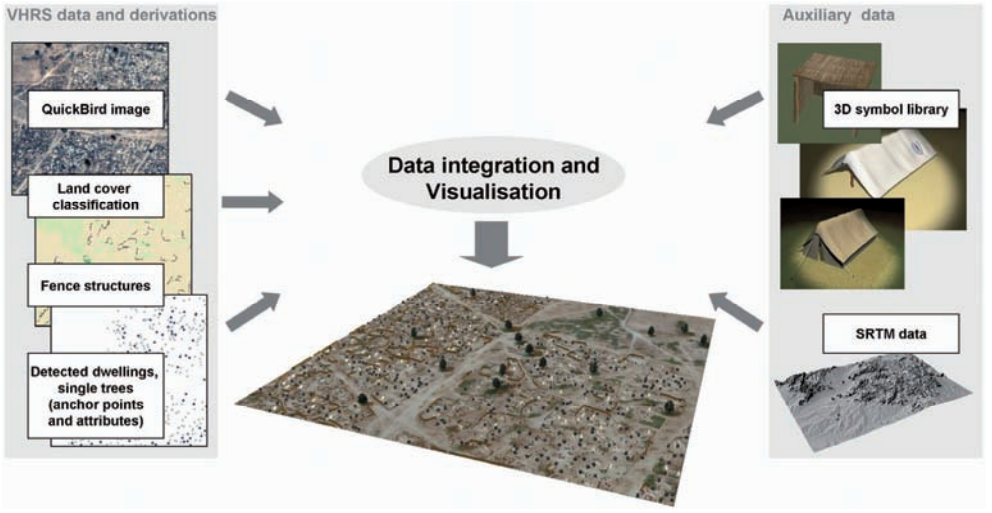

Fig. 5: Overview of data integration for pseudo-realistic 3D visualization.

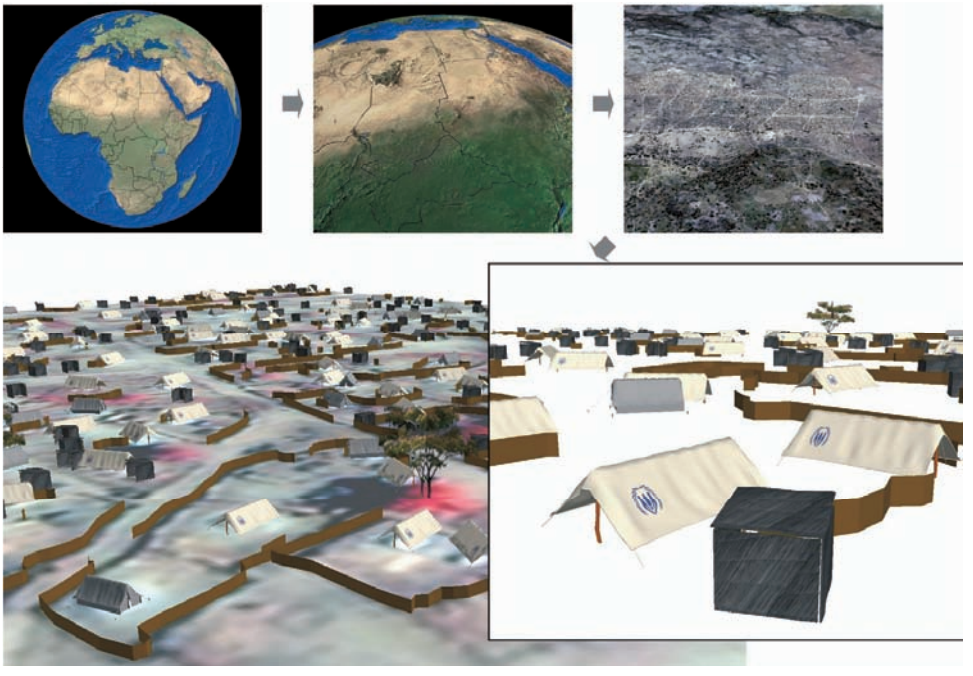

Fig. 6: Pseudo-realistic visualization in a globe environment.

which allows for its integrating the scene into the regional context. Hence, an infinitely variable and scale-independent zoom from global over continental-regionally to locally is supported (cf. Fig. 6). In addition it might be of interest to provide the result within free available 3D data viewers (e. g. ArcReader), overcoming problems of informa-

tion dissemination due to restrictions in software licensing.

Discussion

Population mapping and monitoring

Population monitoring in a refugee camp under the given conditions differs from population monitoring in more common places. For the present research, the detailed spatial resolution has been a great advantage, but a pixel size qualifying as a satisfying resolution may even be higher. A rough and quick estimation is possible – also considering that field research is impossible in some remote areas, especially within a short period of time. In the Goz Amer study, the pan-sharpened VHSR data material allowed for detecting entire objects of varying size and geometry, without leaving scattered remnants of incoherent pixels. The concept of neighbourhood, distance and location was successfully introduced, especially in shadowed areas. Spatial relationships helped to discern between classes, where high similarity in spectral behaviour occurred. However, spatial concepts alone did not separate fence structures from other elongated dark objects. Evidently fence objects interfered with other edge features accentuated by the Sobel edge detector. Massive fluxes of refugees may occur within one day. Hence, quick information generation regarding the movement or replacement of people needs to be provided to administration and relief support. Change detection techniques and rapid multi-temporal analysis are to be integrated in the workflow. This is one of the major research tasks for the future. Difficulties arise, as a binary comparison of absence and presence of tents being erected or dismantled may not reflect the number of people living there at this particular moment. Whole sections of the camp may be abandoned for a certain period of time. In this case night time data (e. g. from the *Defence Meteorological Satellite Program*, *Operational Linescan System*), could provide valuable additional information by indicating human activities (bonfires, stove cooking). No doubt, the use of VHSR data such as QuickBird or Ikonos is expensive. On the other hand, the *International Charter on Space and Major Disasters* obliges data providers and analysts for a close collaboration in crisis situations without financial barriers. The QuickBird data used for this study has been obtained through this charter. Even if data are not for free, from a humanitarian point of view it makes sense spending the money on high quality data in order to adequately implement supporting actions. Finally, the detailed scale on which the analysis performs and the expected higher quality of the result may lead to a more precise and cost-effective help, which could justify the additional costs for data acquisition.

Visualization and relief support

Discussions on the usefulness of a pseudo-realistic 3D visualization for relief operations arose several times within the GMOSS expert group. It was concluded that this can be seen as a novel and complementary approach for standard mapping. It implies additional value to be considered in crisis management. Mainly the flexibility is appreciated. Admittedly the degree of realism is a crucial point: for example the degree of detail concerning the 3D symbol library may pretend a higher accuracy than the use of standard symbols. Also the orientation of the 3D symbols derived from the main line of the extracted objects generates a more realistic impression compared to equally orientated symbols. But still the question remains: which of these alternative visualizations really correspond to the nature of this particular refugee camp? Is it the strict and ordered placement of tents or an irregular orientation along the main axis as depicted on the imagery? Is then the visualisation maybe too much ‘pseudo’?

Acknowledgements

This study has been conducted under the framework of the EU Network of Excellence GMOSS (http://gmoss.jrc.it/index.

asp). It mainly results from collaborative work between two work packages, i. e. *Population Monitoring* and *Data Integration and Visualization*. We highly appreciate discussions and knowledge transfer among the participants. We would like to cordially thank Thomas Spielbüchler, historian and political scientist at Salzburg University, and adept in Sudan affairs, for the grant of his expert knowledge in the geopolitical background. We are likewise thankful to Gregor Hochleitner, who has created the 3D symbol library of dwellings. Finally, Thomas Blaschke and Peter Zeil we owe thanks for fruitful and stimulating discussions, and the reviewers for improving the quality of the manuscript.

References

Baatz, M. & Schäpe, A., 2000: Multiresolution Segmentation – an optimization approach for high quality multi-scale image segmentation. – In: Strobl, J., Blaschke, T. & Griesebner, G. (eds.): Angewandte Geographische Informationsverarbeitung XII. – pp. 12–23,Wichmann-Verlag, Heidelberg.

Bjorgo, E., 2002: Space Aid: Current and Potential Uses of Satellite Imagery in UN Humanitarian Organizations. – http://www.us ip.org/virtualdiplomacy/publications/reports/12.html (Sept. 2005)

Caritas Österreich, 2004: Sudan/Tschad, Situation dramatisch; http://www.caritas.at/ international (April 2005).

Ehrlich, D., Schneiderbauer, S. & Louvrier, C., 2004: Needs assessment for an unfolding disaster Zimbabwe 2003–04. – Technical Note No. 1 (Internal JRC report).

FAO Statistical Databases: http://faostat.fao.org/ (Mai 2006)

Harvey, D., 2002: Estimating census district populations from satellite imagery: some approaches and limitations. – Internat. J. Remote Sensing, **23** (10): 2071–2095.

Hofer, F., 2005: Population monitoring utilizing remote sensing and GIS technologies. – Master Thesis (unpublished).

Lang, S. & Tiede, D., 2005: Behausungsextrahierung und -visualisierung zur Bevölkerungsabschätzung im sudanesischen Flüchtlingslager Goz Amer (Tschad). – In: Strobl, J., Blaschke, T. & Griesebner, G. (eds.), 2005: Angewandte Geoinformatik 2004, Beiträge zum 16. AGIT-Symposium Salzburg. – pp. 397–402, Herbert Wichmann Verlag, Heidelberg.

Liu, J. G., 2000: Smoothing Filter-based Intensity Modulation: a spectral preserve image fusion technique for improving spatial details. – Internat. J. Remote Sensing **21**.

Reeves, E., 2005: Ghosts of Rwanda: The Failure of the African Union in Darfur (Part 1). – http://www.sudantribune.com (Nov. 2005)

UNHCR, 2004: Refugee map; http://www.unhcr.ch/chad/(April 2004)

Welthungerhilfe, 2004: Lage der Flüchtlinge im Tschad. – http://www.welthungerhilfe.de/WHHDE/themen/sudan/ (04/20 05)

Addresses of the authors:

Dr. Stefan Lang
Centre for Geoinformatics (Z_GIS)
Salzburg University
Schillerstr. 30, A-5020 Salzburg
e-mail: stefan.lang@sbg.ac.at

Dipl.-Geogr. Dirk Tiede
Centre for Geoinformatics (Z_GIS)
Salzburg University
Schillerstr. 30, A-5020 Salzburg
dirk.tiede@sbg.ac.at

Mag. Ferdinand Hofer
Office of Science and Technology
Embassy of Austria
Washington DC, 20008
USA

Manuskript eingereicht: März 2006
Angenommen: Mai 2006

VAKAT

Berichte

ISPRS Workshop on Multiple Representation and Interoperability of Spatial Data

22–24 February 2006 in Hannover

At the end of February the 'ISPRS workshop on Multiple Representation and Interoperability of Spatial Data' took place in Hannover. The workshop was an initiative of two ISPRS working groups: II/3 (Multiple representations of image and vector data) and II/6 (System integration and interoperability). Although these two working groups are within one ISPRS commission (Spatio-temporal data handling and information) the focus of the workshop was not always clear. On the other hand, this also led to a wide variety of topics which was very interesting for the participants. Generalization was in any case a topic that came up during the whole workshop. The workshop itself was neatly organized (as Germans are known for); with a nice congress hotel and sufficient time for both social and information exchange. There were about 40 participants from twelve countries.

The keynote speech was given by Professor W. Förstner (University of Bonn), president of ISPRS Com. III. The speech was about *'natural and artificial scale of geoinformation'* with a few very nice examples of 'multiple scales at the same position'. He mentioned the city views with continuous scale-ranges from close by (Level of Detail 0) to far away (Level of Detail 4), according to the City Model division of Thomas Kolbe. The principle of Level of Details was effectively illustrated by Förstner with an animation of the work of Escher. Besides that Förster gave a nice example of generalization (abstraction) in using natural language in our daily lives, i. e. in case of emergencies. There is a clear difference in 'There is fire at Churchstreet 12th, second floor, room 2.24.0' and 'I see a plume of smoke when I look outside my window'. It was good to see that Förstner recognizes the importance of non-photorealistic 3D City Models in geo-applications as well as an essential role for cartographic aspects within computer graphics.

The paper of N. Regnauld (Ordnance Survey, UK) in the first session '*Generalization Web Services*' was about efficiency improvement for developing automatic generalization solutions. His message was clear. Research is only looking for proof of concepts. As a consequence generalization research does hardly lead to reusable prototypes. Only a few – and mostly simple – results are taken over by the industry. This problem can be met by 'Generalization Web Services'. Nicolas had tested this concept by providing one of his algorithms to the WebGen platform of M. Neun (University of Zürich) which Neun presented in the second presentation. Neun based his web service on standardized web technology, i. e. Simple Object Access Protocol (SOAP). T. Foerster (ITC) is currently working on making this service OGC compliant by implementing it in an OGC Web Processing Service.

The second session was on '*Ontology and Semantic Integration*'. A remark from the audience that ontology is just another saying for 'Knowledge Representation' made clear that ontology is still a confusing term. Reading Nietzsche's 'Beyond good and evil' might help by understanding more about ontologies. E. Tomai (Institute of Applied and Computational Mathematics, Heraklion, Crete) presented her work in which she integrated two different ontologies by focusing on instances rather than on classes of ontologies. J. Stoter (ITC Enschede, co-author of this report) talked about semantic data integration within the MRDBMS environment of the Dutch Topographic Survey (TD Kadaster). Part of her presentation focused on integration of the ontology of TD Kadaster with ontologies from other domains. It included machine ontologies, semantic web and Web Ontology Language

(OWL). The session was closed by a paper of W. Shi and L. Meng (Technical University of Munich) on the *integration of multi-disciplinary spatial data*.

In the afternoon J. de Waele (Nationaal Geografisch Instituut Belgium) talked about the *integration of road networks by linking the 1:10.000 database with the 1:50.000 database in order to align cartographic production of those two databases*.

The remainder of the afternoon was dedicated to two parallel discussions: one on issues related to integrating Geo-ontologies and one on the use and usefulness of Generalization Web Services. In the ontology session it was concluded that the term ontology is maturing within the geo-community, although the term is still a source of confusion. Ontologists and geo-it professionals need to work closely together and need to be willing to look at each others terminology and needs in order to make considerable progress in applying geo-ontologies.

The conclusion of the session on Generalization Web Services was that it should be clear for what user the service is intended (generalization researcher, planner or a user who wants to simplify her data but does not know anything about generalization). The specific use(r) lays down specific requirements for the service. The major difficulties of setting up web services were identified as:

- Lack of procedural knowledge
- A common data model is required (for a service for non-expert users)
- Formalizing algorithm and interfaces
- Wrapping the algorithm and maintaining the web services requires work and responsibility of a specific institute
- Copyright issues, both for cartographic data and for algorithms that are made available over the web
- Web Processing Services (e. g. the OGC WPS) could be used but they provide no algorithm specification

The second day E. Verbree (Delft University of Technology, co-author of this report) started in the '*Generalization*' session with a presentation on the en- and decoding of planar maps through conformal triangulation. J. Haunert (University of Hannover) presented his research on *'Hierarchical structures for rule base incremental generalization'*. He showed a nice implementation in ArcGIS of the aggregation of polygons. M. Kada (University of Stuttgart) had an animated talk about 3D building generalization based on half space modeling.

In the session on '*Hierarchies in images and in text*' J. Heuwold (University of Hannover) talked about the automatic scale-dependent adaption of object models to support the automatic extraction of objects from images. Unfortunately this was the only presentation on images. M. Müller (University of Karlsruhe) spoke about the transmission of the Brazilian Cadastre, which is a textual system, to a system that is based on a description with real-world coordinates. To make this happen different kinds of property descriptions need to be translated into real-world coordinates which is a hard job. L. Harrie (Lund University) had a nice idea to automate vegetation symbol placement on Ordnance Survey 1:50.000 maps.

In the last session (on *''Matching'*) S. Mustière (IGN France) tried to match networks in the BD Topo database (~ 1:10.000) of IGN with networks in the BD Carto database (~ 1:50.000). He had a nice approach with good results: first find all the sets of possible similar nodes and secondly the sets of possible similar arcs after which the matching can take place. The 'fitness of the match' is expressed in a 'confidence' value. In the last and final talk S. Volz (University of Stuttgart) presented a similar story but now with two street networks at approximately the same scale (from ATKIS and Geographic Data Files). All papers can be downloaded from http://www.ikg.uni-hannover.de/isprs/workshop.htm

Jantien Stoter (ITC, Enschede) and Edward Verbree (Delft University of Technology)

5th Turkish German Joint Geodetic Days

vom 28. bis 31. 3. 2006 in Berlin

Zum fünften Mal fanden die Deutsch-Türkischen Geodätentage statt. Sie wurzeln in der langjährigen engen Kooperation zwischen der Technischen Universität Berlin und der Istanbul Technical University (ITU). Es konnten dieses Jahr etwa 160 Teilnehmer aus 16 Ländern begrüßt werden.

Kern der Eröffnungsveranstaltung waren ein Vortrag von JOHN TRINDER, Australien, Präsident der ISPRS, und der anschließende Empfang im Türkischen Haus an der Urania.

Die Tagung lief teilweise zweigleisig ab. Außerdem wurden einige eingereichte Vorträge als Poster präsentiert. Leider konnte eine Vielzahl von angekündigten Vorträgen nicht gehalten werden, weil die Vortragenden nicht erschienen waren. Andere, möglicherweise interessante Vorträge, waren wegen des knappen Zeitbudgets von den Organisatoren nicht ins Programm aufgenommen worden. Dabei ist den Organisatoren kein Vorwurf zu machen.

Das Tagungsprogramm begann mit einer Plenarveranstaltung mit Vorträgen unter anderem von Prof. ORHAN ALTAN zum Thema „*Geoinformation for Disaster Management*“ und Prof. KARL KRAUS „*Least Squares Matching for Airborne Laser Scanner Data*“. Letzterer beschrieb eine Technologie zur Steigerung der Genauigkeit von Laserscannerdaten. In den dann folgenden Sitzungen wurden Vorträge zu Photogrammetrie, Fernerkundung und Geoinformation teilweise auch parallel gehalten.

In der Session zum Thema *Nahbereichsphotogrammetrie* beschrieb SUTHAU Methoden zur Vermessung und Modellierung von Dinosaurierskeletten und KÜLÜR sprach zum Thema „*An Automated System to Model Small Objects Using Structured Light*“.

Der Freitag begann mit einer Session zum Thema luftgestützter Photogrammetrie. Zunächst berichtete WIEDEMANN über einen „*Combined Photogrammetric Flight with ALTM and Digital Camera*“. Im Vortrag „*New Airborne Sensors and Platforms for Solving Experimental Applications in Photogrammetry and Remote Sensing*“ von KEMPER wurde über alternative Sensorträger berichtet. Über die Kalibrierung von Zeilenkameras berichtetet KOCAMAN in „*Self-Calibrating Triangulation of Airborne Linear Array CCD Cameras*“. ALBERTZ beschrieb einen interessanten Ansatz „*The Generation of True Orthoimages – A New Approach*“. Die Session beschloss WEHR mit „*CW-Laser-Scanning State-Of-The-Art AT INS and Future Multispectral Sensors*“.

Leider fanden die Sessions *Cultural Heritage* und *Computer Vision* parallel statt. In der Computer Vision Sitzung berichtete unter anderem LÄBE über „*Automatic Relative Orientation of Images*“ und RODEHORST in seinem Vortrag „*Comparison and Evaluation of Feature Point Detectors*“ über Interest-Operatoren.

In der abschließenden Plenarsitzung berichtete unter anderem JACOBSEN über „*Mapping From Space – A Cooperation of Zonguldak Karaelmas University and University of Hannover*“ und WÄHLISCH über „*Mapping of the Saturnian Satellites – Results From Cassini*“.

Die Tagung war geprägt vom Engagement junger Leute und bietet als solche für die jungen Leute eine sehr gute Plattform. Die Organisation erfolgte durch die Teams von Prof. ALTAN (Istanbul TÜ), sowie von Prof. ALBERTZ und Prof. GRÜNDIG (TU Berlin).

Die angenehme und interessante Tagung wurde leider überschattet von der schweren Erkrankung von Prof. KARL KRAUS, der kurz nach seinem Vortrag am Mittwoch ins Krankenhaus gebracht wurde, wo er eine Woche später verstarb.

ALBERT WIEDEMANN, Berlin

Förderpreis für Geoinformatik 2006

am 1. März 2006 in München verliehen

Im Rahmen des 11. Münchner Fortbildungsseminars Geoinformationssysteme an der TU München wurde zum fünften Mal der Förderpreis für Geoinformatik vergeben. Die Verleihung des Preises ist fester Be-

Teilnehmer der Förderpreisverleihung 2006 mit Prof. M. SCHILCHER, Vierter von Rechts und den Gewinnern CHRISTINE DALL, 1. Preis, Zweite von Rechts, JAN HERRMANN, 2. Preis, Dritter von Rechts und ALBRECHT WEISER, Dritter von Links. (Foto: Plabst)

standteil der Förderung des wissenschaftlichen Nachwuchses, die sich der Verein Runder Tisch GIS e.V. zum Ziel gesetzt hat.

21 Nachwuchswissenschaftler von Universitäten und Fachhochschulen bewarben sich mit ihren hervorragenden Arbeiten um den Förderpreis Geoinformatik 2006 des Runder Tisch GIS e.V. Etwa die Hälfte der Arbeiten wurde in den Studiengängen bzw. Fachbereichen GIS, Geoinformatik und Geographie erstellt. Die bunte Vielfalt interdisziplinär geprägter Themen aus Grundlagen- und anwendungsorientierter Forschung wird zudem durch Bewerbungen aus der Informatik, den Energie- und Wirtschaftswissenschaften, der Landschaftsarchitektur und Umweltplanung, der Geologie und den Naturwissenschaften ergänzt. Es lohnt sich also, einen Blick auf die Zusammenfassungen der eingereichten Arbeiten zu werfen, die auf der Homepage des Runder Tisch GIS e.V. zu finden sind.

Mit dem 1. Preis wurde Dipl.-Geogr. CHRISTINE DALL für ihre Masterarbeit an der Universität Salzburg ausgezeichnet. Sie überzeugte die international besetzte Jury aus sechs Professoren mit ihrer herausragenden Arbeit zum Thema *Crime Mapping in Hamburg und der Suche nach alternativen Darstellungsformen der Straftatenverteilung*.

Der Preisträger von 2005, Dr.-Ing. ANDREAS DONAUBAUER, ernannte die Preisträgerin 2006 zur „GIS-Königin des Jahres" und überreichte ihr einen Scheck über 1500 Euro.

Den 2. Preis über 1000 Euro erhielt Dipl.-Inf. JAN HERRMANN für seine Diplomarbeit an der TU München *Entwicklung und Implementierung einer raumbezogenen Zugriffskontrolle für Geo Web Services*.

Der 3. Preis mit 500 Euro ging an Dipl.-Ing. ALBRECHT WEISER für seine Diplomarbeit an der FH Mainz zum Thema *Automatisierte Generierung von Styled Layer Descriptor-Dateien aus ESRI ArcGIS-Projekten zur Publikation mit OGC-konformen Mapservern*.

Im Anschluss an die Preisverleihung, in den Pausen des Seminars und in der Posterausstellung wurde von den Seminarteilnehmern vielfach die Gelegenheit genutzt, mit den ausgezeichneten jungen Kolleginnen und Kollegen ins Gespräch zu kommen.

Mit dem Förderpreis Geoinformatik des Runder Tisch GIS e.V. werden jährlich drei herausragende Dissertationen, Diplom- oder Masterarbeiten aus dem deutschsprachigen Raum ausgezeichnet, die im Umfeld der Geoinformatik entstanden sind.

Interessenten können sich den 31. Oktober 2006 als Termin für die Einreichung von Arbeiten zum Förderpreis Geoinformatik 2007 bereits jetzt vormerken. Nähere Informationen sind auf der Homepage des Runder Tisch GIS e.V. nachzulesen: http://www.rundertischgis.de

GABRIELE AUMANN, München

Arbeitskreis Landkreise zum Thema Geoinformationssysteme gegründet

Im Anschluss an das *11. Münchner Fortbildungsseminar Geoinformationssysteme* (GIS) an der Technischen Universität München vom 1. bis 3. März 2006 fand die Kick-off-Veranstaltung für den AK Landkreise am Runden Tisch GIS e.V. großen Anklang: Von 27 Teilnehmern waren 14 Vertreter

bayerischer Landkreise. „Wir wollen einen offenen Arbeitskreis, in dem vordringlich die Belange der Landkreise berücksichtigt werden, sich aber auch Vertreter der Anbieter und der Hochschulen sowie Freiberufler auf der informellen Ebene einbringen können", betonte der Vorstandsvorsitzende des Runder Tisch GIS e.V., Prof. Matthäus Schilcher. Die Auswertung der Vorstellungsrunde ergab zunächst als Schwerpunkthemen Informationsaustausch, Datenbeschaffung und Interessenvertretung. „Mit dem AK Landkreise haben die Vertreter der Landkreise die Chance, ihren Anliegen und Interessen im Bereich Geoinformationssysteme eine Stimme zu geben und diese gebündelt als Sprachrohr an Verbände und Entscheidungsträger heranzutragen", erläutert die Leiterin des neuen Arbeitskreises, Dr. Gertraud Sutor, www.runder tischgis.de

Gertraud Sutor, München

Heitfeld-Preis

Der Heitfeld-Preis für Angewandte Geowissenschaften wird von der GeoUnion Alfred-Wegener-Stiftung in einem Turnus von zwei Jahren vergeben. Er ist mit einem Preisgeld von 10 000 Euro dotiert und wird aus den Erträgen einer großzügigen Stiftung des Namensgebers an die GeoUnion AWS finanziert.

Der Heitfeld-Preis wird als nationaler Preis für im wesentlichen in Deutschland erbrachte Leistungen verliehen. Es werden herausragende Einzelleistungen wie auch die Ehrung des Gesamtwerkes eines Wissenschaftlers vor allem der ersten und/oder mittleren Lebens- oder Berufsphase erfasst. Eigenbewerbungen sind nicht statthaft. Vorschläge zur Verleihung des Heitfeld-Preises können von Einzelpersonen oder Personengruppen (Institutionen, wissenschaftliche Gesellschaften) erbracht werden.

Die Vorschläge werden von dem Heitfeld-Preis-Kuratorium, welches vom Präsidium der GeoUnion AWS bestellt wird, auf der Grundlage von Fachgutachten entschieden. Das Preis-Kuratorium besteht aus 5 Mitgliedern (2 Geologen, 1 Geophysiker, 1 Mineraloge sowie einem Vertreter einer weiteren Disziplin der Geowissenschaften der Festen Erde). Es sollen führende Vertreter ihres Fachs sein.

Die GeoUnion AWS vergibt den Preis auf einer herausragenden geowissenschaftlichen Veranstaltung; die Preisträger werden in den einschlägigen wissenschaftlichen Organen veröffentlicht und gewürdigt.

In den vergangenen Jahren hat sich der Heitfeld-Preis zu einer der angesehensten Ehrungen auf dem Gebiet der Angewandten Geowissenschaften in Deutschland entwickelt.

Dr. G. Greiner, Geschäftsführer der GeoUnion Alfred-Wegener-Stiftung, e-mail: greiner@gfz-potsdam.de

International Union of Geodesy and Geophysics IUGG

Die **Internationale Union für Geodäsie und Geophysik** ist einer der großen wissenschaftlichen Dachverbände der Welt und gliedert sich in 7 fachliche Assoziationen. Eine davon ist die International Association of Geodesy (IAG). Über 100 Staaten sind Mitglieder der Union oder ihrer Teile, ferner etwa 60 globale Vereinigungen.

Hauptzweck der IUGG ist die Förderung und Koordination von Forschung über die Erde und den erdnahen Weltraum. Sie gründet spezielle Kommissionen zu langfristigen Forschungsthemen und Spezial-Studiengruppen (SSG) zu aktuellen Themenkreisen. Ferner unterhält die Union eine Reihe wissenschaftlicher Dienste (*Service*), unter anderem zur Erdrotation und zu GPS. Alle 4 Jahre finden große zweiwöchige Kongresse mit 5-10.000 Teilnehmern statt, zuletzt im Jahre 2005 in Cairns (AUS).

Die 23. IUGG General Assembly wurde veranstaltet vom 30. Juni bis 11. Juli 2003 in Sapporo, Japan. Die 24. IUGG General Assembly findet statt vom 2. bis 13. Juli 2007 in Perugia, Italien, unter dem Motto: *„Earth, Our Changing Planet"*.

Wichtige internationale Kooperationspartner sind Gliederungen der UNO, der Internationale Wissenschaftsrat ICSU und zahlreiche Organisationen der Geowissenschaften wie z. B. EGS, EGU, IAG, IAMAP, IAH, IHO, COSPAR.

Das Büro der IUGG wird gegenwärtig geleitet von Präsident Uri Shamir, Israel. Vizepräsident ist Tom Beer, Australien.

Quelle: http://www.iugg.org/

International Association of Geodesy IAG

Die IAG ist eine Assoziation der IUGG (Internationale Union für Geodäsie und Geophysik), die ihrerseits dem Dachverband der ICSU angehört.

Gliederung der IAG in fünf Sektionen:
I – Positionierung,
II – Neue Technologien der Raumfahrt,
III – Berechnung des Gravitationsfeldes,
IV – Allgemeine Theorien und Methoden,
V – Geodynamik.

Spezielle Kommissionen:
– Globale u. regionale Vermessungsnetze,
– Raumfahrt-Techniken,
– Satellitenmethoden im Erdschwerefeld,
– Gravimetrie,
– Geoid,
– Grundlagen (Mathematik, Physik),
– Erdgezeiten, Erdkruste,
– Fundamentale und Bezugssysteme,
– Geodynamik,
– Globales Eis,
– Internationales Seerecht,
– Ausbildung und Hochschulen.

Spezielle Studiengruppen (SSG) für kurzfristige Themenkreise (20–30).

Subkommissionen für längerfristige Forschungsthemen.

Internationale Dienste:
- IGS – International GPS Service,
- IERS – International Earth Rotation Service (Erdrotation, Datendienst),
- IGeS – International Geoid Service,
- ILRS – International Laser Ranging Service (EDM zu Satelliten und Erdmond),
- IVS – International VLBI Service (Interferometrie, Radioastronomie),
- PSMSL – The Permanent Service for Mean Sea Level (Meeresspiegel, Geoid),
- BIPM – Bureau International des Poids et Mesures (Eichung, Zeitdienste).

Alle 2 Jahre finden große zweiwöchige Kongresse mit etwa 1000 Teilnehmern und Dutzenden einzelner Tagungen statt. Eine intensive Kooperation besteht auch zur FIG (Fédération Internationale des Géomètres), welche im Gegensatz zur „Geodesy" die technisch-geodätische Seite vertritt.

Quellen:
http://www.iag-iag.org
http://www.gfy.ku.dk/~iag/

Standardisierung – Normung

für Geoinformation, Fernerkundung und Photogrammetrie

DIN ©2006 **DIN Deutsches Institut für Normung e.V.**
http://www.din.de

Das DIN ist ein eingetragener Verein mit Sitz in Berlin (DIN Deutsches Institut für Normung e. V., gegründet 1917). DIN ist die für die Normungsarbeit zuständige Institution in Deutschland und vertritt die deutschen Interessen in den weltweiten und europäischen Normungsorganisationen. Dieser Status wurde im Vertrag mit der Bundesrepublik Deutschland am 5. Juni 1975 anerkannt.

Das DIN ist der runde Tisch, an dem sich Hersteller, Handel, Verbraucher, Handwerk, Dienstleistungsunternehmen, Wissenschaft, technische Überwachung, Staat, d. h. jedermann, der ein Interesse an der Nor-

mung hat, zusammensetzen, um den Stand der Technik zu ermitteln und unter Berücksichtigung neuer Erkenntnisse in Deutschen Normen niederzuschreiben.

Das Präsidium des DIN besteht gegenwärtig aus 45 leitenden Vertretern aus Industrie, Wirtschaft und Politik Deutschlands, Österreichs und der Schweiz. Präsident des DIN ist Dipl.-Kfm. Dietmar Harting, Espelkamp, erster Stellvertreter Dipl.-Ing. Heinz Helmut Kempkes, Remscheid.

Die fachliche Arbeit der Normung wird in Arbeitsausschüssen bzw. Komitees durchgeführt. Für eine bestimmte Normungsaufgabe ist jeweils nur ein Arbeitsausschuss bzw. ein Komitee zuständig, die zugleich diese Aufgaben auch in den regionalen und internationalen Normungsorganisationen wahrnehmen. Im Regelfall sind mehrere Arbeitsausschüsse zu einem Normenausschuss im DIN zusammengefasst. Zurzeit gibt es *76 Normenausschüsse (NA)*.

Die Fachgebiete Geoinformation, Geodäsie, Kartographie, Fernerkundung, Photogrammetrie sind im Wesentlichen im *NA 005 Bauwesen (NABau)* erfasst. Die Luft- und Raumfahrt ist im NA 131 (NL), die Grundlagen des Umweltschutzes sind im NA 172 (NAGUS) konzentriert.

Der Normenausschuss Bauwesen (NABau) ist im DIN für die nationale Normungsarbeit nachstehender Bereiche zuständig und vertritt für die entsprechende supranationale Normungsarbeit den nationalen Standpunkt für Grund- und Planungsnormen (im Bauwesen), Abdichtung, Feuchteschutz, Vermessungswesen, Geoinformation, Verkehrswegebau u.v.a. Dabei werden Vornormen und Normen für Baustoffe und Bauteile mit den zugehörigen Normen für die Prüfverfahren sowie Planungs- und Bemessungsnormen (z. B. Eurocodes für den konstruktiven Ingenieurbau) aufgestellt.

Für die Photogrammetrie sind bisher folgende Normen erarbeitet worden:

DIN 18716	Photogrammetrie und Fernerkundung
DIN 18716-1	Grundbegriffe und besondere Begriffe der photogrammetrischen Aufnahme
DIN 18716-2	Besondere Begriffe der photogrammetrischen Auswertung
DIN 18716-3	Begriffe der Fernerkundung
DIN 18740	Qualitätsanforderungen an photogrammetrische Produkte (siehe PFG, 1/2006, S. 79/80).
DIN 18740-1	Anforderungen an Bildflug und analoges Luftbild
DIN 18740-2	Anforderungen an das gescannte Luftbild
DIN 18740-3	Anforderungen an das Orthophoto
DIN 18740-4	Anforderungen an das digitale Luftbild (in Bearbeitung)

CEN – Comité Européen de Normalisation (Europäisches Komitee für Normung)

http://www.cenorm.be

Das Europäische Komitee für Normung CEN wurde 1961 durch EWG- und EFTA-Länder gegründet. CEN hat seinen Sitz in Brüssel. Das Technische Komitee „Geographic Information“ CEN/TC 287 bearbeitet Normen zur Geoinformation. Heute werden vor allem die für den Aufbau der europäischen Geodateninfrastruktur INSPIRE notwendigen ISO-Normen übernommen und an europäische Bedürfnisse angepasst. Das CEN/TC 287 besteht aus fünf Arbeitsgruppen (WGs):

- WG 1: Framework for Standardization in Geoinformatics (GI)
- WG 2: Models and Applications for GI
- WG 3: Geographic Information Transfer
- WG 4: Locational Reference Systems for GI
- WG 5: Spatial data infrastructure

Folgende Normen wurden bisher verabschiedet (published):

EN ISO 19101	Geographic information – Reference model (ISO 19101:2002)
EN ISO 19105	Geographic information – Conformance and testing (ISO 19105:2000)

EN ISO 19106:2004 Geographic information – Profiles (ISO 10106:2004)
EN ISO 19107 Geographic information – Spatial schema
EN ISO 19108 Geographic information – Temporal schema (ISO19108:2002)
EN ISO 19111 Geographic information – Spatial referencing by coordinates (ISO 19111:2003)
EN ISO 19112 Geographic information – Spatial referencing by geographic identifiers (ISO 19112:2003)
EN ISO 19113 Geographic information – Quality principles (ISO 19113:2002)
EN ISO 19114 Geographic information – Quality evaluation procedures (ISO 19114:2003)
EN ISO 19115 Geographic information – Metadata (ISO 19115:2003)
EN ISO 19116:2004 Geographic information – Positioning services
prEN ISO 19125-1:2004 Geographic information – Simple feature access-Part 1: Common architecture
EN ISO 19125-2:2004 Geographic information – Simple feature access-Part 2: SQL option (ISO 19125-2:2004)

Folgende Normenentwürfe werden zurzeit erarbeitet:

prEN ISO 19109:2005 Geographic information – Rules for application schema (ISO 19109:2005)
prEN ISO 19110:2005 Geographic information – Methodology for feature cataloguing (ISO 19110:2005)
prEN ISO 19117:2005 Geographic information – Portrayal (ISO 19117:2005)
prEN ISO 19118:2005 Geographic information – Encoding (ISO 19118:2005)
prEN ISO 19119:2005 Geographic information – Services (ISO 19119:2005)
prEN ISO 19123:2005 Geographic information – Schema for coverage geometry and functions (ISO 19123:2005)
prEN ISO 19133:2005 Geographic information – Location-based services – Trakking and navigation
prEN ISO 19135:2005 Geographic information – Procedures for item registration
prCEN/TR 15449 Geographic information – Standards, specifications, technical reports and guidelines, required to implement Spatial Data Infrastructure
ISO/DIS 19111 Geographic information – Spatial referencing by coordinates

Zahlreiche weitere Normen befinden sich im Stadium der Vorbereitung.
(Dokumente: Beuth Verlag GmbH, 10772 Berlin).

ISO – International Organization for Standardization
http://www.iso.ch

Die ISO wurde 1945 gegründet. Sie koordiniert 118 nationale Normungsgremien. Die Normungsarbeit ist untergliedert in ca. 2700 Komitees, Arbeitsgruppen u. a. Das Technische Komitee ISO/TC 211 „Geographic information/Geomatics" besteht seit 1994 und erarbeitet Normen für dieses Sachgebiet. Chairman des ISO/TC 211 ist Olaf Østensen, Norwegen. Für die Realisierung der Normungsarbeit sind zurzeit folgende Arbeitsausschüsse (Working Groups/WG) eingesetzt:

TC 211/WG 4 Geospatial services
TC 211/WG 6 Imagery (mit Photogrammetrie, Fernerkundung)
TC 211/WG 7 Information communities
TC 211/WG 8 Location based services
TC 211/WG 9 Information management

Das ISO/TC 211 bearbeitet zurzeit folgende Projekte:

ISO/CD 6709 Standard representation of latitude, longitude and altitude for geographic point locations
ISO/DTS 19101-2 Geographic information – Reference model – Part 2: Imagery
ISO/DIS 19104 Geographic information – Terminology
ISO/DIS 19111 rev Geographic information – Spatial referencing by coordinates
ISO 19115:2003 cor. 1 Geographic information – Metadata

ISO/CD 19115-2 Geographic information – Metadata – Part 2: Metadata for imagery and gridded data
ISO 19119:2005 Amd. 1 Geographic information – Services. Amendment 1
ISO/DTS 19129 Geographic information – Imagery, gridded and coverage data framework
ISO/CD 19130 Geographic information – Sensor data models for imagery and gridded data
ISO/DIS 19131 Geographic information – Data product specification
ISO/DIS 19132 Geographic information – Location based services – Reference model
ISO/DIS 19134 Geographic information – Location based services – Multimodal routing and navigation
ISO/DIS 19136 Geographic information – Geography Markup Language
ISO/DIS 19137 Geographic information – Core profile of the spatial schema
ISO/DTS 19138 Geographic information – Data quality measures
ISO/DTS 19139 Geographic information – Metadata – XML schema implementation
ISO/CD 19141 Geographic information – Schema for moving features
ISO/CD 19142 Geographic information – Web Feature Service
ISO/CD 19143 Geographic information – Filter encodeing
ISO/CD 19144 Geographic information – Classification systems

OGC – Open Geospatial Consortium, Inc.

http://www.opengeospatial.org/

Das OGC ist ein internationales Industriekonsortium für die Entwicklung von offenen GIS-Standards, heute vor allem bezüglich des Internet, des Mobilfunks und der Navigationssysteme. OGC basiert auf der Mitgliedschaft von mehr als 300 Firmen, Regierungsstellen und Universitäten.

Der Sitz der Gesellschaft ist in den USA mit Außenstellen in Europa (UK) – OGCE – und Australasien (Australien, Neuseeland) – OGCA – .Das OGC wird geleitet von Präsident Mark Reichardt, Generaldirektor David Schell und einem 20-Personen umfassenden Board of Directors, dem aus Deutschland Dr. Axel Nawrocki von der Hansa Luftbild AG angehört.

Erprobte Lösungen stehen vor allem im Web-Bereich zur Verfügung. Bisherige Ergebnisse sind u. a.:

– SensorML (Sensor Model Language) für Photogrammetrie und Fernerkundung zur Modellierung von Sensoren auf beweglichen und stationären Plattformen
– Integration von JPEG2000 und GML (Einbindung photogrammetrischer Parameter in GML/JPEG2000).

Quellen:
– Bill & Zehner, Lexikon der Geoinformatik 2001
– W. Kresse, PFG 7/2005, S. 552–554
– P. Reiß, PFG 1/2006, S. 79/80
– homepages DIN, CEN, ISO, OGC

Klaus Szangolies, Jena

Hochschulnachrichten

Technische Universität München

Schulungsangebot
Runder Tisch GIS e.V.:
OGC Standards, OGC Web Services

Im Jahre 2005 hat der Runde Tisch GIS e. V. zum ersten Mal ein Schulungsprogramm aufgelegt. Der Schwerpunkt des Angebotes lag beim Thema OGC-Standards.

Erfreulicherweise wurde das Schulungsangebot gut angenommen. Dies hat dazu ermutigt, das Angebot für 2006 um einige Kurse zu erweitern. Hier die einzelnen Kurse:

OGC Standards in Geodateninfrastrukturen:
– Überblick und Einordnung
– Praktische Anwendungen

OGC Web Services für Entwickler
– Herausforderung Sicherheit bei OGC Web Services:
  • Überblick und Einordnung
  • Praktische Anwendungen

Fähigkeiten und Grenzen von GIS-Software im Open-Source-Bereich

Bewertungsverfahren für den wirtschaftlichen Einsatz von GIS im kommunalen Bereich

GIS-Datenqualität – Leitlinien bei der Vergabe von Aufträgen

AFIS-ALKIS-ATKIS Basiswissen

SVG für Anfänger

Das komplette Angebot sowie Informationen zu den einzelnen Kursen finden Sie unter http://www.rtg.bv.tum.de/index.php/article/archive/191/

Dr. Gabriele Aumann, München
Runder Tisch GIS e. V.
c/o Technische Universität München
Fachgebiet Geoinformationssysteme
Arcisstr. 21, D-80290 München
Tel.: +49-89-289-22857
Fax: +49-89-289-2878

ETH Zürich

Weiterbildungszertifikatslehrgang
Räumliche Informationssysteme
ETH-Hönggerberg Zürich, Schweiz.

6.–10.11.2006, 4.–8.12.2006, 8.–12.1.2007, 5.–9.02.2007, 12.–16.3.2007. Auskünfte durch Frau S. Sebestyen, Tel.: +41-44-633-3157, e-mail: sebestyen@geod.baug.ethz.ch und Frau K. Wolff, Tel.: +41-44-633-3054, e-mail: wolff@geod.baug.ethz.ch http://www.photogrammetry.ethz.ch/ndk/

Buchbesprechungen

Nicole Ueberschär & André M. Winter, 2006: Visualisierung von Geodaten mit SVG im Internet. Bd. 1: Scalable Vector Graphics – Einführung, clientseitige Interaktionen und Dynamik. XIV, 296 S. Kartoniert. Herbert Wichmann Verlag, Hüthig GmbH & Co. KG, Heidelberg. ISBN 3-87907-431-3.

Dieses Buch ist eine detaillierte und vielseitige Anleitung zur Herstellung graphisch hochwertiger und interaktiver Karten mit Hilfe von SVG. Die Anwendungen reichen vom graphischen Bildschirm bis zum Handydisplay.

Das Buch besteht aus 14 Kapiteln, drei Anhängen und einem Beispielarchiv auf einer geschützten Internetseite.

Bis zum Kapitel 7 werden die statischen Graphikelemente von SVG erläutert. Dazu gehören die vier klassischen Graphiktypen Punkt, Linie, Fläche und Text, die jeweils so detailliert vorgestellt werden, wie es für

eine ansprechende Kartengraphik erforderlich ist. In Kapitel 8 folgt eine Einführung in die Animationstechnik. Gezielt eingesetzt kann durch sie die Lesbarkeit der Karte gut unterstützt werden. Vorgestellt werden „wachsende Linien", die mit einem Bleistiftsymbol verknüpft das Von-Hand-Zeichnen der Linien nachbilden. Das Kapitel 9 bietet unter dem Titel Scripting eine anwendungsbezogene Einführung in JavaScript. Das Kapitel 10 erläutert das in SVG verwendete Datenmodell, das Document Object Model (DOM). Hier ist auch die Erzeugung von Signaturen und Tortendiagrammen angesiedelt. Im Weiteren ist vor allem das Kapitel 12 hervorzuheben. Dort werden die scheinbar trivialen Funktionen Zoom und Pan dem Leser nahe gebracht und erläutert, wie beispielsweise bei Maßstabs- und Ausschnittsänderungen der Hauptkarte eine interaktive Übersichtkarte statisch an ihrer Position bleibt und die Steuerung der Hauptkarte per Mausklick erlaubt. Die übrigen Kapitel 11, 13 und 14 behandeln das graphische Hervorheben, DOM-Methoden und die Einbindung fremder Namespaces.

Der Anhang befasst sich mit der Ausgabe von SVG-Daten aus den Desktop-Publishing-Programmen CorelDraw und Adobe Illustrator sowie aus den ESRI-Programmen. Im Anhang B wird die Einbettung von SVG in HTML erläutert. Der Anhang C stellt die wichtigsten aktuellen SVG-Viewer gegenüber.

Das Beispielarchiv umfasst über 200 SVG-Dateien, die eine sehr gute Ergänzung zum Buch darstellen und den ersten Schritt zu selbst gestalteten SVG-Karten außerordentlich erleichtern.

Der Text des Buches ist locker und spritzig geschrieben. Man hat immer den Eindruck, bei den Autoren im Schulungskurs zu sitzen und direkt angesprochen zu sein. Alle Beispielcodes bauen auf erprobten SVG-Dateien auf. Wichtige Passagen und erläuterte Details sind farblich markiert.

Besonders hilfreich ist der vielfältige Bezug zu den aktuellen SVG-Viewern Adobe SVG Viewer 3.x, Corel SVG Viewer 2.1, Mozilla Firefox 1.5, Opera 8.5, Batik Squiggle 1.6 und Microsoft Internet Explorer 6.x. Die Einschränkungen und Bugs dieser Viewer werden präzise benannt und Workarounds angegeben, zumindest soweit der Themenumfang des Buches reicht.

Auch ein paar kritische Anmerkungen seien gestattet. Das Buch wird als Band 1 vorgestellt. Es wird aber nicht deutlich, ob es einen zweiten Band gibt oder geben wird, und wie der thematisch ausgerichtet sein könnte.

Alle Skriptbeispiele benutzen JavaScript. Das kann zu speziellen Lösungen führen, ist aber legitim, zumal die anderen gängigen Skriptsprachen wie PHP und Python benannt werden. Wahrscheinlich würde eine generische Lösung den Rahmen des Buches sprengen und weniger einsteigerfreundlich sein.

Der Anspruch des Buches ist die Anleitung zur Erstellung einer SVG-Karte mit einem Texteditor. Es wird gezeigt, dass keines der auf dem Markt verfügbaren Softwarepakete SVG-Dateien so ausgibt, dass alle kartographischen Anforderungen erfüllt sind. Nacharbeit ist immer erforderlich, unter anderem, um interaktive Karten herzustellen. Daher muss ein guter Kartograph heute in großem Maße auch ein geschickter Programmierer sein. Das Buch bietet dazu das Handwerkszeug und ist sowohl Einsteigern als Grundkurs als auch Fortgeschrittenen als Nachschlagewerk zu empfehlen.

Wolfgang Kresse, Neubrandenburg

GIS und Sicherheitsmanagement von Josef Strobel & Cornelius Roth, (Hrsg.), 2005: GIS und Sicherheitsmanagement. 181 S., Kartoniert. Herbert Wichmann Verlag, Hüthig GmbH & Co. KG, Heidelberg. ISBN 3-87907-432-1.

Wie die Herausgeber des Buches in ihrem Vorwort betonen, möchten sie mit dieser thematischen Schwerpunktsetzung einen neuen weiteren Bereich, in dem Geoinformatik als verbindendes Element wirkt, in den Fokus des Interesses rücken. Dazu wurden die 23 Beiträge der gleichnamigen Fachtagung bzw. Schwerpunktveranstaltung auf der letztjährigen AGIT überarbeitet und zu-

sammen mit der Eröffnungsrede und Stimmen aus der die Tagung abschließenden Podiumsdiskussion in einem Band von insgesamt 181 Seiten zusammengestellt.

Im Vorwort wird für den Bereich des Sicherheitsmanagement GIS insbesondere in der Funktion einer Integrationsplattform gesehen. Allgemein besteht Bedarf an effizienter Pro- und Re-Aktion, im Besonderen an Infrastrukturen für ein effektives, räumliches Management von lebenserhaltenden Ressourcen. Dabei sind zeitnahe Geoinformationen und pragmatische Einfachheit von Anwendungen gefordert, da Einsatzkräfte keine GIS-Spezialisten sind und auch nicht sein müssen. Entsprechend kreisen die in der Podiumsdiskussion gestellten und diskutierten Fragen darum, wie der Wissenstransfer von der Forschung in einfache, funktionale Werkzeuge für den Notfall sicherzustellen ist, dies nicht allein über politische Rahmenbedingungen gesteuert sondern durch die Zusammenarbeit und den Dialog von Forschung, Anwenderschaft und Wirtschaft.

Ganz an den Anfang des Buches gestellt wurde die Eröffnungsrede durch Mag. Rainer Frank vom Österreichischen Bundesministerium für Verkehr, Innovation und Technologie zu *„Forschung und Sicherheit – politische und wirtschaftliche Interdependenzen vor dem Hintergrund neuer Bedrohungen*“. Er endet seinen Beitrag mit dem Hinweis, dass Konferenzen wie diese die Öffentlichkeit über neue Entwicklungen in der sicherheitsrelevanten Hochtechnologie und deren Nutzen für die Gesellschaft informieren würden.

Das Buch wurde in vier Teile gegliedert. Jedem der Teile ist eine kurze Einführung durch den Herausgeber C. Roth vorangestellt. Der erste Teil zu *„Geodateninfrastrukturen (GDI) für das Sicherheitsmanagement*“ umfasst vier Artikel. Es wird ORCHESTRA vorgestellt, ein derzeit durch die EU gefördertes Projekt zur Entwicklung einer offenen, service-orientierten Systemarchitektur für das Risikomanagement in Europa. Der Artikel zu GDI im Notfall- und Katastrophenmanagement stellt gekonnt die Notwendigkeit von Koordination und Kommunikation der beteiligten Akteure neben der Bereitstellung von Daten und Informationen für optimale Lösungen dar, dies am Beispiel Brandenburgs. Die ÖNORM A2263-1 zur Übermittlung von Lokationsangaben wird in einer Art technischer Dokumentation vorgestellt, dem Leser aber nicht vermittelt, warum diese für das Sicherheitsmanagement von Relevanz ist. Und schließlich wird dem Nutzen von Ontologien im Katastrophenschutz nachgegangen, wobei es sich um eine gute allgemeine Einführung zum Wissensmanagement handelt mit Verweisen auf laufende Projekte. Wie C. Roth schreibt, gehört die Errichtung von GDI zu einem mittlerweile etablierten Trend in der Geoinformatik. Das sehr weite Feld wird hier durch vier Artikel sehr unterschiedlicher Ausrichtung nur gestreift.

Teil II *„Einsatzorganisationen und GIS*“ fasst wiederum vier Artikel zusammen. Sie beschreiben alle den Einsatz von GIS bzw. georäumlichen Informationen bei der Feuerwehr. Das Notfallmanagement-System der Rettungsleitstelle der Stadt Darmstadt wird umfassend vorgestellt. Das mobile Entscheidungsunterstützungssystem MONA, wie es für die Feuerwehr Duisburg entwickelt und derzeit getestet wird, ist ebenfalls sehr ausführlich beschrieben. Dagegen wird das bei der Berliner Feuerwehr zum Einsatz kommende Gefahrenabwehrsystem GeoFES nur sehr kondensiert vorgestellt. Aus der stichworthaften Zusammenstellung von Funktionalitäten und den zahlreichen Abbildungen lässt sich das Potential des Systems aber erahnen. Die Informations- und Dokumentationsverarbeitung an der Einsatzstelle der Werkfeuerwehr der Technischen Universität München setzt Tablet PC Hardware ein. Auf das robuste mobile Gerät können vom Einsatzleitrechner Daten übermittelt werden. Bei diesem letzten Beitrag aus dem zweiten Teil stellt sich die Frage, warum dieser Praxisbericht nicht im nächsten Teil, *„Einsatzleitsysteme und Mobile Dienste*“, angesiedelt ist.

An dessen Anfang steht ein sehr allgemein gehaltener Artikel zur Open-Source-GIS-Software der Firma DIALOGIS für raum-

bezogenes Informationsmanagement. Der Beitrag kommt dabei leider völlig ohne Bezug zu Einsatzleitsystemen und Mobilen Diensten aus, geschweige denn zum Thema Sicherheitsmanagement. Der Beitrag *„Erstellung einfacher Lagekarten im Katastrophenschutz“* der Bezirkshauptmannschaften Oberösterreichs stellt einen sehr einfachen aber pragmatischen Ansatz vor. Ein „Notfallkoffer“ als Zusammenstellung von Hard- und Software dient für den Notfall und steht auch im Zuge der Rufbereitschaft zur Verfügung. *„GIS in Einsatzleitungen – Geodaten im Krisen- und Katastrophenmanagement“* ist der Versuch einer generell gültigen Darstellung, die jedoch nur sehr wenig an Information bietet. Ein weiterer Praxisbericht erläutert die Kopplung von GIS und Navigationssoftware für Entstörungsdienste der Energieversorger. Hier sind einige Fachbegriffe leider nicht erläutert, sonst ist der Beitrag aber flott zu lesen. Letzteres trifft für den Beitrag zur Navigation mittels RFID (Radio Frequency Identification) bei der Fußball-WM 2006 nicht zu. Trotzdem erhält der Leser einen Eindruck von den technischen Potentialen in Verbindung mit RFID-Eintrittskarten. Und schließlich berichtet das Österreichische Bundesheer von der Geodatenaufbereitung für seinen Tsunami-Katas-tropheneinsatz in Sri Lanka, dies leider nur sehr oberflächlich und somit von wenig Nutzen für den interessierten Leser.

Während die Mehrzahl der in Teil II und III enthaltenen Beiträge ganz oder fast ohne Literaturreferenzen auskommt, beinhaltet der vierte Teil *„Naturgefahren und Risikobewertungen“* einige nach wissenschaftlichen Maßstäben ausgearbeitete Artikel. Im einzigen in Englisch verfassten Beitrag wird die Übertragbarkeit eines für die Alpen entwickelten Ansatzes auf Island dargestellt zur Analyse und Bewertung des Naturgefahrenpotentials von Straßen. Im Beitrag zur Schadenpotentialanalyse für den regionalen Maßstab am Beispiel Tirols, Südtirols und Graubündens nehmen die Ergebnisse und die Diskussion leider vergleichsweise wenig Platz ein. Der Beitrag zur Modellierung der Rutschanfälligkeit am schwäbischen Albtrauf einschließlich einer Gefährdungskarte lässt nichts zu wünschen übrig, ist entsprechend rundum gelungen. Die Beschreibung des Hochwasserinformationssystems in Baden-Württemberg sowie die der Hochwassersimulation in Sonthofen ähneln wieder mehr Praxisberichten. Der Artikel zur Tsunami-Gefährdungskarte für Istanbul lässt wichtige Informationen zum Vorgehen bei der Erstellung vermissen. Während der Beitrag zu den Online-Karten für den Tiroler Lawinenwarndienst den Fortschritt des Projekts erkennen lässt, wird bei den beiden abschließenden Beiträgen zum Wegemanagementsystem für eine erhöhte Sicherheit beim Bergwandern in den Alpen sowie zum Aufbau einer Naturgefahren-GDI für Kärnten, hier in noch stärkerem Maße, deutlich, dass diese beiden Projekte noch in den Anfängen stecken.

Auch wenn auf der Rückseite des Titelblatts größtmögliche Sorgfalt durch den Verlag zugesichert wird, so mangelt es diesem Buch daran. Der Leser wundert sich, dass bereits im Vorwort der erste Abschnitt in einer Überarbeitung wiederholt wird oder dass im Inhaltsverzeichnis ein Titel doppelt vorkommt. Zudem finden sich in den einzelnen Beiträgen z.T. zahlreiche Fehler. Es ist doch Aufgabe des Verlags in Zusammenarbeit mit den Herausgebern, für ein, auch sprachlich, korrektes Buch zu sorgen. Auch die Abbildungen lassen oft zu wünschen übrig: sei es, dass die schwarzweiße Wiedergabe den eigentlichen Inhalt nicht erkennen lässt, dass eingebettete Fonts im Druck nicht unterstützt wurden, dass Abbildungen zu klein integriert und somit schwer „lesbar“ sind, oder dass gar die Graphikqualität den Ansprüchen im Druck nicht gerecht wird.

Insgesamt liegt uns ein sehr heterogenes Buch vor, welches sich zwar laut Text auf dem Rückumschlag an sämtliche sich für die Bereiche Naturgefahren, Sicherheitsforschung und GIS Interessierende bzw. in diesen Bereichen Tätige richtet. Aber durch die sehr unterschiedliche Ausführung der Beiträge dürfte keine dieser Gruppen mit dieser Zusammenstellung zufrieden gestellt sein. Unbefriedigend ist insbesondere, wie mit Li-

teraturhinweisen umgegangen wird. Auch stellt sich die Frage, warum Teile auf Englisch enthalten sind.

Trotz aller Unzulänglichkeiten, die zu bedauern sind, liegt nach Kenntnislage der Rezensentin mit diesem Buch erstmalig eine Zusammenstellung von Artikeln zum Thema *„GIS und Sicherheitsmanagement"* (fast durchgängig) auf Deutsch vor. Die Heterogenität der Beiträge erklärt sich bestimmt auch darin, dass Akteure aus Forschung, Wirtschaft und Anwendung zu Wort kommen. Hier liegt das Verdienst der Veranstalter dieser Fachtagung: sie haben den Dialog zwischen den Akteuren gefördert und eventuell auch zu deren Zusammenarbeit angeregt.

GERTRUD SCHAAB, Karlsruhe

Vorankündigungen

2006

1.–3. September: **ISPRS** 7th Joint **ICA/ EuroGeographic International Workshop on** "*Incremental Updating & Versioning*" in **Haifa**, Israel. Auskünfte durch: Ammatzia Peled, Tel.: +972-48-34 3591, Fax: +972-48-34 3763, e-mail: peled@geo. haifa.ac.il, http://geo.haifa.ac.il/~icaupdt/

3.–7. September: **APOC 2006** (Asia-Pacific Optical Communications) in **Gwangju**, Südkorea. Auskünfte: http://spie.org/app/conferences/index.cfm

4.–7. September: **ISPRS Mid-term Symposium Commission VIII** *"Remote Sensing Applications for a Sustainable Future"* in **Haifa**, Israel. Auskünfte durch: Ammatzia Peled, Pres. Com.VIII, Tel.: +972-48-34 35 91, Fax: +972-48-34 3763, e-mail: peled@geo.haifa.ac.il, www.commission8.isprs.org

5.–8. September: **RSPSoc Annual Conference** in **Cambridge**, UK. Auskünfte durch: Patsy Wilson-Smith, e-mail: adminis strator@uflm.cam.ac.uk, www.rspsoc.org

11.–13. September: 26. **Wissenschaftlich-Technische Jahrestagung der DGPF** *„Geoinformatik und Erdbeobachtung"* in **Berlin**-Adlershof. Auskünfte: www.dgpf.de

11.–16. September: **SPIE Europa Symposium** *Optics/Photonics in Security and Defense*. Gleichzeitig: **SPIE Europa Symposium** *Remote Sensing* in **Stockholm**. Auskünfte: http://spie.org/app/conferences/ index.cfm

12.–14. September: 28. **DAGM – Tagung 2006** in **Berlin**. Auskünfte durch: Konferenz-Sekretariat Frau Andrea Semionyk, Frauenhofer Institut für Telekommunikation, Heinrich-Hertz-Institut, Image Processing Department. Einsteinufer 37, D-10587 Berlin, Tel.: +49-30-31002-561, Fax: +49-30-3927200, e-mail: dagm06@hhi.de, http://dagm06.hhi.de

13.–15. September: **Speckle 2006 International Conference** in **Nimes**, Frankreich. Auskünfte: http://spie.org/app/conferences/index.cfm

13.–15. September: **9. AGIS-Seminar** „**GIS & Internet**" in **Neubiberg**. Auskünfte durch: AG Geoinformationssysteme GIS (AGIS) der Universität der Bundeswehr München. Tel.: 089-6004-2451, Fax: 089-6004-3906. www.agis.unibw.de

14.–22. September: 9th **International Symposium on High Mountain Remote Sensing Cartography** in **Graz** mit mehrtägiger Alpenexkursion. Auskünfte: e-mail wolfgang.sulzer @uni-graz.at, http://www.kfunigraz.ac.at/geowww/hmrsc/hmrsc_9.htm

18./19. September: 43. **AgA-Tagung** "Arbeitsgemeinschaft **Automation in Kartographie, Photogrammetrie und GIS**" der DGfK im Hasso-Plattner-Institut **Potsdam**. Auskünfte und Einreichung von Beiträgen: www.ikg.uni-hannover.de/aga

18.–20. September: **International Conference on Image Analysis & Recognition** (ICIAR 2006) in **Póvoa de Varzim**, Portugal. Auskünfte durch: Secretariat, Tel.: +351-22-508-1623, Fax: +351-22-508-1624, e-mail: gafonso@fe.up.pt, www.iciar.uwaterloo.ca/

19. September: **Expertenrunde „Runder Tisch GIS"** e.V. mit dem Thema »Wirtschaftlichkeit von GIS im kommunalen e-Government« in **München**. Auskünfte: Dr. Gabriele Aumann, e-mail: gabriele.aumann@bv.tum.de, www.rundertischgis.de

19.–22. September: **ISPRS Mid-term Symposium Commission III** *"Photogrammetric Computer Vision* **PCV'06**" in **Bonn**. Auskünfte durch: Prof. Wolfgang Förstner, Pres. Com.III, Tel.: +49-228-732 2713, Fax: +49-228-732 2712, e-mail: wf@ipb.uni-bonn.de, www.commission3.isprs.org, www.ipb.uni-bonn.de/isprs/pcv06/

20. September: ISPRS WG IV/6 **UbiGIS 2006 Workshop** in **Münster**. Auskünfte durch: Alexander Zipfe, e-mail: zipf@geoinform.fh-mainz.de, www.ubigis.org

24.–29. September: XII **SELPER** International Symposium **GIS & Remote Sensing applied to Natural Risk & Territory Management** in **Cartagena de Indias**, Kolumbien. Auskünfte durch Sekretariat Tel.: +571-480 9453, Fax: +571-369 4096, e-mail: simposio@selper.org.co, http://www.selper.org.co/pdfs/symposium_information.pdf

25./26. September: 2nd **International Symposium on Geo-Information for Disaster Management** in **Goa** (The Hotel Marriot), Indien. Auskünfte: www.grss-ieee.org/menu.taf?menu=Conferences&detail=Conferences

25.–27.September: **SPIE Boulder Damage Symposium** in **Boulder**, CO, USA. Auskünfte: http://spie.org/app/conferences/index.cfm

25.–27. September: **ISPRS Mid-term Symposium Commission V** *„Image Engineering and Vision Metrology"* in **Dresden**. Auskünfte durch: Prof. Hans-Gerd Maas, Pres. Com.V, Tel.: +49-351-463-33680, Fax: +49-351-463-37266, e-mail: hmaas@rcs.urz.tu-dresden.de, www.commission5.isprs.org, www.tu-desden.de/ipf/symposium/

27.–30. September: **ISPRS Mid-term Symposium Commission IV** *„Geospatial Data-bases for Sustainable Development"* in **Goa**, Indien. Auskünfte durch: Shailesh Nayak, Pres. Com.IV, Tel.: +91-79-2691 4141, Fax: +91-79-26915, e-mail: shailesh@sac.isro.org, www.commission4.isprs.org

28.–30. September: 2nd Workshop of the **EARSeL Special Interest Group on Land Use and Land Cover** in **Bonn**. Auskünfte durch: Zentrum für Fernerkundung der Landoberfläche, Universität Bonn, c/o Ellen Götz, Walter-Flex-Str. 3, D-53113 Bonn, Tel.: 0228-73-4978, Fax: 0228-73-6857, zfl@uni-bonn.de, http://www.zfl.uni-bonn.de/earsel/earsel.html und EARSel, Secretariat, Gesine Böttcher, c/o Institute of Photogrammetry and GeoInformation, Nienburger Str. 1, D-30167 Hannover, Tel.: 0511-762 2482, Fax: 0511-762 2483, e-mail: secretariat@earsel.org, http://www.earsel.org

1.–4. Oktober: **SPIE Optics East** in **Boston**, USA. Auskünfte: http://spie.org/app/conferences/index.cfm

1.–8. Oktober: **GMOSS Summer School 2006** in **Salzburg**. Titel: Monitoring of Human Security: People-Homes-Infrastructure. http://www.sbg.ac.at/zgis/gmoss/SS2006/

1.–12. Oktober: **Z_GIS Summer School 2006** in **Salzburg**. Titel: ENERegion-Regional Potentials for Renewable Energy Generation. Solarthermie und Photovoltaik, Windenergie, Wasserkraft und Einsatz von

Biomasse als Hauptthemen. http://www.sbg.ac.at/zgis/ss06/

2.–6. Oktober: 57th **International Astronautical Congress der IAA** in **Valencia**, Spanien. Auskünfte: www.iaaweb.org

4.–6. Oktober: 2nd **Goettingen GIS & Remote Sensing Days** *„Global Change Issues in Developing and Emerging Countries*" in **Göttingen**. Auskünfte durch: Martin Kappas, e-mail: GGRS@uni-goettingen.de, www.ggrs.uni-goettingen.de

8.–13. Oktober: XXIII. **Internationaler FIG Kongress** *"Shaping the Change*" in **München**. Auskünfte durch: FIG Office, Tel.: +45-38-861081, Fax: +45-38-86 0252, e-mail: fig@fig.net und Thomas Gollwitzer, Kongressdirektor, Tel.: 49-9-414022-200, Fax: +49-9-414022-101, e-mail: congress.director@fig2006.de, www.fig2006.de/

9.–13. Oktober: IX **Global Spatial Data Infrastructure Conference** in **Santiago**, Chile. Auskünfte durch: Instituto Geografico Militar (IGM), e-mail: gsdi9@igm.cl, www.igm.cl

9.–13. Oktober: 27th **Asian Conference on Remote Sensing (ACRS2006)** in **Ulaanbaatar**, Mongolei. Auskünfte durch: Conference Secretariat, Tel./Fax: +976-11-32 7824, e-mail: msaandar@mongol.net, http://www.acrs2006.ub.mn

10.–12. Oktober: **INTERGEO 2006** *„Wissen und Handeln für die Erde*" in **München**, ICM-Messegelände. Kongressdirektor: Dipl.–Ing. Walter Henninger. Auskünfte durch: e-mail: www.dvw.de, www.intergeo 2006.de und www.hinte-messe.de

17./18. Oktober: **ISPRS** IC WG I/V 2nd **International Workshop** *"The Future of Remote Sensing*" in **Antwerpen**, Belgien. Auskünfte durch: Jürgen Everaerts, Tel.: +32-14-336834, Fax: +32-14-322795, e-mail: jurgen.everaerts@vito.be, www.pegasus4europe.com/

25.–29. Oktober: **Cities and Media: Cultural Perspectives on Urban Identities in a Mediatized World.** ESF-LiU (European Science Foundation-Linköping University) Research Conference in **Vadstena**, Schweden. Chairs: J. Fornäs, Norkkoping & N. Couldry. Auskünfte durch: ESF Research Conferences Unit, 1 quai lezay-Marnésia, BP 90015, 67080 Strasbourg cedex, France, e-mail: conferences@esf.org, www.esf.org/conferences

30. Oktober-2. November: 6th International Conference on **Earth Observation & Geo-information Sciences in Support of Africa's Development (AARSE2006)**, African Association of Remote Sensing of the Environment in **Cairo**, Ägypten. Auskünfte durch: Sayed M. Arafat, Tel.: +202-622 5818, Fax: +202-622 5800, e-mail: smarafat@narss.sci.eg, www.narss.sci.eg/aarse2006, http://spie.org/app/conferences/index.cfm

30. Oktober–4. November: **ISPRS Joint Conferences** WG V/2, CIPA, VAST, EG 2006 in **Cyprus**. Auskünfte durch: Marinos Ioannides, Tel.: +357-22-40 6413, Fax: +357-22-48 8676, e-mail: chairman@cipa2006.org, http://www.vast2006.org/

3.–11. November: 9th International Conference of the **Global Spatial Data Infrastructure (GSDI-9) Spatial Information: Tools for Reducing Poverty** in **Santiago**, Chile. Auskünfte: Organizing Committee, Tel.: +56-2-410 9427, e-mail: gsdi9@igm.cl, www.igm.cl/gsdi9/

6.–10. November: **ASPRS Fall Meeting** in **San Antonio** Crowne Plaza Hotel, Texas, USA. Auskünfte durch: ASPRS, Tel.: +1-301-493-0290, Fax: +1-301-493-0208, e-mail: asprs@asprs.org, www.asprs.org/asprs/meetings/calen dar.html

13./14. November: **NatureProtection: GIS**. International Symposium on Geoinformatics in Eurorean Nature Protection Regions in **Dresden**. Auskünfte durch: Prof. Elmar Csaplovics, TU Dresden, Helmholtzstr.10, 01069 Dresden, Tel.: +49-351-463-33372,

Fax: +49-351-463-37266 und: Birgit Hantusch, Leibniz-Institut für ökologische Raumentwicklung e.V., Weberplatz 1, 01217 Dresden, Tel.: +49-351-4679-273, Fax: +49-351-4679-212

13.–17. November: **Asia-Pacific Remote Sensing** in **Goa**, Indien. Auskünfte: http://spie.org/app/conferences/index.cfm

20.–24. November: 13th **Australasian Remote Sensing & Photogrammetry Conference 2006** in **Canberra**. Auskünfte durch: Erica Stevens, Tel.: +61-2-6257-3299, Fax: +61-2-6257-3256, e-mail: arspc @icms.com.au, www.arspc.org

2007

31. Januar/1. Februar: **6. Oldenburger 3D-Tage 2007. Photogrammetrie-Laserscanning-Optische 3D-Messtechnik**. Auskünfte durch: Prof. Thomas Luhmann, Institut für Angewandte Photogrammetrie und Geoinformatik und Institut für Mess- und Auswertetechnik der FH Oldenburg. www.fh-oow.de/3dtage

11.–17. Februar: 14. **Internationale Geodätische Woche** des Instituts für Geodäsie der Leopold-Franzens-Universität Innsbruck in **Obergurgl**, Tirol, Österreich. Auskünfte durch: Dr. Thomas Weinhold, A-6020 Innsbruck, Technikerstr.13, Tel.: +43-512-507-6757 oder 6755, Fax: +43-512-507-2910, e-mail: geodaetischewoche@uibk.ac.at, http://geodaesie.uibk.ac.at/geod_wo.html

29.–31. Mai: **ISPRS** IC WG I/V + V/I, WG I/2 + 3 5th International Symposium on **Mobile Mapping Technology** (**MMT2007**) in **Padua**, Italien. Auskünfte durch: Dr. Naser El-Sheimy, Chair IC WG I/V, Tel.: +1-403-220-7587, Fax: +1-403-284-1980, e-mail: naser@geomatics.ucalgary.ca, www.cirgeo.unipd.it/sitocirgeo/mm_frst.html

29.Mai-1. Juni: **ISPRS** WG I/5, IV/3 **Workshop "High Resolution Earth Imaging for Geospatial Information**" in **Hannover**. Auskünfte durch: Karsten Jacobsen, e-mail: karsten@ipi.uni-hannover.de und Christian Heipke, e-mail: heipke@ipi.uni-hannover.de, http://www.ipi.uni-hannover.de

2.–6. Juni: **FIG XXX General Assembly and Working Week** in **HongKong**. Auskünfte durch: FIG Office, e-mail: fig@fig.net, www.fig.net/events/events2007.htm

19.–21. Juni: 27. **Wissenschaftlich-Technische Jahrestagung der DGPF** und **Jahrestagung der SGPBF** der Schweiz in **Muttenz** (Basel). Auskünfte: www.dgpf.de und Prof. Stephan Nebiker, Fachhochschule Nordwestschweiz, Institut Vermessung und Geoinformation, Gründenstr. 40, CH-4132 Muttenz, Tel.: +41-61-467-4336, Fax: +41-61-467-4460, e-mail: stephan.nebiker@fhnw.ch, www.sgpbf.ch

27.–29. Juni: **Joint Workshop** von ISPRS und DGfK **Visualization and Exploration of Geospatial Data** in **Stuttgart**. Auskünfte durch: Prof. Jochen Schiewe, e-mail: jschiewe@igf.uni-osnabrueck.de, www.igf.uni-osnabrueck.de/isprs07/

4.–6. Juli: **AGIT 2007** in **Salzburg**. Auskünfte durch: Dr. Stefan Lang, Z_GIS Centre for Geoinformatics, Universität Salzburg, Hellbrunnerstr. 34, A-5020 Salzburg, Tel.: +43-662-8044 5262, Fax: +43-662-8044 5260, e-mail: stefan.lang@sbg.ac.at, Thomas Blaschke, e-mail: Thomas.Blaschke@sbg.ac.at, www.uni-salzburg.at/zgis/lang, www.agit.at/obia

3.–7. September: **51. Photogrammetrische Woche 2007** in **Stuttgart**. Auskünfte durch: Martina Kroma, Tel.: +49-711-121 3386, Fax: +49-711-121 3297, e-mail: martina.kroma@ifp.uni-stuttgart.de, www.ifp.uni-stuttgart.de/aktuelles/veranstaltungen.html

12.–14. September: **ISPRS** WG I/4, IV/9 **Workshop & Annual Conference of the Remote Sensing and Photogrammetry Society** (RSPSoc) 2007 in **Newcastle upon Tyne**, UK. Auskünfte durch: Jon Mills, e-mail: j.p.mills@ncl.ac.uk und David Holland, e-mail: david.holland@ordnancesurvey.co.uk

19.–21. September: **ISPRS** WG III/4+5,IV/3 **Workshop "Photogrammetric Image Analysis" (PIA07)** in **München**. Auskünfte durch: Uwe Stilla, Tel.: +49-89-289-22671, Fax: +49-89-280 9573, e-mail: stilla@bv.tum.de, www.ipk.bv.tum.de/isprs/pia07

1.–6. Oktober: **ISPRS XXI CIPA International Symposium** in **Athen**. Auskünfte durch Organizing Committee, e-mail: cipathens_2007@survey.ntua.gr, Congress Secretariat, e-mail: Cipa07_secr@triaenatours.gr, http://www.survey.ntua.gr/hosted/cipathens_2007/

2008

14.–19. Juni: **FIG XXXI General Assembly & Working Week** in **Stockholm**. Auskünfte: FIG Office, e-mail: fig@fig.net, www.fig.net/events/2008/fig_2008_stockholm.pdf

3.–11. Juli: **XXI ISPRS Kongress** in **Beijing**, China. Auskünfte durch: CSGPC, Tel.: +86-10-6833 9005, Fax: +86-10-6831 1564, e-mail: fanbsm@public.bta.net.cn, www.isprs2008-beijing.com

Zum Titelbild

IKONOS – EU Space Imaging – GeoEye

A new generation of one meter very high resolution space born remotely sensed imagery shifted the science of remote sensing and gave way for new research opportunities and challenging questions. The year 1999 can be seen as a landmark for optical space borne remote sensing, especially for urban remote sensing purposes. For the first time ever digitally acquired and processed imagery with a spatial ground cell size of one meter became available.

Since the first optical space borne satellite imagery has been recorded in the early 1970s, remote sensing is focusing on urban areas, our human habitats. Data recorded by these early Landsat Multi Spectral Scanner sensors provided spatial resolution of 57 m x 79 m. Such a spatial resolution has found suitable for a medium to small application scale of about 1:250.000. The spatial resolution has been improved by Landsat Thematic Mapper to 30 m resulting in an application scale of 1:75.000. Both systems provide a spectral resolution ranging from the visible to the infrared portion, enabling them for the analysis of vegetation cover as well as for the mapping of man made objects.

However the spatial resolution could not be proofed successfully for a detailed urban monitoring. That changed dramatically when the first high resolution satellite imagery became available to researchers in 2000. *Space Imaging*, based in Thornton, Colorado, U.S. launched their satellite "IKONOS" successfully in 1999 into an orbit about 450 km above earth surface. It was the second launch of an IKONOS satellite, the first launch unfortunately failed.

The IKONOS sensor layout is designed to acquire the portion of visible electromagnetic spectrum and in addition the infrared multispectral information very similar to that recorded by Landsat TM/ETM. As consequence IKONOS pan imagery can be seen as a kind of magnifier, enlarging objects at the ground by almost 900 times compared to Landsat TM. Image data of both systems can be combined very efficiently; thus TM/ETM data is used for the analysis of large areas and IKONOS data is embedded in the analysis process as a deep zoom in, enlarging small features with a detailed structure.

Four impressive examples of IKONOS multispectral capabilities can be observed on the front cover. Those IKONOS imagery show typical urban features, all located in Munich (from upper left clock wise): the

newly established soccer stadium (*Allianz Arena*), the famous *Oktoberfest*, the area of the 2005 Federal Garden Exhibition (*Bundesgartenschau*) directly located on the former airport Munich Riem and the *historic city center of Munich*. For those not so familiar with Munich attractions from above, the significant twin towers of the *Frauenkirche* give an impression from a not remote sensing perspective.

IKONOS can be moved in any direction: side, forward looking and after looking, respectively. That capability increases the theoretical revisit rate of the sensor up to every third day for each location on earth. The sensor has shown the benefits of fast revisit cycles with the close to real time documentation of natural and man made hazards. Examples for the tsunami flooding, recorded short after the wave hits parts of Indonesia can by found at http://www.spaceimaging.com. Imagery recorded with different viewing angles provides stereo capability and it can be seen as anaglyph imagery in a 3D view (page 261). Use the red-blue glasses inside this special issue and look after the anaglyph image produced from IKONOS stereo pairs by the German Aerospace Center (DLR).

Urban areas represent a large number of many different objects, a huge variety of small features. For clear distinction and an automated mapping of these urban objects from digitally recorded imagery a wide radiometric range is necessary. An 11 bit radiometric range is offered by IKONOS imagery, leading to typical radiometric fingerprints for almost each urban feature. The major advantage of that imagery compared to aerial photos is the entire digital processing chain. Images are recorded by CCD cells similar to that known from digital cameras. The raw imagery is then preprocessed and geo-rectified to different levels of accuracy. At least newly developed digital image analysis techniques provided by highly sophisticated software packages have been proofed excellent for the object-based analysis of this high resolution imagery.

European Space Imaging is located in Munich, Germany, and is the Regional Affiliate of GeoEye for IKONOS satellite imagery in Europe. European Space Imaging operates its own receiving station located at the DLR in Oberpfaffenhofen. That enables a real time image acquisition on demand. The area footprint received at Oberpfaffenhofen covers whole Europe and some parts of North Africa and Asia as well. For more information about IKONOS image products, application and order contact European Space Imaging through their website: http://www.euspaceimaging.com/ or: Tel.: +49-89-1301 42-0, Fax: +49-89-130142-22, e-mail: General Enquiries: info@EUSpace Imaging.com Customer Support: support@EUSpaceImaging.com, Sales & Marketing: sales@EUSpaceImaging.com
Office location & Mailing address: Arnulfstrasse 197, 80634 Munich, Germany

Matthias S. Moeller, Tempe, Arizona